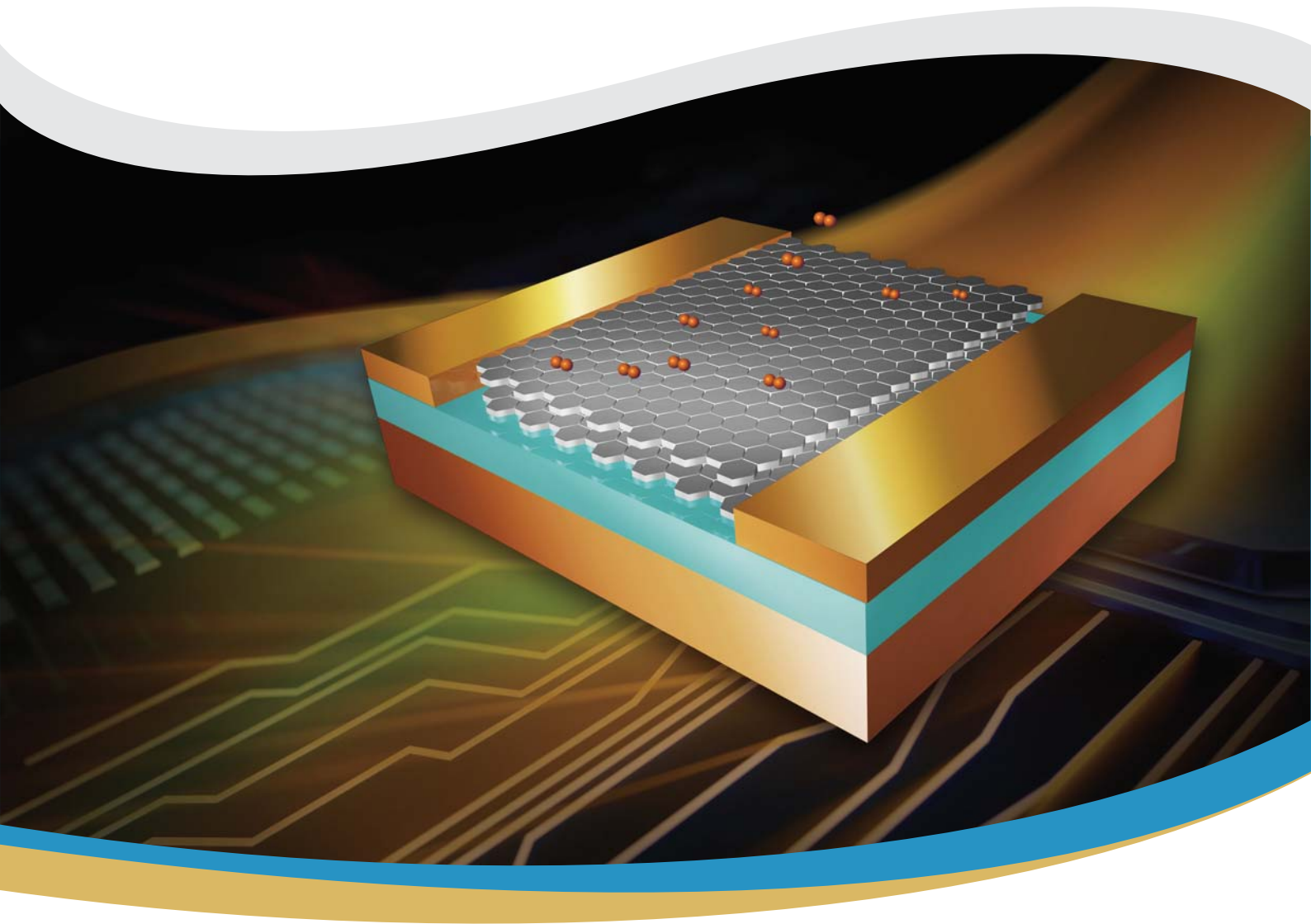


Proceedings of the

Nano-Micro Conference 2017



Shanghai China

June 19th - 23rd, 2017



Proceedings of the Nano-Micro Conference 2017

edited by

Yafei Zhang, Zhi Yang, Liying Zhang, Rong He, Zhihua Zhou

Nano-Micro Conference 2017

Shanghai, China

June 19-23 2017

Local Organizer

Key Laboratory for Thin Film and Microfabrication of Ministry of Education, China
National Key Laboratory of Science and Technology on Micro/Nano Fabrication, China
School of Electronics, Information and Electrical Engineering
Shanghai Jiao Tong University
Shanghai, China

Sponsored By



SHANGHAI JIAO TONG
UNIVERSITY



Nano-Micro
Letters



Shanghai Jiao Tong University
Nano-Micro Letters
Key Laboratory for Thin Film and Microfabrication of Ministry of Education, China
National Key Laboratory of Science and Technology on Micro/Nano Fabrication, China

Publisher

Nature Research Society
120 Baker Street, Westminster, W1U 6TU, London, United Kingdom



Published

November 1st 2017

TITLE: PROCEEDINGS OF THE NANO-MICRO CONFERENCE 2017
EDITORS: YAFEI ZHANG, ZHI YANG, LIYING ZHANG, RONG HE, ZHIHUA ZHOU
ISBN: 978-1-9997506-1-9

General Information

Nano-Micro Conference 2017 is an international conference focused on Nano-Micro Science and Engineering. The aim of this conference is to bring together world-renowned experts, academicians, senior scientists, industry executives and project leaders from all over the world to discuss new developments and frontier researches in the multidisciplinary field of Nano-Micro Science and Engineering.

Conference Chair

Yafei Zhang, Shanghai Jiao Tong University, China

Workshop Chairs

Weimin Chen, Linköping University, Sweden

Yujie Feng, Harbin Institute of Technology, China

Genquan Han, Xidian University, China

Kazuo Kadowaki, University of Tsukuba, Japan

Chaoyang Li, Kochi University of Technology, Japan

Guang Li, Donghua University, China

Hongjun Liu, Xi'an Institute of Optics and Precision Mechanics, CAS, China

Ho Seok Park, Sungkyunkwan University, Korea

Qiquan Qiao, South Dakota State University, USA

Liqiang Mai, Wuhan University of Technology, China

Donald K. Roper, University of Arkansas, USA

Yumeng Shi, Shenzhen University, China

Kimiyasu Shiraki, University of Toyama, Japan

Kang L. Wang, University of California Los Angeles, USA

Zhenhai Xia, University of North Texas, USA

Zhangxiong Wu, Soochow University, China

Yaxin Zhang, University of Electronic Science and Technology of China, China

Jim P. Zheng, Florida State University, USA

Advisory Committee Chair

Kang L. Wang, University of California Los Angeles, USA

Scientific Program Committee Chair

Zhi Yang, Shanghai Jiao Tong University, China

Organizing Committee Chair

Mingwang Fu, The Hong Kong Polytechnic University Hong Kong SAR

Session Chairs

Giuseppina Cerrato, University of Torino, Italy

Weimin Chen, Linköping University, Sweden

Yi Dan, Sichuan University, China

Minoru Fujishima, Hiroshima University, Japan

Toshiaki Hattori, University of Tsukuba, Japan

Jyh-Chiang Jiang, National Taiwan University of Science and Technology, Taiwan

Kazuo Kadowaki, University of Tsukuba, Japan

Xufeng Kou, ShanghaiTech University, China

Atsushi Kanno, National Institute of Information and Communications Technology, Japan

Chaoyang Li, Kochi University of Technology, Japan

Qiang Li, Zhejiang University, China

Ho Seok Park, Sungkyunkwan University, Korea

XiaoYu Peng, Chongqing Institute of Green and Intelligent Technology, CAS, China

Kimiyasu Shiraki, University of Toyama, Japan

Yutaka Takaguchi, Okayama University, Japan

Heqing Tang, South-Central University for Nationalities, China

Weining Wang, Virginia Commonwealth University, USA

Renhua Wu, Shantou University Medical College, China

Zhangxiong Wu, Soochow University, China

Zhenhai Xia, University of North Texas, USA

Xinlong Xu, Northwest University, China

Yanfeng Zhang, Peking University, China

Qun Zhao, The University of Georgia, USA

Bao-Ping Zhang, Xiamen University, China

Yongchun Zhao, Huazhong university of Science and Technology, China

Advisory Committee

Cyrille Andre Boyer, The University of New South Wales, Australia
Siang-Piao Chai, Monash University Malaysia, Malaysia
Trong-On Do, Université Laval, Canada
Jorge Gascon, Delft University of Technology, Netherlands
Rongchao Jin, Carnegie Mellon University, USA
Kazunori Kataoka, The University of Tokyo, Japan
Ali Kosar, Sabancı University, Turkey
Yogendra Kumar Mishra, Christian-Albrechts-Universität zu Kiel, Germany
Shizhang Qiao, University of Adelaide, Australia
Josep Nogués Sanmiquel, Catalan Institute of Nanoscience and Nanotechnology, Spain
Nico A.J.M Sommerdijk, Eindhoven University of Technology, Netherlands
Gleb Yushin, Georgia Institute of Technology, USA

Scientific Program Committee

Valentina Donzella, University of Warwick, United Kingdom
Morteza Eslamian, Shanghai Jiao Tong University, China
Reza Azizian, Massachusetts Institute of Technology, USA
Emin Açikkalp, Bilecik Şeyh Edebali University, Turkey
Davide Barreca, Istituto di Chimica della Materia Condensata e di Tecnologie per l'Energia, Italy
David Aradilla, The French Alternative Energies and Atomic Energy Commission, France
Mingshang Jin, Xi'an Jiaotong University, China
Moonis Ali Khan, King Saud University, Saudi Arabia
Boris Ildusovich Kharissov, Universidad Autónoma de Nuevo León, Mexico
Yasser Mahmoudi Larimi, Queen's University Belfast, United Kingdom
Luis Lugo, Universidade de Vigo, Spain
Kyoung-sik Moon, Georgia Institute of Technology, USA
Sameh A. Nada, Benha University, Egypt
MV Reddy, National University of Singapore (NUS), Singapore
Xu Rong, Nanyang Technological University, Singapore
Ali Shirzadmehr, Islamic Azad University, Iran
Meisam Tabatabaei, Agricultural Biotechnology Research Institute of Iran, Iran
David Maria Tobaldi, University of Aveiro, Portugal
Alan X. Wang, Oregon State University, USA
Chunsheng Wang, University of Maryland, USA
Greg Watson, University of the Sunshine Coast, Australia
Jingwei Xie, University of Nebraska Medical Center, USA
Dimitrios Zeugolis, National University of Ireland, Galway, Ireland

Organizing Committee

Alexandru Vlad, Université catholique de Louvain, Belgium

Ioana Demetrescu, University of Bucharest, Romania

Mingwang Fu, The Hong Kong Polytechnic University, Hong Kong SAR

Rajan Jha, Indian Institute of Technology Bhubaneswar, India

Varaprasad Kokkarachedu, Centro de Investigación de Polímeros Avanzados, Chile

Vincent Ladmiral, Université de Montpellier, France

Amparo López-Rubio, Institute of Agrochemistry and Food Technology, Spain

Zhong Li, Taiyuan University of Technology, China

Sina Sadreddini, Islamic Azad University, Iran

Somchai Wongwises, King Mongkut's University of Technology Thonburi, Thailand

Liyang Zhang, Shanghai Jiao Tong University, China

Zhihua Zhou, Shanghai Jiao Tong University, China

Zuowan Zhou, Southwest Jiaotong University, China

Modeling and Analysis of Bow-Tie Antenna Integrated Resonant-Tunneling-Diode Relaxation Oscillators for Wireless Radio Applications

Hirokazu Yamakura,* Michihiko Suhara*

Department of Electrical and Electronic Engineering, Tokyo Metropolitan University, 1-1, Minami-Osawa, Hachioji, Tokyo, 192-0397 Japan

Corresponding Author. Email: yamakura-hirokazu@ed.tmu.ac.jp, suhara@tmu.ac.jp

Received: 19 May 2017, Accepted: 12 June 2017, Published Online: 15 September 2017

Citation Information: Hirokazu Yamakura, Michihiko Suhara, Nano-Micro Conference, 2017, 1, 01001. doi: 10.11605/cp.nmc2017.01001

Abstract

We propose a self-complementary bow-tie antenna-integrated resonant-tunneling-diode relaxation oscillator and investigate its oscillation/radiation characteristics. In the investigation, we establish a physics-based equivalent circuit model of the oscillator for taking the all physical phenomena related to the diode and the antenna into consideration simultaneously. In this paper, we report the equivalent circuit modeling and the large-signal oscillation/radiation analysis of the oscillator.

Introduction

Terahertz (THz) technology has been received great deal of interest in terms of applications for spectroscopy, imaging, wireless communications, etc. In the wireless communication, the THz range is specifically one of the most attractive regions owing to the existence of the non-allocated frequency band. One of the main challenges of the THz wireless communication is the shortage of the emission RF power of the oscillator. We guess the challenge can be overcome by using the wideband-spectrum relaxation wave, whose entire emission RF power exceeds that of the narrowband sinusoidal wave, as the carrier.

From this perspective, we have proposed an oscillator consisting of a resonant tunneling diode (RTD) and a broadband bow-tie antenna (BTA) [1] for generating a wideband-spectrum relaxation wave and their theoretical models expressed by equivalent circuits respectively [2,3]. Such a semiconductor-based oscillator for THz applications is generally fabricated as a monolithically-integrated configuration of an oscillation device, a radiation antenna, etc. As the performance of such an oscillator depends upon a both of their physics, which usually differ from each other, the performance evaluation method and the design guideline for the oscillator should be established as a physical-coupled scheme considering the all effects regarding the oscillator simultaneously.

In this paper, we focus on a physics-based modeling for the entire oscillator-structure we proposed and its oscillation/radiation performance evaluated by using the physics-based model.

Modeling

Schematics of the proposed oscillator are illustrated in Figure 1.

A peripheral circuit in front serves as a bias circuit and that in back is added for adjusting the total impedance of the peripheral circuits. We establish a physics-based equivalent circuit model of each component, RTD, BTA, and the circuits, since it is considerably impossible to analyze the quantum phenomena of the RTD together with the elec-

tromagnetic (EM) properties of the other components by a single solver.

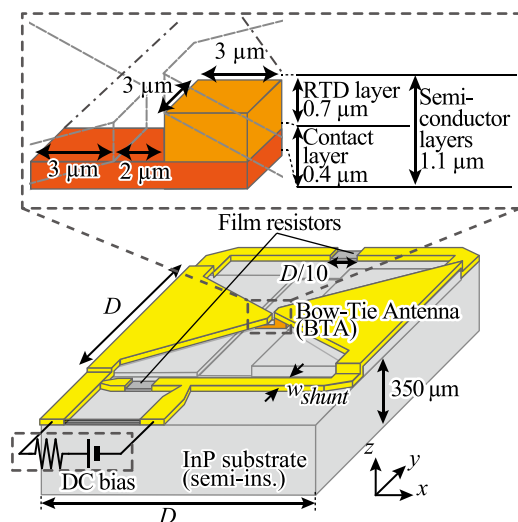


Figure 1 Schematics of a proposed oscillator.

Simple block expressions of the oscillator are described in Figure 2.

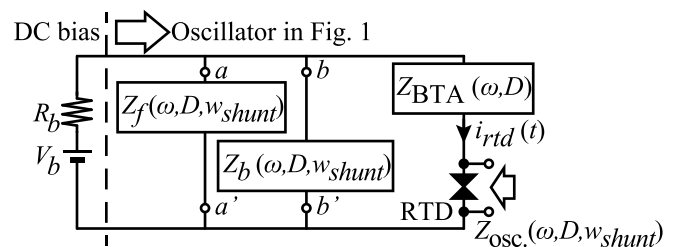


Figure 2 Block expressions of an equivalent circuit for the oscillator shown in Figure 1.

The impedance variables, $Z_f(\omega, D, w_{shunt})$, $Z_b(\omega, D, w_{shunt})$, and $Z_{BTA}(\omega, D)$, correspond to the equivalent circuit of the peripheral circuit in front, that in back, and the BTA, respectively. The RLC expression of $Z_{BTA}(\omega, D)$ has been reported in Ref. [2]. Additionally, the circuit model of the RTD and its theoretical expression has also been reported in Refs. [3, 4], respectively.

The variables, $Z_f(\omega, D, w_{shunt})$ and $Z_b(\omega, D, w_{shunt})$, are com-

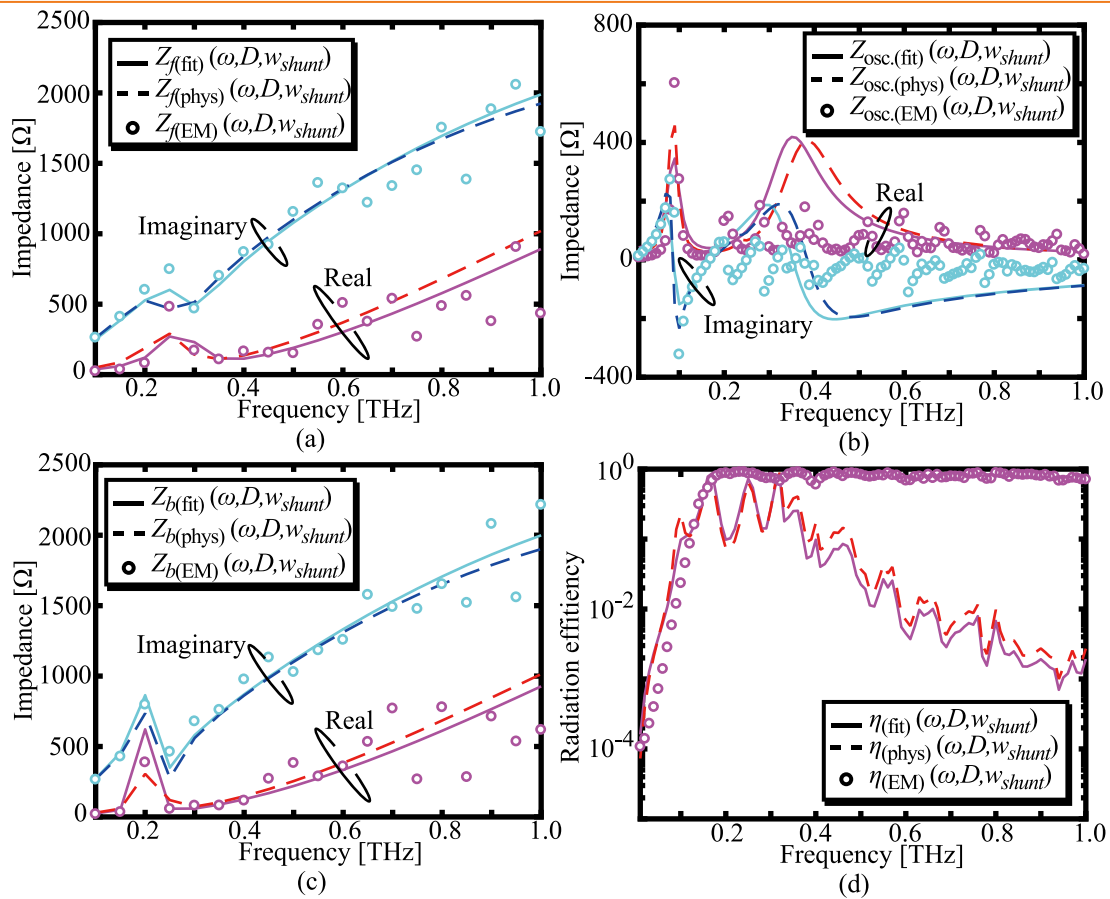


Figure 3 Typical fitting results regarding the impedance characteristics of (a) the peripheral circuit in front, (b) that in back, and (c) the entire oscillator, and (d) the radiation characteristics. Radiation efficiency, $\eta(\omega, D, w_{shunt})$, is defined by the ratio of the oscillation power on the semiconductor layers to the radiation power on the BTA. Solid lines are depicted by using the de-embedded values of the circuit parameters. Dash lines are calculated by the physical/material parameters. The antenna size, D , and the line width, w_{shunt} are set to 300 and 10 μm , respectively.

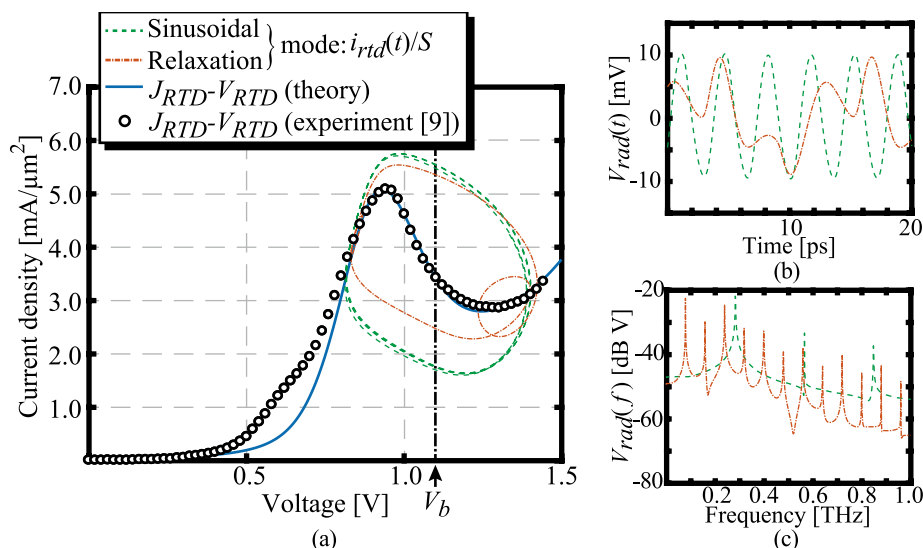


Figure 4 (a) Measured/theoretical current density-voltage (J - V) characteristics of the employed RTD and the calculated results of the time-dependent orbit of the current density, $i_{rt}(t)/S$, in the RTD. (b) Waveforms of the radiation voltage and (c) corresponding frequency spectra. Chain and dotted lines indicate the relaxation and the sinusoidal oscillation mode, where the line width, w_{shunt} is set to 10 and 20 μm , respectively. Antenna size, D , is set to 300 μm .

posed of several RLC elements which can be explained by the electromagnetic properties: the surface impedance due to the skin effect [5], the straight micro stripline [6], fringe capacitance [7], and parasitic components regarding the semi-insulating substrate. The circuit elements involved in $Z_f(\omega, D, w_{shunt})$ and $Z_b(\omega, D, w_{shunt})$ are evaluated by the EM field distribution in the vicinity of the circuits calculated by the finite element method-based simulator, namely, COMSOL.

Their approximate numerical values of the elements are also estimated by the physical interpretation based on the structural and material properties. More precise values are numerically de-embedded by using the optimization method, namely, the particle swarm optimization [8]. More details regarding the circuit identification process have also been reported in Ref. [2].

Figure 3 summarizes the typical fitting results of the im-

pedance and radiation characteristics regarding the peripheral circuit/entire oscillator.

From Figure 3, the equivalent circuit expression is quantitatively valid for the evaluation of the radiation/oscillation characteristics by the circuit analysis around the first resonance frequency of the oscillator.

Oscillation Analysis

The non-linear oscillation analysis of the proposed oscillator is performed by using the equivalent circuit above mentioned. The non-linearity of the RTD is involved by

considering the measured current-voltage (I-V) characteristics [9]. The supplied voltage, V_b , is set to a constant value to keep the negative differential conductance of the RTD maximum. More details regarding the oscillation analysis methodology have been reported in Refs. [10, 11].

Figure 4 displays the current density-voltage (J-V) characteristics of the RTD and the time-dependent orbit of the current density, $i_{\text{rt}}(t)/S$, in the RTD, where S indicates the mesa area.

We classify the oscillation modes depicted the dotted and chain lines in Figure 4 designated as the "sinusoidal" and the "relaxation" mode, respectively. The modes are quantitatively distinguished by the cycle number of the $i_{\text{rt}}(t)/S$ trajectory in Figure 4; if the cycle number is unity, the mode is a "sinusoidal mode"; else, it is a "relaxation mode". The entire emission RF power of the relaxation mode shown in Figure 4 is ~ 6 dBm greater than that of the sinusoidal mode when the upper limit value of band is approximately set to 400 GHz. It is suggested that the relaxation wave can compensate for the shortage of the emission RF power if we employ a certain band appropriately. Moreover, it is found that the oscillation mode can be designed by adjusting the two parameters, D and w_{shunt} , appropriately.

According to Shannon-Hartley theorem [12], the capacity of a wireless channel is directly proportional to the channel bandwidth. Therefore, the wideband-spectrum relaxation wave can contribute to the possibility of large-capacity wireless transmissions together with compensating for the RF power shortage.

Conclusion

We investigated radiation/oscillation characteristics of the resonant tunneling diode-based relaxation oscillator by using its physics-based equivalent circuit model. The advantage of a wideband-spectrum relaxation wave as the carrier was revealed in terms of the entire emission RF power. Our further studies will represent the link-budget analysis of the relaxation carrier wave-based THz wireless link to clarify the advantage of the relaxation carrier regarding the link performance.

References

- [1] H. Yamakura, Y. Ishiguro, Y. Kato, M. Suhara. 41-th International Conference of Infrared, Millimeter, and THz waves. M5P.12.24, Sept., 2016. doi: [10.1109/IRMMW-THz.2016.7758647](https://doi.org/10.1109/IRMMW-THz.2016.7758647)
- [2] H. Yamakura, M. Suhara. IEICE Transactions on Electronics. 2016, E99-C(12), 1312-1322. doi: [10.1587/transele.E99.C.1312](https://doi.org/10.1587/transele.E99.C.1312)
- [3] K. Asakawa, M. Naoi, Y. Iki, M. Shinada, M. Suhara. Physica Status Solidi (C). 2010, 7(10), 2555-2558. doi: [10.1002/pssc.200983885](https://doi.org/10.1002/pssc.200983885)
- [4] H. Shin-ya, M. Suhara, N. Asaoka, M. Naoi. IEICE Transactions on Electronics. 2010, E93-C(8), 1295-1301. doi: [10.1587/transele.E93.C.1295](https://doi.org/10.1587/transele.E93.C.1295)
- [5] J. J. Sanz-Fernandez, R. Cheung, G. Goussetis, C. Mateo-Segura.

IEEE Transactions on Antennas and Propagation. 2011, 59(6), 2205-2216. doi: [10.1109/TAP.2011.2143654](https://doi.org/10.1109/TAP.2011.2143654)

[6] I. Bahl, P. Bhartia. Microwave solid state circuit design, 2nd edition, pp.59, Wiley, 2003.

[7] S.H. Kim, J.G. Fossum, J.W. Yang. IEEE Transactions on Electron Devices. 2006, 53(9), 2143-2150. doi: [10.1109/TED.2006.880369](https://doi.org/10.1109/TED.2006.880369)

[8] J. Kennedy and R. Eberhart. Proceedings of IEEE International Conference on Neural Networks. 1995, 4, 1942-1948. doi: [10.1109/ICNN.1995.488968](https://doi.org/10.1109/ICNN.1995.488968)

[9] M. Reddy, S. C. Martin, A. C. Molnar, R. E. Muller, R. P. Smith, P. H. Siegel, M. J. Mondry, M. J. W. Rodwell, H. Kroemer, S. J. Allen. IEEE Electron Device Letters. 1997, 18(5), 218-221. doi: [10.1109/55.568771](https://doi.org/10.1109/55.568771)

[10] K. Asakawa, Y. Itagaki, H. Shin-ya, M. Saito, M. Suhara. IEICE Transactions on Electronics. 2012, E95-C(8), 1376-1384. doi: [10.1587/transele.E95.C.1376](https://doi.org/10.1587/transele.E95.C.1376)

[11] N. Okumura, K. Asakawa, M. Suhara. IEICE Transactions on Electronics. 2017, E100-C(5), 430-438. doi: [10.1587/transele.E100.C.430](https://doi.org/10.1587/transele.E100.C.430)

[12] C. E. Shannon. Tee Bell System Technical Journal. 1948, 27(3), 379-423. doi: [10.1002/j.1538-7305.1948.tb01338.x](https://doi.org/10.1002/j.1538-7305.1948.tb01338.x)

Open Access

This article is licensed under a [Creative Commons Attribution 4.0 International License](https://creativecommons.org/licenses/by/4.0/).

© The Author(s) 2017

Transient Device Simulation Using Deterministic Boltzmann Equations Solvers

Sung-Min Hong*

Gwangju Institute of Science and Technology, 123 Cheomdan-gwagiro (Oryong-dong), Buk-gu, Gwangju 61005, Republic of Korea

Corresponding Author. Email: smhong@gist.ac.kr

Received: 01 June 2017, Accepted: 20 June 2017, Published Online: 15 September 2017

Citation Information: Sung-Min Hong, Nano-Micro Conference, 2017, 1, 01002. doi: 10.11605/cp.nmc2017.01002

Abstract

The transient simulation of semiconductor devices using a deterministic Boltzmann equations solver is presented. In order to avoid the numerical difficulties originated from the conventional H-transformation, the kinetic-energy-based scheme is adopted. Within the kinetic-energy-based scheme, the transport parameters become time-independent, therefore, implementing the transient simulation capability can be done easily. Preliminary results for a device are shown.

Introduction

The terahertz (THz) technology has gained much research interest worldwide. However, realization of a THz emitter with a small form factor is still a difficult task. The plasma instability in the two-dimensional (2D) electron gas has been proposed as a possible mechanism to enable an extremely fast semiconductor device operating in the THz frequency range [1].

Recently, we have reported the numerical simulation results of plasma oscillation in two-dimensional electron gas [2]. A periodic steady-state solver has been used to obtain the oscillating solution efficiently. The set of governing equations contains the 2D Poisson equation, the electron continuity equation, and the electron current density equation. The time derivative of the current density and the convective derivative are considered in the electron current density equation. It has been numerically verified that inclusion of those terms are mandatory to support sufficiently strong plasma instability in the 2D electron gas.

However, it is noted that the set of governing equations adopted in [2] is based on the moments of the Boltzmann equation. It is not sufficiently accurate to describe the behavior

of plasma waves quantitatively [3]. A more advanced modelling approach is required. In order to solve this issue ultimately, the Boltzmann equation solver with the transient simulation capability is mandatory.

Although the stochastic Boltzmann equation solvers (the Monte Carlo simulators) have been used to simulate a device operating in the THz frequency range (for example, [4]), the stochastic nature of the Monte Carlo simulators introduces some numerical difficulties. Therefore, the deterministic Boltzmann equation solver is desirable. In this work, our motivation is to present some transient simulation results using a deterministic Boltzmann equation solver.

Projected Boltzmann Equation

The Boltzmann equation is a microscopic transport equation. It governs the spatiotemporal motion of the electron gas in a semiconductor device. Since it is defined on the phase space, evaluating its solution is a highly non-trivial task.

As discussed above, the stochastic Monte Carlo method can be applied to solve the Boltzmann equation efficiently. However, nowadays, the deterministic Boltzmann equation solvers [5] have gained popularity. In these solvers, the angle-dependent part of the electron distribution function is expanded

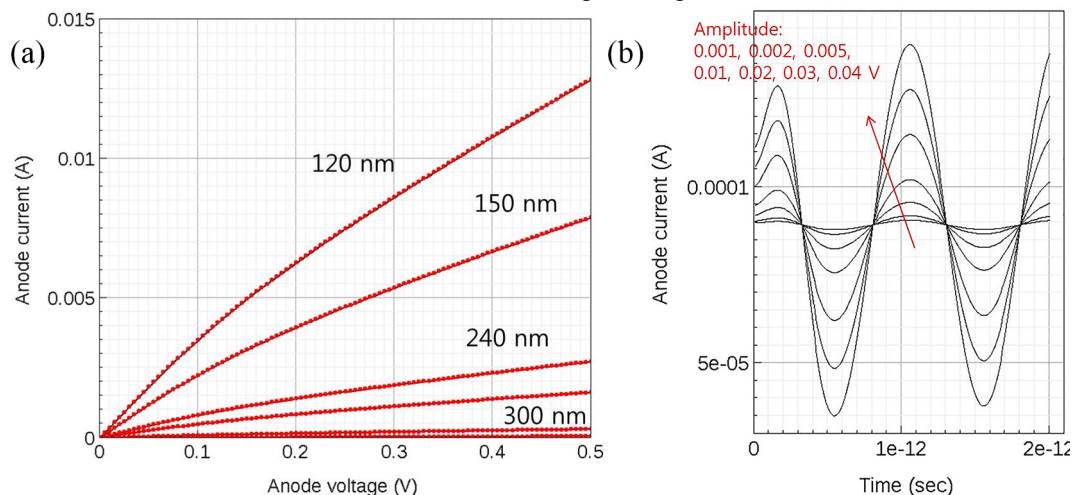


Figure 1 (a) DC IV characteristics of various N^+NN^+ devices, which are obtained from the deterministic Boltzmann equation solver. (b) Transient results of an N^+NN^+ device whose total length is 1200 nm. The DC bias voltage is 0.8 V. AC voltages of 1 THz with various amplitudes are applied to the anode terminal. The first two periods are simulated.

with basis functions. Depending on the dimensionality of the momentum space, there can be a few variants of deterministic Boltzmann equation solvers. In this work, the three-dimensional momentum space is understood. Therefore, the spherical harmonic expansion [6] is the appropriate technique. A numerical stabilization scheme called the H-transformation [6] has played an important role in the development of this simulation technique. In the H-transformation, the total energy (which is a sum of the kinetic energy and the potential energy) instead of the kinetic energy is used as the energy variable.

Unfortunately, when the transient simulation is concerned, the H-transformation introduces a serious difficulty [7]. The time-varying potential energy yields the time-varying transport parameters. Unavoidable interpolation procedure prevents the transient simulation capability eventually. Of course, the fundamental solution to the above problem is to invent yet another numerical stabilization scheme, which does not suffer from the time-varying transport parameters. Since it is currently a formidable task, in this work, we simply apply the kinetic-energy-based scheme [8] to get the preliminary solutions.

Numerical Results

A spherical harmonics expansion solver has been newly implemented into our in-house device simulation framework [2]. All parameters for Si are taken from [6]. The lowest expansion order is used. Various N^+NN^+ devices are simulated. Figure 1(a) shows the DC IV characteristics of those devices. The transient simulation results of the 1200-nm-long device are shown in Figure 1(b). The DC bias voltage is 0.8 V. The frequency of the AC voltage is 1 THz. It is clearly demonstrated that our deterministic Boltzmann equation solver can perform the transient simulation at such a high frequency without any numerical problem.

Conclusion

In this work, the transient device simulation results using a deterministic Boltzmann equation solver based on the spherical harmonics expansion has been presented. In order to avoid the numerical difficulties originated from the H-transformation, the kinetic-energy-based scheme is adopted. The numerical results demonstrate that both of DC and AC analyses can be performed without any numerical problem. It is expected that this simulator can be applied to the THz devices based on the plasma instability.

Acknowledgements

This work was supported by Samsung Research Funding Center of Samsung Electronics under Project Number SRFC-IT1401-08.

References

- [1] Taiichi Otsuji, Takayuki Watanabe, Stephane A. Boubanga Tombet, Akira Satou, Wojciech M. Knap, Vyacheslav V. Popov, Maxim Ryzhii, Victor Ryzhii. *IEEE Transactions on Terahertz Science and Technology*, 2013, 3(1), 63-7. doi: [10.1109/TTHZ.2012.2235911](https://doi.org/10.1109/TTHZ.2012.2235911)
- [2] Sung-Min Hong, Jae-Hyung Jang. *IEEE Transactions on Electron Devices*. 2015, 62(12), 4192-4198. doi: [10.1109/TED.2015.2489220](https://doi.org/10.1109/TED.2015.2489220)
- [3] Zeinab Kargar, Tobias Linn, Dino Ruić, Christoph Jungemann. *IEEE Transactions on Electron Devices*. 2016, 63(11), 4402-4408. doi: [10.1109/TED.2016.2608422](https://doi.org/10.1109/TED.2016.2608422)
- [4] Javier Mateos, Toms Gonzalez. *IEEE Transactions on Terahertz Science and Technology*. 2012, 2(5), 562-569. doi: [10.1109/TTHZ.2012.2209970](https://doi.org/10.1109/TTHZ.2012.2209970)
- [5] Sung-Min Hong, Anh-Tuan Pham, Christoph Jungemann. *Deterministic Solvers for the Boltzmann Transport Equation*, ISBN 978-3-

7091-0777-5, Springer Verlag Wien/New York, 2011.

[6] A. Gnudi, D. Ventura, G. Baccarani, F. Odeh. *Solid-State Electronics*, 1993, 36, (4), 575-581. doi: [10.1016/0038-1101\(93\)90269-V](https://doi.org/10.1016/0038-1101(93)90269-V)

[7] K. Rupp, C. Jungemann, S.-M. Hong, M. Bina, T. Grasser, A. Jünger. *Journal of Computational Electronics*. 2016, 15(3), 939-958. doi: [10.1007/s10825-016-0828-z](https://doi.org/10.1007/s10825-016-0828-z)

[8] C. Jungemann, A. T. Pham, B. Meinerzhagen, C. Ringhofer, M. Bollhöfer. *Journal of Applied Physics*, 2006, 100, 024502. doi: [10.1063/1.2212207](https://doi.org/10.1063/1.2212207)

Open Access

This article is licensed under a [Creative Commons Attribution 4.0 International License](https://creativecommons.org/licenses/by/4.0/).

© The Author(s) 2017

Enhanced Catalysis by Optical Nanoantenna Reduced on Transition Metal Dichalcogenide

Donald Keith Roper,^{1,2*} Jeremy Dunklin,² Alexander O'Brien²

¹Microelectronics Photonics Graduate Program

²Ralph E Martin Department of Chemical Engineering (University of Arkansas) NANO 206, 731 W. Dickson St. Fayetteville, AR 72701

Corresponding Author. Email: dkroper@uark.edu

Received: 03 June 2017, Accepted: 15 June 2017, Published Online: 01 October 2017

Citation Information: Donald Keith Roper, Jeremy Dunklin, Alexander O'Brien. *Nano-Micro Conference*, 2017, 1, 01003. doi: 10.11605/cp.nmc2017.01003

Abstract

Photocatalysis of hydrogen from water is limited by incomplete absorption of solar radiation and by uncontrolled disposition of generated carriers. Nanoantenna (NA)-induced coupling of photons to excitons could enhance photocatalytic solar fuel generation by increasing broadband optical absorption and by injecting energetic electrons where NA interfaces with semiconductor catalyst. This work examined catalysis of hydrogen evolution reaction (HER) by monolayer (1L) transition metal dichalcogenide (TMD) with and without decoration by optical NA. Spectroscopic and microscopic characterization of heterostructures of 1L-TMD and NA self-assembled via exfoliation and redox chemistry was compared with discrete dipole simulation. Electrodes inked with 1L tungsten disulfide (WS₂) onto which NA was electrochemically reduced exhibited higher HER relative to 1L-WS₂ in neat or physically NA-decorated forms as measured by linear sweep and cyclic voltammetry. Coordinated simulation and measurement of supports improved design of 1L-TMD-NA photocatalysts and their implementation in chemical, biological, energy and water systems.

Introduction

Two-dimensional (2D) transition metal dichalcogenide (TMD) semiconductor crystals offer optoelectronic inducibility with superior electron mobility and gate tunability. This enables enhanced photocatalytic activity of interest for chemical and biological catalysis, energy, sensing, desalination, and nanoelectromechanical systems. Heterostructures of monolayer (1L) TMD crystals decorated with optical nanoantenna (NA) could improve their catalytic efficiency. However, measured catalytic efficiency of such heterostructures relative to undecorated 1L-TMD is rare and characterization of opto-electronic effects at 1L-TMD-NA heterointerfaces is largely empirical. Integration of microscopic and spectroscopic analysis with simulation of 1L-TMD-NA has been limited by computational expense and complexity, particularly for dynamic interactions at nanometer (nm) scales. Compact, multi-scale, integrated analysis of optical, electronic and catalytic effects could identify extraordinary features to guide design and implementation.

Results and Discussion

Electrochemical measurements were carried out in a three-electrode cell with a 3-mm diameter glassy carbon (GC) working electrode, a graphite rod counter electrode, and an Ag/AgCl reference electrode (Pine Research Instrumentation, Durham, NC). The cell was filled with 8 milliliters (mL) of concentrated sulfuric acid, 0.5M H₂SO₄. The reference electrode was kept in a salt bridge of 3M sodium chloride (NaCl). A microliter of aqueous ethanol ink containing 6 micrograms (μg) liquid phase exfoliated (LPE) tungsten disulfide (WS₂) powder (Sigma-Aldrich, St. Louis, MO), 3 μg Ketjen black

(EC-600JD, AkzoNobel, Chicago, IL) and 1.5 μg Nafion ionomer (Sigma-Aldrich, St. Louis, MO) was drop cast onto a glassy carbon (GC) electrode. After allowing the ink to set for 10 minutes, the three-electrode system was placed in the cell. The cell and electrodes were contained in an unlit fume hood. Electrodes were connected to a WaveNow potentiostat (Pine Research Instrumentation, Durham, NC). Linear sweep voltammetry (LSV) was performed by measuring current as potential was varied at a rate of 5 mV/s over a range of -0 to -800 mV versus the Ag/AgCl reference electrode, i.e., reversible hydrogen electrode (RHE). Bubbles forming at the electrode tip indicated hydrogen evolution. LSV was performed in triplicate. To provide background measurement, voltammetry was run with the polished working electrode prior to adding catalyst. Cyclic voltammetry (CV) performed for twenty cycles to measure persistence of catalytic activity over time.

Values of peak current density measured by LSV and CV for catalysis by LPE 1LWS₂ on a GC electrode ranged from -70 to -100 mA/cm² at -0.5 eV vs. RHE. Figure 1 shows representative CV and controls. Adjusting the position of the electrode to facilitate buoyant removal of hydrogen bubbles improved the peak current density across this range. The onset potential was approximately 250 mV without buoyant removal of hydrogen and about -300 mV after electrode adjustment. This range of measured peak current densities was greater than values previously reported for comparable measures of hydrogen evolution from WS₂. From a similar experimental setup, a current density of -25 mA/cm² at approximately -0.45V vs SCE [1] or about -0.21V vs RHE was reported. That system consisted of three-electrodes; 25 μg of WS₂ nanoflake catalyst was drop cast onto the GC electrode. Ketjen black was added to increase the conductivity of the solution. Other

similar experiments reported current densities of -20 mA/cm^2 at -0.5 V vs RHE and -2.2 mA/cm^2 at -0.2 V vs RHE, respectively [2,3]. Scarce reports of WS_2 catalysis in GC systems suggests comparison with molybdenum disulfide (MoS_2) in which disulfide edge sites similarly catalyze hydrogen evolution reaction (HER). One such study reported a current density of -13 mA/cm^2 at -0.2 V vs RHE [4]. Without the edge site enhancement, another study reported results for MoS_2 of ca. -5 mA/cm^2 at -0.5 V vs RHE [2].

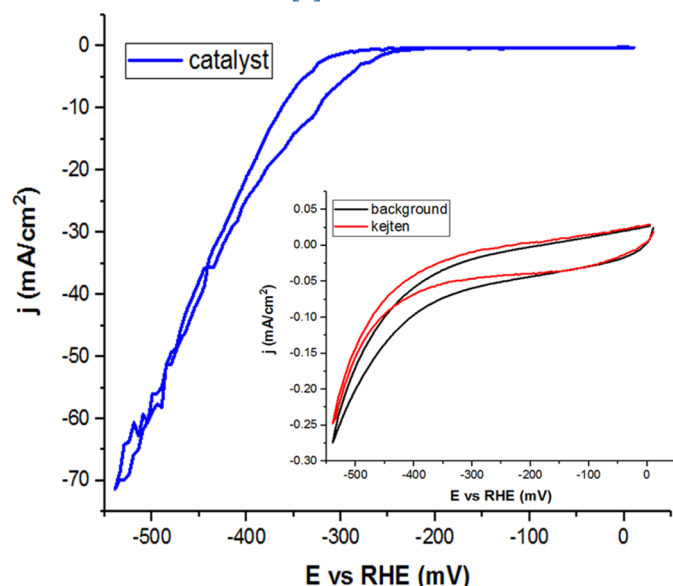


Figure 1. Catalytic activity of WS_2 measured by cyclic voltammetry (CV; blue). Inset: CV of bare electrode (black) and Nafion/Ketjen matrix (red).

Use of TMDs as photocatalysts has been constrained by difficulty tuning the intrinsic optoelectronic excitation and damping mechanisms. Optical absorption in monolayer tungsten disulfide (WS_2), for example, is limited to $>2 \text{ eV}$ ($<620 \text{ nm}$). This keeps broadband UV-vis absorption below ca. 2%. Moreover, the photoluminescence (PL) response of WS_2 is layer-number dependent [5]. Decoration of 1L-TMD by plasmonic metal nanoparticle (NP) has enabled broadband tunability of resultant photon-exciton interactions in catalytic hydrogen generation [6,7]. The enhanced photon-exciton interactions have been attributed to hot electron transfer (HET) from plasmonic NA to TMD substrate. HET, which occurs at interfaces between non-insulating media, e.g., TMD and NA, increases plasmon damping beyond radiative and nonradiative mechanisms [8]. Such damping has been reported to transfer plasmon energy to adjacent 1L semiconducting TMDs [9,10]. Moreover, NP decoration of WS_2 was reported to enhance PL 11-fold via exciton coupling with plasmonic electric near fields [11]. However, plasmonic HET had only been evaluated across interfaces of AuNP physically deposited on TMD; and characterization of HET from NA to WS_2 has been empirical, lacking a computational framework.

To examine effect of NA on WS_2 catalytic hydrogen evolution, Au was reduced onto edge sites of liquid phase exfoliated (LPE) 2H- WS_2 from an aqueous Au(III) solution based on a previously reported method [12,13]. Thiols dangling at WS_2 nanosheet edges underwent a redox reaction with AuCl_3 to yield a covalent Au-S bond as confirmed by transmission electron microscopy (TEM; Figure 2) and X-ray photoelectron spectroscopy (XPS) [14]. In contrast, covalent bond formation was not observed when AuCl_3 was reacted with chemical ex-

foliated 1T- WS_2 . Oxidation of thiols to disulfides at edges of LPE-2H- WS_2 coincident with reduction of Au (III) to Au(0) was anticipated to increase catalytic HER in Au-decorated 2H- WS_2 [15,16]. Using LSV, AuNP-decorated 1L2H- WS_2 catalyst exhibited a 5-fold enhancement relative to undecorated monolayer and >10 -fold increase relative to other reported TMD-based electrodes when exchange current density was normalized by film thickness [14]. For the comparison, equivalent mass of WS_2 per unit area electrode was used and mean flake length was maintained at $\langle L \rangle = 67 \text{ nm}$. All films exhibited 100 mV/decade slopes, consistent with reported nanolayered TMD HER electrocatalysts.

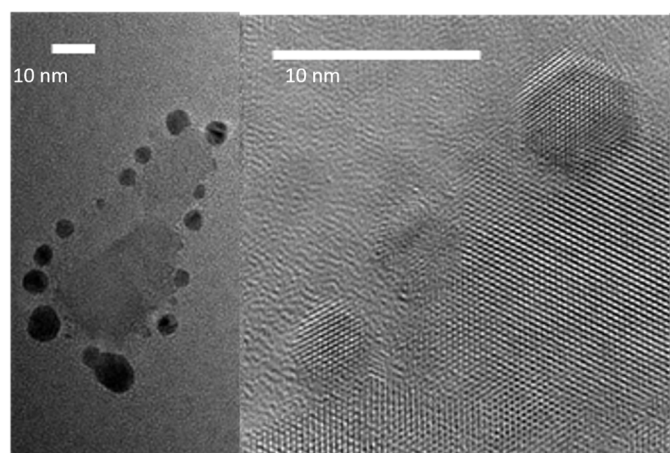


Figure 2. Transmission electron microscopy (TEM) of 1LTMD flake decorated with nanoantenna (NA).

To quantitate HET from plasmonic NA to catalytic WS_2 , discrete dipole approximation (DDA) of Maxwell's equations using DDSCAT v7.3 [17] was conducted based on a previously reported method for 1L graphene [18] and MoS_2 [19]. Computed far field spectra of 1L- WS_2 -NA heterostructures exhibited localized surface plasmon resonance (LSPR) and WS_2 excitonic transitions [20]. Decoration of 1L WS_2 by AuNA enhanced broadband extinction, particularly at the 620 nm A exciton red-shifted from the LSPR. Tuning the LSPR to specific excitonic transitions is anticipated to increase enhancement [21]. Edge decoration increased optical extinction efficiency relative to basal plane deposition. An $11 \pm 5\%$ quantum efficiency of HET from ca. 20 nm AuNPs reduced on WS_2 nanosheets was estimated by comparing electron energy loss spectroscopy (EELS) measured and DDA simulation [22].

Conclusion

In summary, reduction of plasmonic NA onto 1L-2H- WS_2 edges formed covalent Au-sulfur bonds. Such 1L- WS_2 -NA heterostructures increased catalytic HER relative to 1L-2H- WS_2 in physically decorated-NA or undecorated forms and enhanced plasmon damping attributable to direct electron transfer at the catalytic TMD-NA heterointerface. Application of this redox chemistry and integration of microscopic and spectroscopic measures and simulation enable improved photocatalysis using 1L-TMD-NA and implementation in a variety of chemical, biological, energy and water systems.

Acknowledgments

The authors acknowledge support from the National Science Foundation (NSF) Graduate Research Fellowship (awarded to J.R.D); The University of Arkansas Foundation; Walton Charitable Foundation; and Charles W. Oxford Professorship of

Emerging Technologies. The authors thank Prashant Acharya and Lauren Greenlee for guidance and technical assistance.

References

- [1] Cheng, L.; Huang, W.; Gong, Q.; Liu, C.; Liu, Z.; Li, Y.; Dai, H. Ultrathin WS₂ Nanoflakes as a High-Performance Electrocatalyst for the Hydrogen Evolution Reaction. *Angewandte Chemie International Edition*. **53**, 7860–7863 (2014). doi:10.1002/anie.201402315
- [2] Zahra Gholamvand; David McAteer; Claudia Backes; Niall McEvoy; Andrew Harvey; Nina C. Berner; Damien Hanlon; Conor Bradley; Ian Godwin; Aurlie Rovetta; Michael E. G. Lyons; Georg S. Duesbergac; Jonathan N. Coleman, Comparison of liquid exfoliated transition metal dichalcogenides reveals MoSe₂ to be the most effective hydrogen evolution catalyst. *Nanoscale* **8**, 5737–5749 (2016). doi:10.1039/C5NR08553E
- [3] Chen, T.-Y.; Chang, Y.-H.; Hsu, C.-L.; Wei, K.-H.; Chiang, C.-Y.; Li, L.-J., Comparative study on MoS₂ and WS₂ for electrocatalytic water splitting. *International Journal of Hydrogen Energy*. **38**, 12302–12309 (2013). doi:10.1016/j.ijhydene.2013.07.021
- [4] Junfeng Xie; Hao Zhang; Shuang Li; Ruoxing Wang; Xu Sun; Min Zhou; Jingfang Zhou; Xiong Wen (David) Lou; Yi Xie, Defect-Rich MoS₂ Ultrathin Nanosheets with Additional Active Edge Sites for Enhanced Electrocatalytic Hydrogen Evolution. *Advanced Materials*. **25**, 5807–5813 (2013). doi:10.1002/adma.201302685
- [5] Qing Hua Wang; Kourosh Kalantar-Zadeh; Andras Kis; Jonathan N. Coleman; Michael S. Strano, Electronics and optoelectronics of two-dimensional transition metal dichalcogenides. *Nature Nanotechnology*. **7**, 699–712 (2012). doi:10.1038/nnano.2012.193
- [6] Yin, Z.; Chen, B.; Bosman, M.; Cao, X.; Chen, J.; Zheng, B.; Zhang, H., Au nanoparticle-modified MoS₂ nanosheet-based photoelectrochemical cells for water splitting. *Small*. **10**, 3537–3543 (2014). doi:10.1002/sml.201400124
- [7] Yimin Kang; Yongji Gong; Zhijian Hu; Ziwei Li; Ziwei Qiu; Xing Zhu; Pulickel M. Ajayan; Zheyu Fang, Plasmonic hot electron enhanced MoS₂ photocatalysis in hydrogen evolution. *Nanoscale* **7**, 4482–4488 (2015). doi:10.1039/C4NR07303G
- [8] Manjavacas, A.; Liu, J. G.; Kulkarni V.; Nordlander, P., Plasmon-induced hot carriers in metallic nanoparticles. *ACS Nano*. **8**, 7630–7638 (2014). doi:10.1021/nn502445f
- [9] S. B. Lu; L. L. Miao; Z. N. Guo; X. Qi; C. J. Zhao; H. Zhang; S. C. Wen; D. Y. Tang; D. Y. Fan, Broadband nonlinear optical response in multi-layer black phosphorus: an emerging infrared and mid-infrared optical material. *Optics Express*. **23**, 11183–11194 (2015). doi:10.1364/OE.23.011183
- [10] Huang, X.; Tan, C.; Yin, Z.; Zhang, H., Hybrid nanostructures based on two-dimensional nanomaterials. *Advanced Materials*. **26**, 2185–2204 (2014). doi:10.1002/adma.201304964
- [11] Johannes Kern; Andreas Trügler; Iris Niehues; Johannes Ewering; Robert Schmidt; Robert Schneider; Sina Najmaei; Antony George; Jing Zhang; Jun Lou; Ulrich Hohenester; Steffen Michaelis de Vasconcellos; Rudolf Bratschitsch, Nanoantenna-Enhanced Light-Matter Interaction in Atomically Thin WS₂. *ACS Photonics* **2**, 1260–1265 (2015). doi:10.1021/acsphotonics.5b00123
- [12] Jang, G.-G.; Roper, D. K., Balancing redox activity allowing spectrophotometric detection of Au(I) using tetramethylbenzidine dihydrochloride. *Analytical Chemistry*. **83**, (2011). doi:10.1021/ac102668q
- [13] Berry K. R.; Russell A. G.; Blake P. T.; Roper, D. K., Gold nanoparticles reduced in situ and dispersed in polymer thin films: optical and thermal properties. *Nanotechnology*. **23**, 11 (2012). doi:10.1088/0957-4484/23/37/375703
- [14] Dunklin, J. R.; et al., Exploiting the redox edge chemistry of liquid-exfoliated 2H-WS₂ to yield highly monolayer-rich gold decorated nanosheets in dispersion. Submitted.
- [15] Mendoza-Sánchez B.; Gogotsi Y., Synthesis of Two-Dimensional Materials for Capacitive Energy Storage. *Advanced Materials*. **28**, 6104–6135 (2016). doi:10.1002/adma.201506133
- [16] Martin Pumera; Zdeněk Soferb; Adriano Ambrosia, Layered transition metal dichalcogenides for electrochemical energy genera-

tion and storage. *Journal of Materials Chemistry A*. **2**, 8981 (2014). doi:10.1039/c4ta00652f

- [17] Bruce T. Draine; Piotr J. Flatau, Discrete-dipole approximation for scattering calculations. *Journal of the Optical Society of America A*. **11**, 1491–1499 (1994). doi:10.1364/JOSAA.11.001491
- [18] Drew DeJarnette; D. Keith Roper, Electron energy loss spectroscopy of gold nanoparticles on graphene. *Journal of Applied Physics* **116**, 054313 (2014). doi:10.1063/1.4892620
- [19] Forcherio, G. T.; Benamara, M.; Roper D. K.; Electron energy loss spectroscopy of hot electron transport between gold nanoantennas and molybdenum disulfide by plasmon excitation. *Advanced Optical Materials*. **5**(3), 1600572 (2017). doi:10.1002/adom.201600572
- [20] Dunklin, J. R., Plasmon-enhanced interfacial energy transfer in nanocomposite media (Ph.D. Thesis). University of Arkansas. (2017)
- [21] Forcherio, G. T.; Roper, D. K., Spectral Characteristics of Noble Metal Nanoparticle-Molybdenum Disulfide Heterostructures. *Advanced Optical Materials*. **4**(8), 1288–1294 (2016). doi:10.1002/adom.201600219
- [22] Forcherio, G. T.; Dunklin, J. R.; Backes, C.; Vaynzof, Y.; Benamara, M.; Roper, D. K., Gold nanoparticles physicochemically bonded onto tungsten disulfide nanosheet edges exhibit augmented plasmon damping, *AIP Advances*. **7**, 075103 (2017). doi:10.1063/1.4989774

Open Access

This article is licensed under a [Creative Commons Attribution 4.0 International License](https://creativecommons.org/licenses/by/4.0/).

© The Author(s) 2017

Generation and Detection of Terahertz Radiation from Laser-Plasmas

Xiao-Yu Peng,* Hai-Wei Du

Chongqing Institute of Green and Intelligent Technology, Chinese Academy of Sciences
 No. 266 Fangzheng Avenue, Beibei District, Chongqing, China

Corresponding Author. Email: xypeng@cigit.ac.cn

Received: 25 May 2017, Accepted: 15 June 2017, Published Online: 02 October 2017

Citation Information: Xiao-Yu Peng, Hai-Wei Du. Nano-Micro Conference, 2017, 1, 01004. doi: 10.11605/cp.nmc2017.01004

Abstract

Broadband terahertz (THz) radiation from laser-plasma interaction and a corresponding broadband THz time domain spectroscopy based on optically-air-biased-coherent-detection technique are presented. One of the single-shot detection techniques for THz time domain spectroscopy, the spectral-encoding technique, is also reviewed [1]. Distortions of the signals measured by this technique and the corresponding strategies to reduce them are demonstrated [2].

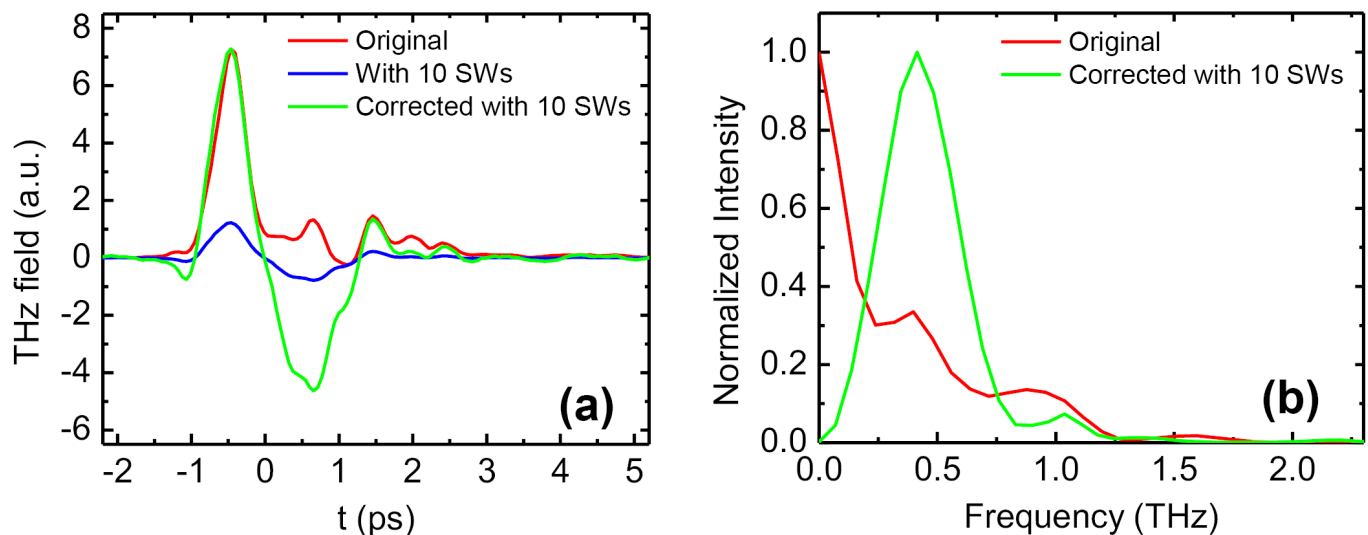


Figure 1. (a) Attenuated and corrected THz waveforms using 10 Si wafers as attenuators vs. the original strong THz signal. (b) THz spectrum of the corrected THz signal with 10 Si wafers vs. that of the original one.

References

- [1] X.-Y. Peng; J.-H. Teng; X.-H. Zhang; Y.-L. Foo, Distortion analysis of pulsed terahertz signal measured with spectral-encoding technique. *Journal of Applied Physics* 108, 093112 (2010); doi:10.1063/1.3499639
- [2] X.-Y. Peng; J. Teng; H. Liu; H. Tanoto; H. Guo; Z.-M. Sheng; J. Zhang, Distortion reduction in strong terahertz signals using broadband attenuators with flat transmittance. *Journal of Physics D: Applied Physics*, 49, 015501 (2016). doi: 10.1088/0022-3727/49/1/015501

Open Access

This article is licensed under a [Creative Commons Attribution 4.0 International License](https://creativecommons.org/licenses/by/4.0/).

© The Author(s) 2017

Photonic crystal cavity optomechanics for the applications of low phase noise frequency source and high-performance sensing

Yongjun Huang,^{1*} Guangjun Wen,¹ Chee Wei Wong²

¹School of Communication and Information Engineering, University of Electronic Science and Technology of China, Chengdu, 611731, China

²Fang Lu Mesoscopic Optics and Quantum Electronics Laboratory, University of California at Los Angeles, Los Angeles, CA 90095, USA

Corresponding Author. Email: yongjunh@uestc.edu.cn

Received: 31 May 2017, Accepted: 16 June 2017, Published Online: 03 October 2017

Citation Information: Yongjun Huang, Guangjun Wen. Nano-Micro Conference, 2017, 1, 01005. doi: 10.11605/cp.nmc2017.01005

Abstract

Based on the air-slot line-defected photonic crystal nano-cavity [1], here we develop a monolithic integration of photonic crystal optomechanical oscillators and on-chip high speed Ge detectors (see Figure 1) by using the silicon CMOS platform. With the generations of both high harmonics (up to 59th order) and subharmonics (down to 1/4), due to strong mutual couplings between optomechanical self-sustained oscillation and self-pulsation oscillation, our chipset provides multiple low phase noise frequency tones [2] for applications in both frequency multipliers and dividers. The synchronization between two mechanical modes [3] and dynamical chaos [4] in the optomechanical cavity are reported as well. These characteristics enable optomechanical oscillators as a frequency reference platform for radio-frequency-photonic information processing.

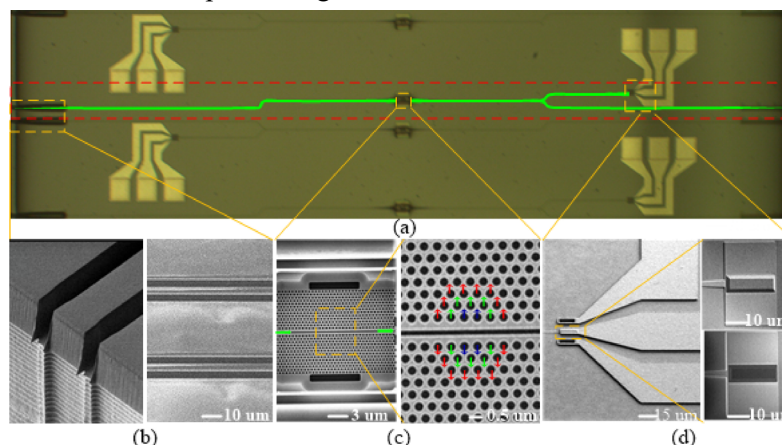


Figure 1. Fabricated optomechanical cavity integrated with on-chip Ge-detector

Moreover, we further demonstrate a chip-scale optomechanical cavity with large mass (see Figure 2) which operates at ~ 77.7 kHz fundamentally and exhibits large optomechanical coupling of 44+ GHz/nm. The mechanical shifting range of ~ 58 kHz and more than 100-order harmonics are obtained with which the free-running frequency instability is lower than 10^{-6} at 0.1 sec integration time [5]. The optomechanical coupling strength can be mechanically controlled by taper fiber and the Drude self-pulsation plasma locking is also reported in this platform [6]. Such large mass optomechanical cavity can be applied for the sensing applications, such as accelerometers and magnetometers.

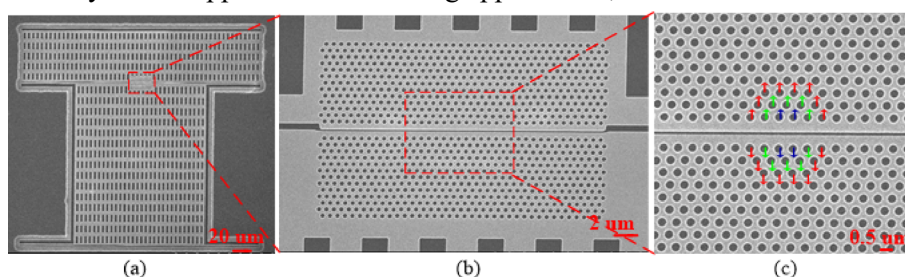


Figure 2. Fabricated large mass optomechanical cavity

References

[1] Yamamoto T.; Notomi M.; Taniyama H.; Kuramochi E.; Yoshikawa Y.; Torii Y.; Kuga T, Design of a high-Q air-slot cavity based on a width modulated line-defect in a photonic crystal slab. *Optics Express*. 16(18), 13809-13817 (2008). doi:10.1364/OE.16.013809

[2] Xingsheng Luan; Yongjun Huang; Ying Li; James F. McMillan; Jiangjun Zheng; Shu-Wei Huang; Pin-Chun Hsieh; Tingyi Gu; Di Wang; Archita Hati; David A. Howe; Guangjun Wen; Mingbin Yu; Guoqiang Lo; Dim-Lee Kwong; Chee Wei Wong, An integrated low

Express. 16(18), 13809-13817 (2008). doi:10.1364/OE.16.013809

phase noise radiation-pressure-driven optomechanical oscillator chip-set. *Scientific Reports*. 4, 6842 (2014). doi:[10.1038/srep06842](https://doi.org/10.1038/srep06842)

[3] Yongjun Huang; Jiagui Wu; Jaime Gonzalo Flor Flores; Mingbin Yu; Dim-Lee Kwong, Synchronization in air-slot photonic crystal optomechanical oscillators, *Applied Physics Letters*, 110, 111107 (2017). doi:[10.1063/1.4978671](https://doi.org/10.1063/1.4978671)

[4] Jiagui Wu; Shu-Wei Huang; Yongjun Huang; Hao Zhou; Jinghui Yang; Jia-Ming Liu; Mingbin Yu; Guoqiang Lo; Dim-Lee Kwong; Shukai Duan; Chee Wei Wong, Mesoscopic chaos mediated by Drude electron-hole plasma in silicon optomechanical oscillators. *Nature Communications*. 8, 15570 (2017). doi:[10.1038/ncomms15570](https://doi.org/10.1038/ncomms15570)

[5] Yongjun Huang; Jaime Gonzalo Flor Flores; Ziqiang Cai; Mingbin Yu; Dim-Lee Kwong; Guangjun Wen; Layne Churchill; Chee Wei Wong, A low-frequency chip-scale optomechanical oscillator with 58 kHz mechanical stiffening and more than 100th-order stable harmonics, *Scientific Reports*. 7, 4383 (2017). doi:[10.1038/s41598-017-04882-4](https://doi.org/10.1038/s41598-017-04882-4)

[6] Yongjun Huang; Jaime G. Flores; Ziqiang Cai; Mingbin Yu; Dim-Lee Kwong; Guangjun Wen; Chee Wei Wong, Controllable optomechanical coupling and Drude self-pulsation plasma locking in chip-scale optomechanical cavities. *Optics Express*. 25(6), 6851-6859 (2017). doi:[10.1364/OE.25.006851](https://doi.org/10.1364/OE.25.006851)

Open Access

This article is licensed under a [Creative Commons Attribution 4.0 International License](https://creativecommons.org/licenses/by/4.0/).

© The Author(s) 2017

Hydration of various solutions observed by terahertz spectroscopy

Toshiaki Hattori*

Division of Applied Physics, Faculty of Pure and Applied Sciences, University of Tsukuba

Corresponding Author. Email: hattori@bk.tsukuba.ac.jp

Received: 02 May 2017, Accepted: 03 June 2017, Published Online: 04 October 2017

Citation Information: Toshiaki Hattori. *Nano-Micro Conference, 2017, 1, 01006* doi: [10.11605/cp.nmc2017.01006](https://doi.org/10.11605/cp.nmc2017.01006)

Abstract

Use of terahertz waves for sensing various type of materials has been an important subject of research. The target materials include biological tissues, various kind of liquids, industrial products, etc. In most of cases, water is the most important absorber of terahertz waves. It is crucial, therefore, to understand the terahertz absorption properties of water in various situations.

It is known that the terahertz absorption of water is strongly affected by the interaction with other molecules in solutions, gels, crystals, or other types of phases. In aqueous solutions, for example, the solute is stabilized by the interaction with surrounding water molecules, and the water molecules incorporated in this interaction are very often strongly bound to the solute, leading to reduced mobility and reduced terahertz absorption.

We have constructed a high-precision terahertz time-domain spectroscopy apparatus for hydration study. Results of hydration study of protein (hen egg white lysozyme) aqueous solution with several ammonium salts [1,2] is briefly described below. Terahertz absorption coefficient of the protein-salt aqueous solutions and salt aqueous solutions were obtained as a function of the salt concentration. The difference between the results of protein-salt aqueous solutions and those of salt aqueous solutions exhibits the nature of the hydration water of the protein and also the effect of salt on them. It was found that the hydration layer of the protein is affected by ions (mostly anions) added to the solution, and that so-called kosmotropic ions (structure makers), such as sulfate ion, reduce the amount of immobile hydration water, whereas chaotropic ions (structure breakers), such as thiocyanate ions, increase it. It is shown that the dynamical properties of hydration water molecules is correlated with the stability of the macromolecules, whereas their density with the solubility.

Measurements on other types of water-rich systems have shown that the mobility of water sometimes increases after hydration, or that the hydration number changes drastically upon a small change in the concentration. Study of hydration using terahertz waves is expected to produce fruitful results in various fields including solution chemistry, sol-gel science, biology, and medicine.

References

[1] Katsuyoshi Aoki; Kentaro Shiraki; Toshiaki Hattori, Observation of salt effects on hydration water of lysozyme in aqueous solution using terahertz time-domain spectroscopy. *Applied Physics Letters*. 103, 173704 (2013). doi:[10.1063/1.4826699](https://doi.org/10.1063/1.4826699)

[2] Katsuyoshi Aoki; Kentaro Shiraki; Toshiaki Hattori, Salt effects on the picosecond dynamics of lysozyme hydration water investigated by terahertz time-domain spectroscopy and an insight into the Hofmeister series for protein stability and solubility. *Physical Chemistry Chemical Physics*. 18, 15060 (2016). doi:[10.1039/C5CP06324H](https://doi.org/10.1039/C5CP06324H)

Open Access

This article is licensed under a [Creative Commons Attribution 4.0 International License](https://creativecommons.org/licenses/by/4.0/).

© The Author(s) 2017

Fast THz Modulator based on the stagger-netlike GaN HEMT active metamaterial

Yuncheng Zhao,¹ Yaxin Zhang,^{1*} Shixiong Liang,² Zhihong Feng,² Ziqiang Yang,^{1*}

¹Terahertz Science Cooperative Innovation Center, University of Electronic Science and Technology of China No.4, Section 2, North Jianshe Road, Chengdu, 610054, China

²National Key Laboratory of Application Specific Integrated Circuit, Hebei Semiconductor Research Institute, Hezuo Road, Shijiazhuang, 050051, China

Corresponding Author. Email: Yaxin Zhang, zhangyaxin@uestc.edu.cn; Ziqiang Yang, zqyang@uestc.edu.cn

Received: 12 June 2017, Accepted: 18 June 2017, Published Online: 04 October 2017

Citation Information: Yuncheng Zhao, Yaxin Zhang, Shixiong Liang, Zhihong Feng, Ziqiang Yang. Nano-Micro Conference, 2017, 1, 01007
doi: 10.11605/cp.nmc2017.01007

Abstract

Terahertz technology promises unique applications in high speed communication, high accuracy imaging and so on [1]. However, one major bottleneck for developing Terahertz application systems is the lack of high-performance dynamic devices for effectively manipulating the Terahertz wave. In recent years, the rapid development of two-dimensional electron gas (2DEG) devices provides a promising way to develop dynamic terahertz devices [2]. Here, we combined a stagger-netlike metamaterial array with high-electron-mobility transistor (HEMT) structure to form a electronic grid-controlled THz modulator. By controlling the carrier concentration of 2DEG, the mode conversion between two kinds of dipolar resonances has been realized. Modulation depth of this device can reach up to 94%. More importantly, in the dynamic test, 600 MHz sinusoidal signals was received by a THz detector. It may provide a way to achieve effective active devices in THz wireless communication system.

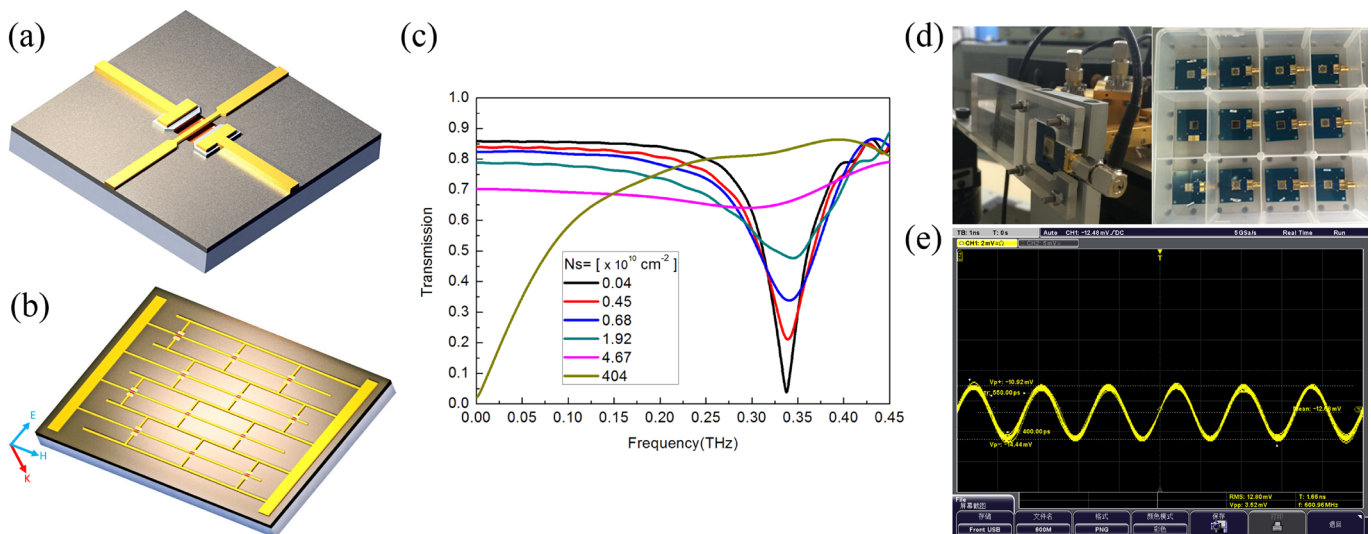


Figure 1. (a) 3-D structure of a GaN HEMT metamaterial unit cell. (b) Schematic of the THz modulator. (c) Simulation transmission spectrum results with different carrier density. (d) Image of packaged THz modulator. (e) The received sinusoidal modulating signals.

References

- [1] P. H. Siegel, Terahertz technology. IEEE Transactions on Microwave Theory and Techniques. 50(3), 910-928 (2002). doi:10.1109/22.989974
- [2] Yaxin Zhang; Shen Qiao; Shixiong Liang; Zhenhua Wu; Ziqiang Yang; Zhihong Feng; Han Sun; Yucong Zhou; Linlin Sun; Zhi Chen; Xianbing Zou; Bo Zhang; Jianhao Hu; Shaoqian Li; Qin Chen; Ling Li; Gaiqi Xu; Yuncheng Zhao; Shenggang Liu, Gbps Terahertz External Modulator Based on a Composite Metamaterial with a Double-Channel Heterostructure. Nano Letters, 15, 3501-3506 (2015). doi:10.1021/acs.nanolett.5b00869

Open Access

This article is licensed under a [Creative Commons Attribution 4.0 International License](https://creativecommons.org/licenses/by/4.0/).

© The Author(s) 2017

Terahertz filter and demultiplexer with photonic crystal waveguide

HongJun Liu,* Zhaolu Wang, Nan Huang, Jing Han

State Key Laboratory of Transient Optics and Photonics Technology, Xi'an Institute of Optics and Precision Mechanics, Chinese Academy of Science, No.17 Xixi Road, New Industrial Park, Xi'an Hi-Tech Industrial Development Zone, Xi'an, Shaanxi, China

Corresponding Author. Email: liuhongjun@opt.ac.cn

Received: 15 May 2017, Accepted: 09 June 2017, Published Online: 05 October 2017

Citation Information: HongJun Liu, Zhaolu Wang, Nan Huang, Jing Han. Nano-Micro Conference, 2017, 1, 01008 doi: 10.11605/cp.nmc2017.01008

Abstract

Terahertz (THz) wave is finding growing applications in various important fields such as space science, communications, and security screening [1]. Besides sources and detectors, development of THz technologies also requires devices to guide and manipulate THz waves. The demand for high performance quasi optic components such as frequency filters, demultiplexer, attenuators, splitters, and polarizers is increasing [2]. We theoretically propose and investigate a magnetically tunable narrow-band terahertz filter and a multi-channel THz wavelength division demultiplexer based on photonic crystal waveguide. The optical properties of the filter have been analyzed in detail. It is found that a single resonant peak with the central frequency of ~ 1 THz is existed in the transmission spectrum, which has a narrow full width at half maximum of < 2 GHz. Moreover, under the control of an external magnetic field, transmission frequency and width of passband are adjustable, which reveals that the 2-D silicon photonic crystal waveguide with point and line defects can serve as a continuously tunable bandpass filter at the terahertz waveband. THz division demultiplexer consists of an input waveguide that perpendicularly coupled with a series of defects cavities, each of which captures the resonance frequency from the input waveguide. Coupled-mode theory and finite element method are used to analyze the transmission properties of the structure. It is found that the transmission wavelength centered around 1 THz can be adjusted by changing the geometrical parameters of defects cavities, which equals to THz waves generated by optical methods such as difference frequency generation and optical rectification.

References

- [1] L. Ho; M. Pepper; P. Taday, Terahertz spectroscopy: Signatures and fingerprints. *Nature Photonics*. 2(9), 541 (2008). doi:[10.1038/nphoton.2008.174](https://doi.org/10.1038/nphoton.2008.174)
- [2] H. Bin; W. Qi Jie; Z. Ying, Broadly tunable one-way terahertz plasmonic waveguide based on nonreciprocal surface magneto plasmons. *Optics Letters*. 37(11), 1895-1897 (2012). doi:[10.1364/OL.37.001895](https://doi.org/10.1364/OL.37.001895)

Open Access

This article is licensed under a [Creative Commons Attribution 4.0 International License](https://creativecommons.org/licenses/by/4.0/).

© The Author(s) 2017

Broadband terahertz absorber based on sinusoidally-patterned graphene

Longfang Ye,* Yao Chen

Institute of Electromagnetics and Acoustics, and Department of Electronic Science, Xiamen University, Xiamen 361005, China
Corresponding Author. Email: lfye@xmu.edu.cn

Received: 25 May 2017, Accepted: 13 June 2017, Published Online: 05 October 2017

Citation Information: Longfang Ye, Yao Chen. Nano-Micro Conference, 2017, 1, 01009 doi: 10.11605/cp.nmc2017.01009

Abstract

Broadband terahertz absorbers have recently attracted considerable attention for their promising applications in terahertz trapping, sensing, imaging, and detecting. In this work, an efficient approach to achieve broadband terahertz absorber based on sinusoidally-patterned graphene with nearly 100% absorption is demonstrated [1]. As shown in Figure 1(a), the proposed absorber is composed of a net-shaped periodically sinusoidally-patterned graphene sheet on the top, a thin gating layer embedded dielectric spacer in the middle, and a metallic reflecting plate on the bottom. We assume the material of the dielectric spacer, the gating layer and metallic plate are the polyethylene cyclic olefin copolymer (Topas) with the permittivity of $\epsilon_{rt} = 2.35$ [2], and the polysilicon with the permittivity of $\epsilon_{rp} = 3$ [3], and gold, respectively. The surface conductivity of the single-layered graphene is obtained from the Kubo formula [4]. The polysilicon gating layer is placed beneath the graphene sheet to control the graphene conductivity via electrostatic doping of the graphene by applying a DC voltage V_g . By introducing such a unique gradient width modulation of the unit graphene sheet structure, the continuous plasmon resonances of the absorber can be excited, and over 65% normalized bandwidth of 90% terahertz absorbance can be achieved under normal incidence for both TE and TM polarizations. As one of the most exciting characteristics, the broadband absorption of this absorber are insensitive to the incident angles and the polarizations. The absorbance remains more than 70% even the incident angles reach 60° for both polarizations. Furthermore, compared to conventional multi-resonator or multi-layered structures, the continuous net-shaped single-layered graphene structure can greatly simplify the electrostatic gating structure in achieving flexible tunability. By controlling the chemical potential of the graphene, the peak absorbance can be continuously tuned from 14% to 100%, as shown in Figure 1(b). This work offers a new perspective on the design of graphene-based tunable terahertz broadband absorbers. The design scheme can be easily scaled to the infrared or visible regimes.

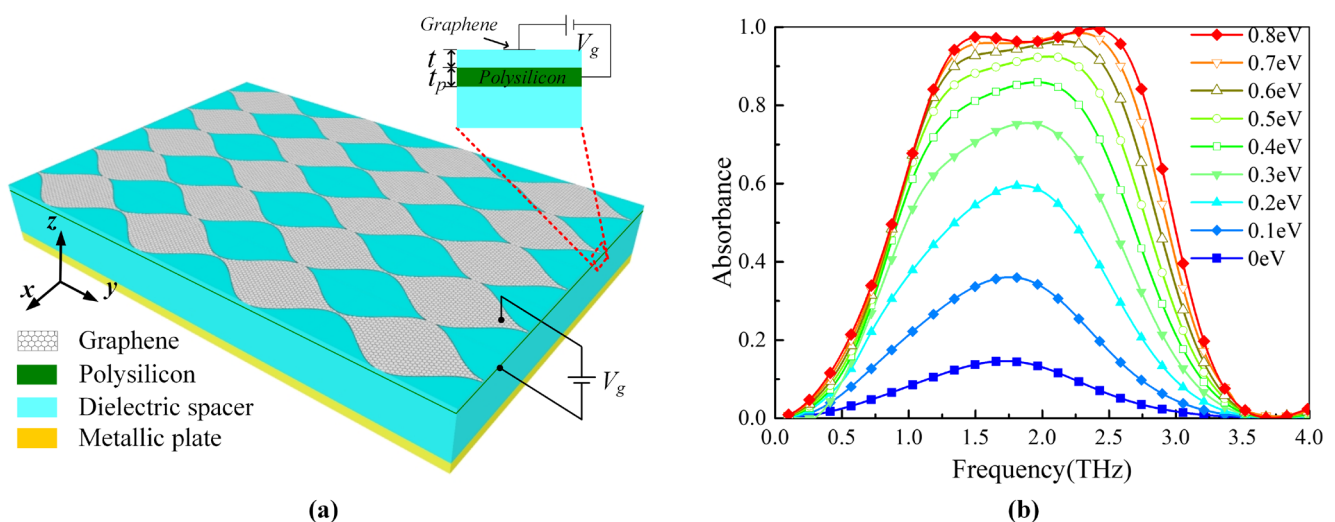


Figure 1. (a) Schematic of the proposed graphene-based broadband terahertz absorber, where the net-shaped periodically sinusoidally-patterned graphene sheet is placed on a dielectric spacer supported on a metallic reflecting plate, where a thin polysilicon layer is placed beneath the graphene sheet as a gating layer to control the graphene conductivity via a DC voltage V_g . (b) Normal-incidence absorbance in the TE polarization of the graphene-based absorber for various values of the graphene chemical potential m_c , where the peak absorbance increases from 14% to nearly 100% when m_c is tuned from 0 to 0.8 eV.

References

- [1] L.F. Ye; Y. Chen; G.X. Cai; N. Liu; J.F. Zhu; Z.Y. Song; Q.H. Liu, Broadband absorber with periodically sinusoidally-patterned graphene layer in terahertz range. *Optics Express*. 25(10), 11223-11232 (2017). doi:10.1364/OE.25.011223
[2] P. D. Cunningham; N. N. Valdes; F. A. Vallejo; L. M. Hayden; B.

- Polishak; X. H. Zhou, Broadband terahertz characterization of the refractive index and absorption of some important polymeric and organic electro-optic materials. *Journal of Applied Physics* 109, 043505 (2011). doi:10.1063/1.3549120
[3] J. S. Gómez-Díaz; J. Perruisseau-Carrier, Graphene-based plasmonic switches at near infrared frequencies. *Optics Express* 21(13),

15490 (2013). doi:[10.1364/OE.21.015490](https://doi.org/10.1364/OE.21.015490)

[4] G. W. Hanson, Dyadic Green's functions and guided surface waves for a surface conductivity model of graphene. *Journal of Applied Physics*. 103, 064302 (2008). doi:[10.1063/1.2891452](https://doi.org/10.1063/1.2891452)

Open Access

This article is licensed under a [Creative Commons Attribution 4.0 International License](https://creativecommons.org/licenses/by/4.0/).

© The Author(s) 2017

Intensity and spectral changes in terahertz quantum cascade lasers induced by the injection of near-infrared optical pulses

Y. Sakasegawa,^{1*} N. Sekine¹, S. Saito¹, A. Kasamatsu¹, I. Hosako¹, M. Ashida²

¹National Institute of Information and Communications Technology, 4-2-1 Nukui-Kitamachi, Koganei, Tokyo 184-8795, Japan

²Graduate School of Engineering Science, Osaka University, Toyonaka 560-8531 Osaka, Japan

Corresponding Author. Email: ysaka@nict.go.jp

Received: 4 June 2017, Accepted: 20 June 2017, Published Online: 06 October 2017

Citation Information: Y. Sakasegawa, N. Sekine, S. Saito, A. Kasamatsu, I. Hosako, M. Ashida, *Nano-Micro Conference, 2017, 1, 01010* doi: 10.11605/cp.nmc2017.01010

Abstract

Terahertz quantum cascade lasers (THz-QCLs) have attracted much attention as possible carrier sources for ultra high-speed wireless communications in the future, which owes to their high output powers and the absence of relaxation oscillations in QCLs. We have recently reported a photogenerated carrier-based optical-to-THz modulation scheme for THz-QCLs [1]. In the presentation, the intensity and spectral changes in THz-QCLs induced by photo-injected carriers at low temperature will be discussed together with the relevant relaxation mechanisms for the injected carriers. Furthermore, to obtain a quantitative understanding of the rich phenomena by the optical injection, we developed a global simulation scheme applicable to a wide variety of optical excitation experiments on QCLs including strong excitation densities (Figure 1) [2]. With the most of internal parameters, e.g., electron temperatures, scattering times, gains, and waveguide loss, treated as spatiotemporal and carrier density-dependent, the rate equation was solved to obtain the number of photon in the cavity. The output power (converted from the number of photons using the time-varying reflectivity at the cavity facet) well reproduces the experimental results.

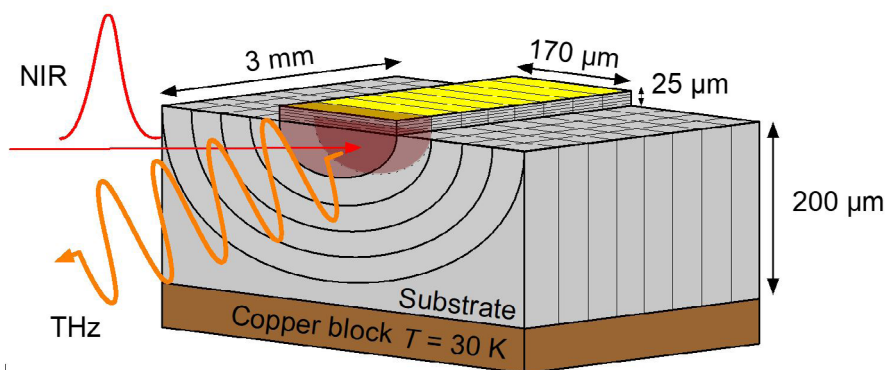


Figure 1. Model grid for the analysis of the optically excited QCL.

Acknowledgements

N.S. acknowledges funding by Collaborative Research Based on Industrial Demand of the Japan Science and Technology Agency.

References

- [1] Y. Sakasegawa; S. Saito; N. Sekine; A. Kasamatsu; M. Ashida; I. Hosako, *Japanese Journal of Applied Physics*. 55, 102701 (2016). doi:10.7567/JJAP.55.102701
- [2] Y. Sakasegawa, N. Sekine, S. Saito, A. Kasamatsu, M. Ashida, and I. Hosako, *Journal of Computational Electronics*. 16, 382 (2017). doi:10.1007/s10825-017-0962-2

Open Access

This article is licensed under a [Creative Commons Attribution 4.0 International License](https://creativecommons.org/licenses/by/4.0/).

© The Author(s) 2017

THz surface Emission spectroscopy and applications

Yuan Yuan Huang, Lipeng Zhu, Xinlong Xu*

Shaanxi Joint Laboratory of Graphene, State Key Laboratory for Incubation Base of Photoelectric Technology and Functional Materials, and Institute of Photonics & Photon-Technology, Northwest University, Xi'an, China

Corresponding Author. Email: xlxuphy@nwu.edu.cn

Received: 27 May 2017, Accepted: 18 June 2017, Published Online: 06 October 2017

Citation Information: Yuan Yuan Huang, Lipeng Zhu, Xinlong Xu, *Nano-Micro Conference, 2017, 1, 01011* doi: [10.11605/cp.nmc2017.01011](https://doi.org/10.11605/cp.nmc2017.01011)

Abstract

Terahertz (THz) wave, bridging electronics and photonics in the electromagnetic spectrum, features many exotic properties and promising applications. However, because of low THz emission efficiency, less sensitive detectors, and few manipulating devices, THz wave is still on the horizon for practical applications since 1980s. With the application of femtosecond laser, THz surface emission spectroscopy has also been developed to serve as a sensitive and contactless tool for the optoelectronic measurement of semiconductor surfaces and interfaces. When a femtosecond laser beam impinges on the semiconductor surface, photocarriers or photodipoles are excited, which then induce THz radiation with the mechanism of photoconductivity or optical rectification. As the THz surface emission is sensitive to the surfaces and interfaces, the modification of the semiconductor surface provides a significant strategy for the design and performance evaluation of many electronic and optoelectronic devices for THz applications. In this talk, we will discuss the THz radiation mechanism for traditional semiconductors by changing the crystal orientation, exciting laser intensity, surface condition, and so on [1-4]. We will also discuss THz radiation from two-dimensional layered semiconductors under linearly polarized femtosecond laser excitation.

References

- [1] Mei Qi; Yixuan Zhou; Yuanyuan Huang; Lipeng Zhu; Xinlong Xu; Zhaoyu Ren; Jintao Bai, Interface-induced terahertz persistent photoconductance in rGO-gelatin flexible films. *Nanoscale*. 9, 637-646 (2017). doi:[10.1039/C6NR06573B](https://doi.org/10.1039/C6NR06573B)
- [2] Xiaojun Wu; Xinlong Xu; Xinchao Lu; Li Wang, Terahertz Emission from Semi-insulating GaAs with Octadecanethiol-passivated Surface. *Applied Surface Science*. 279, 92-96, (2013). doi:[10.1016/j.apsusc.2013.04.040](https://doi.org/10.1016/j.apsusc.2013.04.040)
- [3] Xiaojun Wu; Baogang Quan; Xinlong Xu; Fangrong Hu; Xinchao Lu; Changzhi Gu; Li Wang, Effect of inhomogeneity and plasmons on terahertz radiation from GaAs (100) surface coated with rough Au film. *Applied surface science*. 285, 853-857 (2013). doi:[10.1016/j.apsusc.2013.09.001](https://doi.org/10.1016/j.apsusc.2013.09.001)
- [4] Yuanyuan Huang; Lipeng Zhu; Qiyi Zhao; Yaohui Guo; Zhaoyu Ren; Jintao Bai; Xinlong Xu, Surface Optical Rectification from Layered MoS₂ Crystal by THz Time-Domain Surface Emission Spectroscopy. *ACS Applied Materials & Interfaces*. 9, 4956-4965, (2017). doi:[10.1021/acsami.6b13961](https://doi.org/10.1021/acsami.6b13961)

Open Access

This article is licensed under a [Creative Commons Attribution 4.0 International License](https://creativecommons.org/licenses/by/4.0/).

© The Author(s) 2017

Tune the polarization of terahertz waves via subwavelength metallic gratings

Ren-Hao Fan,* Ru-Wen Peng, Mu Wang

National Laboratory of Solid State Microstructures, School of Physics, and Collaborative Innovation Center of Advanced Microstructures, Nanjing University, Nanjing 210093, China

Corresponding Author. Email: rhfan@nju.edu.cn

Received: 18 May 2017, Accepted: 16 June 2017, Published Online: 06 October 2017

Citation Information: Ren-Hao Fan, Ru-Wen Peng, Mu Wang, *Nano-Micro Conference, 2017, 1, 01012* doi: [10.11605/cp.nmc2017.01012](https://doi.org/10.11605/cp.nmc2017.01012)

Abstract

Here we present our recent work on tuning the polarization of terahertz waves via subwavelength metallic gratings. Firstly, we have experimentally demonstrated a linear polarization rotator that is a three-layer metallic grating structure for manipulating the polarization of broadband terahertz waves. By mechanical rotations of the composite grating layers, this freely tunable device can rotate the polarization of a linearly polarized THz wave to any desired direction with high conversion efficiency [1]. Then we theoretically investigate the propagation of terahertz waves through a graphene-loaded metal grating under external magnetic field. It is found that resonant modes in the system can be converted between transverse-electric and transverse-magnetic polarizations due to Hall conductivity of graphene, as a consequence, asymmetric transmission of terahertz waves through this graphene-loaded metal grating is achieved, and it can be tuned by adjusting either the external magnetic field or the Fermi level of graphene [2]. These tunable terahertz devices have potential applications in various areas, such as material analysis, wireless communication, and terahertz imaging.

References

- [1] R. H. Fan; Y. Zhou; X. P. Ren; R. W. Peng; S. C. Jiang; D. H. Xu; X. Xiong; X. R. Huang; Mu Wang, Freely tunable broadband polarization rotator for terahertz waves. *Advanced Materials*. 27, 1201 (2015). doi:[10.1002/adma.201404981](https://doi.org/10.1002/adma.201404981)
- [2] Y. Zhou; Y. Q. Dong; R. H. Fan; Q. Hu; R. W. Peng; Mu Wang, Asymmetric transmission of terahertz waves through a graphene-loaded metal grating. *Applied Physics Letters*. 105, 041114 (2014). doi:[10.1063/1.4891818](https://doi.org/10.1063/1.4891818)

Open Access

This article is licensed under a [Creative Commons Attribution 4.0 International License](https://creativecommons.org/licenses/by/4.0/).

© The Author(s) 2017

Coherent and Continuous Terahertz Emitters from High- T_c Superconductor Mesa structures

K. Kadowaki,^{1,2*} T. Yuasa,¹ T. Tanaka,¹ Y. Komori,¹ R. Ota,¹ G. Kuwano,¹ Y. Tanabe,¹ K. Nakamura,¹ M. Tsujimoto,^{1,2} H. Minami,^{1,2} T. Kashiwagi,^{1,2} Richard A. Klemm^{3*}

¹Graduate School of Pure & Applied Science, University of Tsukuba, 1-1-1, Tennodai, Tsukuba, Ibaraki 205-8573, Japan

²Division of Materials Science, Faculty of Pure & Applied Sciences, University of Tsukuba, 1-1-1, Tennodai, Tsukuba, Ibaraki 305-8573, Japan

³Department of Physics, University of Central Florida, Orlando, Florida 32816-2385, USA

Corresponding Author. Email: K. Kadowaki, kadowaki@ims.tsukuba.ac.jp; Richard A. Klemm, Richard.Klemm@ucf.edu

Received: 04 June 2017, Accepted: 18 June 2017, Published Online: 07 October 2017

Citation Information: K. Kadowaki, T. Yuasa, T. Tanaka, Y. Komori, R. Ota, G. Kuwano, Y. Tanabe, K. Nakamura, M. Tsujimoto, H. Minami, T. Kashiwagi, Richard A. Klemm, *Nano-Micro Conference*, 2017, 1, 01013 doi: 10.11605/cp.nmc2017.01013

Abstract

After the discovery of high temperature Superconductor $\text{YBa}_2\text{Cu}_3\text{O}_{7-\delta}$ with the superconducting transition temperature $T_c=92$ K, which is well above 77 K, the boiling point of liquid nitrogen, this year has become a celebrative and a commemorative 30th anniversary in the history of superconductivity research. In addition to this memorable occasion, this year is another important anniversary that ten years have passed after the discovery of terahertz electromagnetic wave emission from the mesa structure of Bi2212 single crystals [1]. The important ingredients here is that the superconducting CuO_2 double layers are built in a unit cell of the Bi2212 crystal as it is grown and are sandwiched by the insulating Bi_2O_2 layers, forming a stack of intrinsic Josephson junctions (IJJs). Since the electronic structure as a result of this layered crystal structure the superconducting as well as even normal state is highly two dimensional, the superconducting coupling becomes Josephson-junction like, extremely weak as measured by the c-axis critical current $J_c^c = 10^2 - 10^3$ A/cm² compared with $J_{ab}^c = 10^6 - 10^7$ A/cm², resulting in the reduction of the superconducting plasma frequency to the level of $f_J \sim 10^{11}$ c/s (0.2 ~ 1 meV), which is well below the superconducting gap $\Delta \sim 30$ meV. This Josephson plasma mode can be excited by the *dc*-current through the nonlinear Josephson coupling effect by the *dc*-Josephson effect and the coherent THz emission is generated due to the *ac*-Josephson oscillation with the frequency $f_J = (2e/h)v_J$, where e is the elementary charge of electron, h Planck constant, and v_J the voltage per intrinsic Josephson junctions, when it matches well the cavity mode frequency. Although the understanding of this phenomenon has already been well established by various experiments and theoretical works [2], the practical limitation of the device is not well understood yet. For example, the most important issue is on what determines the maximum power extracted from one intrinsic Josephson junction, and how much power can be generated from the actual mesa structure with N -intrinsic Josephson junctions, where N is the number of intrinsic Josephson junctions in a mesa. The next issue is on what limits the maximum frequency.

The essential parameter related to two issues has evidently been thought the thermal effect due to the Joule heating by the *dc*-current (10 - 50 mW), which produces heat of $\sim \text{MW}/\text{cm}^3$ and naturally causes a serious temperature increase and inhomogeneity, which is often called as a hot-spot. It has been disclosed by us that the formation of the hot-spot gives only a detrimental effect on the THz radiation phenomena so that it is better to avoid it or control it to make the influence minimum on the THz emission. The heating issue has recently been studied intensively [3]. As a result, we have achieved a frequency of 2.4 THz with a power of 30 μW [4] quite reproducibly.

Recently, we have done a systematic case study on the rectangular, square, circular, triangular mesas, *etc.* and found an interesting fact. That is concerning the missing modes, which are expected to be as the strong emission modes but systematically disappear or are missing, perhaps, due to very weak intensities. This seems to occur especially in the degenerated symmetric cases such as in square and circular mesas. We argue this effect as a mode cancellation in the degenerated cavity modes in a symmetric mesa.

References

- [1] L. Ozyuzer; A. E. Koshelev; C. Kurter; N. Gopalsami; Q. Li; M. Tachiki; K. Kadowaki; T. Yamamoto; H. Minami; H. Yamaguchi; T. Tachiki; K. E. Gray; W.-K. Kwok; U. Welp, Emission of Coherent THz Radiation from Superconductors. *Science*. 318, 1291 (2007). doi:10.1126/science.1149802
- [2] Ulrich Welp; Kazuo Kadowaki; Reinhold Kleiner, Superconducting emitters of THz radiation. *Nature Photonics*. 7, 702–710 (2013). doi:10.1038/nphoton.2013.216
- [3] T. Kashiwagi et al., to be published in *Supercond. Sci. Technol.*
- [4] Takanari Kashiwagi; Kazuki Sakamoto; Hiroyuki Kubo; Yuuki

Shibano; Takuma Enomoto; Takeo Kitamura; Kentaro Asanuma; Takaki Yasui; Chiharu Watanabe; Kurama Nakade; Yoshihiko Saiwai; Takuya Katsuragawa; Manabu Tsujimoto; Ryoza Yoshizaki; Takashi Yamamoto; Hidetoshi Minami; Richard A. Klemm; Kazuo Kadowaki, A high- T_c intrinsic Josephson junction emitter tunable from 0.5 to 2.4 terahertz. *Applied Physics Letters*. 107, 082601 (2015). doi:10.1063/1.4929715

Open Access

This article is licensed under a [Creative Commons Attribution 4.0 International License](https://creativecommons.org/licenses/by/4.0/).

© The Author(s) 2017

Terahertz-wave parametric wavelength conversion at room temperature

Shin'ichiro Hayashi,^{1,2*} Kouji Nawata,² Kodo Kawase,³ Hiroaki Minamide²

¹NICT, 4-2-1, Nukui-Kitamachi, Koganei, Tokyo 184-8795, Japan

²RIKEN Center for Advanced Photonics, 519-1399 Aramaki-cho, Aoba, Sendai, 980-0845, Japan

³Graduate School of Engineering, Nagoya University, Furocho, Chikusa, Nagoya, 464-8603, Japan

Corresponding Author. Email: hayashi@nict.go.jp

Received: 02 June 2017, Accepted: 19 June 2017, Published Online: 07 October 2017

Citation Information: Shin'ichiro Hayashi, Kouji Nawata, Kodo Kawase, Hiroaki Minamide, *Nano-Micro Conference*, 2017, 1, 01014 doi: 10.11605/cp.nmc2017.01014

Abstract

Over the past decade, there has been remarkable growth in the field of terahertz frequency science and engineering, which has become a vibrant, international, cross-disciplinary research activity. Wavelength conversion in nonlinear optical materials is an effective method for generating and detecting coherent terahertz waves owing to the high conversion efficiency, bandwidth, wide tunability, and room-temperature operation, and if the tuning range and the peak power can be enhanced, drastic developments in basic researches and industrial applications can be expected.

Here we demonstrate the generation of high-brightness terahertz waves using parametric wavelength conversion in a nonlinear MgO doped LiNbO₃ crystal. We revealed novel parametric wavelength conversion process using stimulated Raman scattering in MgO:LiNbO₃ without stimulated Brillouin scattering using recently-developed microchip Nd:YAG laser. We also demonstrated the coherent detection of generated terahertz waves using nonlinear up-conversion.

A number of applications require high brightness, that is, intense and narrowband, terahertz waves such as observing multi-photon absorption to specific excitation states. We speculate that the high-brightness terahertz wave and its visualization could be powerful tools not only for solving real world problems but also fundamental physics. We expect that these methods will open up new fields and tune up killer applications.

Acknowledgements

The authors would like to thank Prof. T. Taira of IMS, Dr. Sakai of Hamamatsu Photonics, all of previous and present team members, Prof. H. Ito of RIKEN and Prof. M. Kumano of Tohoku University for useful discussions. This work was partially supported by Collaborative Research Based on Industrial Demand of the Japan Science and Technology Agency (JST), and JSPS KAKENHI Grant Numbers 25220606, 25286075, and ImPACT Program of Council for Science, Technology and Innovation.

Open Access

This article is licensed under a [Creative Commons Attribution 4.0 International License](https://creativecommons.org/licenses/by/4.0/).

© The Author(s) 2017

Development of Small Size Terahertz Vacuum Sources in IECAS

Wenxin Liu,* Chao Zhao, Xin Guo

Institute of Electronics, Chinese Academy of Sciences, Beijing, China

Corresponding Author. Email: lwenxin@mail.ie.ac.cn

Received: 05 June 2017, Accepted: 19 June 2017, Published Online: 08 October 2017

Citation Information: Wenxin Liu, Chao Zhao, Xin Guo, *Nano-Micro Conference, 2017, 1, 01015* doi: [10.11605/cp.nmc2017.01015](https://doi.org/10.11605/cp.nmc2017.01015)

Abstract

Terahertz frequencies are among the most under developed electromagnetic spectra, even though their potential applications are promising in biochemical sensing, imaging for medical and security applications, astrophysics and remote atmospheric monitoring, and high-bandwidth communications. Among their wide applications, the lightweight, low voltage and broadband sources of high-power coherent THz radiation are important for military radar, electronic countermeasure systems and communications. Vacuum electronic devices such as the traveling wave tube amplifier (TWTA), backward wave oscillator and extended interaction oscillator show great potential for applications at the frequency because of wide band and high power. At THz band, the most critical part of small size THz vacuum sources is the slow wave structure, which determines the output performances, such as the output power and signal band. In the millimeter and sub-millimeter wave vacuum devices, the various of SWSs including coupling cavity, disk-loaded, helix and complex CC are used. However, they are not suitable for the THz band, resulting from the difficulty of fabricating and integrating.

Folded waveguide (FW) or serpentine circuits, for example, have ~10:1 aspect ratio in the waveguide height dimension. This is much larger than the ideal for both machining, which is limited by the length of the tool shank with acceptable wobble; and photolithography, which is limited by defocusing and absorption of light as it penetrates into deep photoresist. These requirements are the topic of ongoing research in the vacuum electronics community, motivated by the continued interest in high power mm-THz sources. Consequently, there is a great interest in the study and development of FW SWS. For the satisfied with requirement of high speed communication and ViSAR, the TWT has been developed. Based on the FW, the small size THz vacuum devices are developed in China, including UESTC, IECAS CETC 12 and CAEP, etc. In this talk, we report the development of small size THz vacuum devices in IECAS.

At IECAS, three kinds THz devices have been developed, such as the 0.3THz EIO, the peak power exceeds 4W. The 0.1THz EIO generates the output power is larger than 12W. Moreover, the THz TWT has been developed through the small size electron gun, high strength focusing magnetic field and high frequency structure welding. It produces the output power exceeds 2W and the band width is larger than 5GHz. Now we are developing the continued wave TWT for the power exceeds 10W and signal band width larger than 5GHz.

Open Access

This article is licensed under a [Creative Commons Attribution 4.0 International License](https://creativecommons.org/licenses/by/4.0/).

© The Author(s) 2017

300GHz wireless link with a CMOS transceiver

Minoru Fujishima*

Graduate School of Advanced Sciences of Matter, Hiroshima University, 1-3-1 Kagamiyama, Higashi-hiroshima, Japan
Corresponding Author. Email: fuji@hiroshima-u.ac.jp

Received: 01 June 2017, Accepted: 16 June 2017, Published Online: 09 October 2017

Citation Information: Minoru Fujishima, *Nano-Micro Conference, 2017, 1, 01016* doi: [10.11605/cp.nmc2017.01016](https://doi.org/10.11605/cp.nmc2017.01016)

Abstract

Since terahertz provides a wide frequency band, terahertz communication realizes a data rate exceeding 100 Gbps approaching fibre-optic speed. The frequency band from 252 to 275 GHz has already been allocated for communication. Further discussion is being made to use the frequency band exceeding 275 GHz, which has not been assigned yet, for communication use. On the other hand, since terahertz has large atmospheric attenuation and strong directivity, it is limited to short-distance fixed radio communication. However, it is long-distance and mobile application that is intrinsically expected for wireless communication. In this talk, even in terahertz, it is shown that kilometre communication is potentially possible by selecting the frequency appropriately. It is also shown that terahertz communication can be performed using CMOS process, which was said to have inferior high frequency characteristics to compound semiconductors. How will the world change when technologies beyond such conventional common sense are established? The impact of terahertz communication and the contribution of CMOS transceivers are discussed.

References

- [1] K. Katayama; K. Takano; S. Amakawa; S. Hara; A. Kasamatsu; K. Mizuno; K. Takahashi; T. Yoshida; M. Fujishima, A 300GHz 40nm CMOS Transmitter with 32-QAM 17.5Gb/s/ch Capability over 6 Channels. Digest of Technical Papers IEEE International Solid-State Circuits Conference (ISSCC) 2016, 342-343 (1-3 Feb. 2016). doi:[10.1109/ISSCC.2016.7418047](https://doi.org/10.1109/ISSCC.2016.7418047)
- [2] K. Takano; S. Amakawa; K. Katayama; S. Hara; R. Dong; A. Kasamatsu; I. Hosako; K. Mizuno; K. Takahashi; T. Yoshida; M. Fujishima, A 105Gb/s 300GHz CMOS transmitter. 2017 IEEE International Solid-State Circuits Conference (ISSCC), 308-309, 2017. doi:[10.1109/ISSCC.2017.7870384](https://doi.org/10.1109/ISSCC.2017.7870384)
- [3] M. Fujishima; S. Amakawa, Integrated-circuit approaches to THz communications: challenges, advances, and future prospects. IEICE TRANSACTIONS on Fundamentals of Electronics, Communications and Computer Sciences. 100, 516-523 (2017). doi:[10.1587/transfun.E100.A.516](https://doi.org/10.1587/transfun.E100.A.516)

Open Access

This article is licensed under a [Creative Commons Attribution 4.0 International License](https://creativecommons.org/licenses/by/4.0/).

© The Author(s) 2017

Ultra-broadband Wireless Communications in the 0.1-10 Terahertz Band

Chong Han*

University of Michigan-Shanghai Jiao Tong University Joint Institute, Shanghai Jiao Tong University, China

Corresponding Author. Email: chong.han@sjtu.edu.cn

Received: 31 May 2017, Accepted: 19 June 2017, Published Online: 10 October 2017

Citation Information: Chong Han, *Nano-Micro Conference, 2017, 1, 01017* doi: [10.11605/cp.nmc2017.01017](https://doi.org/10.11605/cp.nmc2017.01017)

Abstract

By supporting tens or hundreds GHz bandwidths, Terahertz (THz)-band (0.1-10 THz) communication is envisioned as a key wireless technology of the next decade. The THz band will help overcome the spectrum scarcity problems and capacity limitations of current wireless networks, by providing an unprecedentedly large bandwidth. In addition, THz-band communication will enable a plethora of long-awaited applications, both at the nano-scale and at the macro-scale, ranging from wireless massive-core computing architectures and instantaneous data transfer among non-invasive nano-devices, to ultra-high-definition content streaming among mobile devices and wireless high-bandwidth secure communications.

In this invited speech, an overview of THz-band communications will be provided. First, the current progress and open research directions in terms of THz-band channel modeling will be presented. The main phenomena affecting the propagation of THz signals will be explained and their impact on the channel capacity will be assessed. Second, novel communication mechanisms such as the modulation techniques, resource allocation, timing acquisition schemes, and Ultra-Massive Multiple-Input Multiple-Output (UM-MIMO) will be presented. Finally, the state of the art and open challenges in the network layer design and other relevant research directions will be stated. This presentation is expected to provide the audience with the necessary knowledge to work in a cutting-edge research field, at the intersection of antennas and propagation, and information and communication technologies.

Open Access

This article is licensed under a [Creative Commons Attribution 4.0 International License](https://creativecommons.org/licenses/by/4.0/).

© The Author(s) 2017

Millimeter- and terahertz-wave technology for communication and radar/imaging applications by photonics technology

Atsushi Kanno*

National Institute of Information and Communications Technology, Japan

Corresponding Author. Email: kanno@nict.go.jp

Received: 04 June 2017, Accepted: 19 June 2017, Published Online: 10 October 2017

Citation Information: Atsushi Kanno, Nano-Micro Conference, 2017, 1, 01018 doi: 10.11605/cp.nmc2017.01018

Abstract

Advanced optical fiber communication technologies enable low-loss and broad-bandwidth transmission in the millimeter-wave and terahertz-wave bands via an optical fiber network. Precise optical modulation techniques can directly generate the millimeter-wave signals, and finally, an optical frequency comb signal generated by the modulation also provides the terahertz-wave signals by optical heterodyning systems. These technologies on the signal generation could be utilized for realization of distributed antenna system in the millimeter- and terahertz-wave bands based on the optical fiber network for some specific applications: foreign object debris detection systems for airport runway surveillance and high-speed railway radiocommunication systems between train and trackside. In the talk, we briefly introduce the R&D activities on the millimeter- and terahertz-wave for both wireless communication and radar/non-destructive imaging systems based on photonics.

Open Access

This article is licensed under a [Creative Commons Attribution 4.0 International License](https://creativecommons.org/licenses/by/4.0/).

© The Author(s) 2017

The fascinating split-ring-resonators: progress in design, fabrication and applications of terahertz metamaterials

Mei Zhu*

School of Physics & Electronic Engineering, Taishan University, 525 Dongyue Road, Tai'an City, Shandong Province, China

Corresponding Author. Email: zm_1805@163.com

Received: 01 June 2017, Accepted: 15 June 2017, Published Online: 10 October 2017

Citation Information: Mei Zhu, *Nano-Micro Conference, 2017, 1, 01019* doi: [10.11605/cp.nmc2017.01019](https://doi.org/10.11605/cp.nmc2017.01019)

Abstract

Metamaterials with many unique optical properties are made of periodically arranged sub-wavelength metallic structures that are able to couple to external electromagnetic (EM) waves. One of such structures is the commonly used split-ring-resonators (SRR). In this talk, I will discuss and demonstrate some new progress we made on SRR-based terahertz metamaterials. By looking into the coupling between SRRs and the effect of incident polarization, we proposed a way to continuously modulate their resonances, changing the transmission intensity at resonant frequency from 20% to 80% [1]. We also designed a SRR-based polarization-insensitive broadband filter in THz range and discovered its effect in eliminating asymmetric characteristics in device structure [2]. A stop band with bandwidth of as large as 1.40 THz was achieved. To improve the fabrication process, a facile metal transfer method was employed to create SRR patterns on PDMS surface, planar and otherwise, as well as PDMS-coated surfaces, such as paper, fabric and leaf [3]. Lastly, a design of 3D THz metamaterial device was proposed to be used in biomedical field for cancer cell studies, exploiting its structural similarities with the single-cell-capturing microfluidic devices.

Acknowledgements

Financial support from the National Natural Science Foundation of China (No. 61605139), the Natural Science Foundation of Shandong Province (No. ZR2016FQ15) and the Science and Technology Planning Project of Higher Education of Shandong Province (No. J16LJ10) is acknowledged.

References

- [1] Mei Zhu; Yu-Sheng Lin; Chengkuo Lee, Coupling effect combined with incident polarization to modulate double split-ring-resonator in terahertz frequency range. *Journal of Applied Physics*. 116, 173106 (2014). doi:[10.1063/1.4901062](https://doi.org/10.1063/1.4901062)
- [2] Mei Zhu; Chengkuo Lee, A Design of Terahertz Broadband Filters and its Effect in Eliminating Asymmetric Characteristics in Device Structures. *Journal of Lightwave Technology*. 33, 3280-3285 (2015). doi:[10.1109/JLT.2015.2432017](https://doi.org/10.1109/JLT.2015.2432017)
- [3] Mei Zhu; Chengkuo Lee, Facile metal transfer method for fabricating unconventional metamaterial devices. *Optical Materials Express*. 5, 733-741 (2015). doi:[10.1364/OME.5.000733](https://doi.org/10.1364/OME.5.000733)

Open Access

This article is licensed under a [Creative Commons Attribution 4.0 International License](https://creativecommons.org/licenses/by/4.0/).

© The Author(s) 2017

Micro-fabricated L-shape metasurface terahertz biosensor

Jun Zhou*

University of Electronic Science and Technology of China, No. 4, Section 2, North Jianshe Road, Chengdu, China

Corresponding Author. Email: zhoujun123@uestc.edu.cn

Received: 03 June 2017, Accepted: 19 June 2017, Published Online: 10 October 2017

Citation Information: Jun Zhou, Nano-Micro Conference, 2017, 1, 01020 doi: 10.11605/ep.nmc2017.01020

Abstract

In recent years, more and more attention has been paid on the research and development of terahertz (THz) technologies all over the world. Biosensing is one of the most important applications of THz waves. Metasurface is an artificial two-dimensional material with flexible structures and good electromagnetic wave control capability, which is very suitable for THz wave control and sensing. In this work, a L-shape metasurface THz biosensor was designed, simulated, optimized, micro-fabricated, and finally tested by the time-domain spectroscopy (TDS) system. The simulation and experimental results agree with each other very well. The conclusions show great advantage of metasurface for the THz biosensing application, especially when it is combined with the microfluidic technology in the near future.

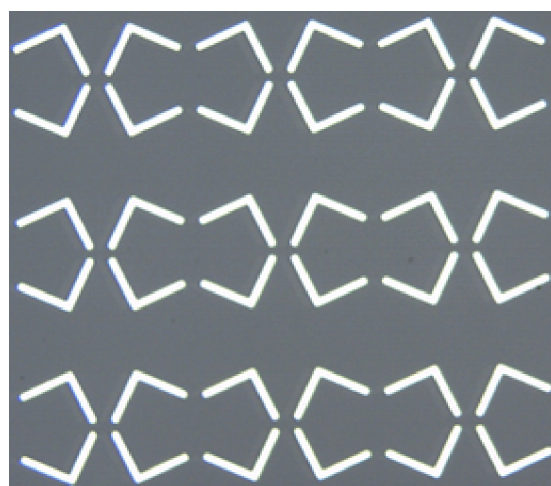


Figure 1. Structure of sensing array

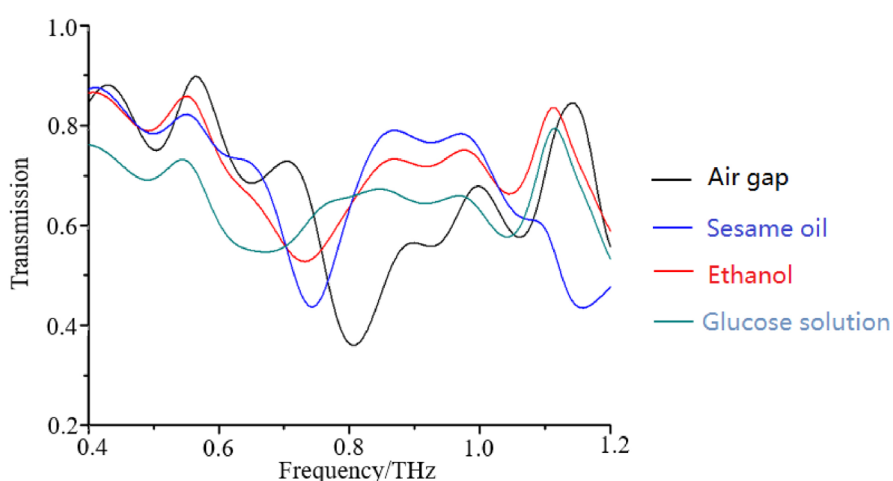


Figure 2. Measured results of some liquid samples

References

- [1] J. B. Pendry, Metamaterials in the sunshine. *Nature Materials*. 5, 599-600 (2006). doi:10.1038/nmat1697
- [2] X. Yan; X. F. Zhang; L. J. Liang, The application and research progress of metamaterial biological sensor in Terahertz. *Spectroscopy and Spectral Analysis*. 34, 2365 (2014).

- [3] L. Q. Cong; S. Y. Tan; R. Yahiaoui; F. P. Yan, Experimental demonstration of ultrasensitive sensing with terahertz metamaterial absorbers: A comparison with the metasurfaces. *Applied Physics Letters*. 106, 26 (2015). doi:10.1063/1.4906109

Open Access

This article is licensed under a [Creative Commons Attribution 4.0 International License](https://creativecommons.org/licenses/by/4.0/).

© The Author(s) 2017

Design and electrochemical performance of nano-micro structured porous materials

Yingke Zhou*

The State Key Laboratory of Refractories and Metallurgy, College of Materials and Metallurgy, Wuhan University of Science and Technology, Wuhan 430081, P. R. China

Corresponding Author. Email: zhouyk888@hotmail.com

Received: 22 May 2017, Accepted: 16 June 2017, Published Online: 12 October 2017

Citation Information: Yingke Zhou, *Nano-Micro Conference, 2017, 1, 01021* doi: 10.11605/cp.nmc2017.01021

Abstract

Graphene and carbon nanotube present unique structure and excellent properties, such as high specific surface area, high conductivity, high thermal conductivity, etc., and play an increasingly important role in the electrochemical energy storage and conversion. The doping of nano-carbon with nitrogen and boron can modulate the electron and energy band structure, and further improve its physical and chemical properties. The pore structure, pore size distribution and wall thickness of the electroactive material display important effect on the electrolyte infiltration, the ion transport and adsorption, and the overall performance of the battery. The use of doped nano-carbon and porous composite structure can improve the conductivity and the electrochemical surface area and reaction sites of the electroactive materials, and significantly increase the efficiency of energy storage and conversion.

This presentation focuses on some progresses of the doped nano-carbon and porous composite structures, including the following three aspects: (1) The controllable synthesis and electrochemical lithium insertion characteristics of the porous electrode materials. Porous materials have been widely used in a variety of fields, but their large-scale controllable synthesis is still a considerable challenge. We have designed a novel templated freeze-drying method to conveniently control the porous properties of materials, which has been successfully applied to the synthesis of various porous phosphates, oxides and composites, and the electrochemical lithium storage properties have been explored. (2) The porous lithium iron phosphate and nitrogen-doped graphene composite. Three-dimensional porous microspheres composed of LiFePO_4 and nitrogen-doped graphene have been synthesized by a solvothermal method. The effect of graphene doping on the nucleation and growth of LiFePO_4 and the influence of the unique self-assembled porous microsphere structure on the electrochemical lithium insertion performance have been studied. (3) Supercapacitance properties of doped graphene. A series of dopant graphene materials have been facilely synthesized by a thermal solid state reaction. The regulation of doping configuration on the electronic structure of graphene and the influence on the supercapacitance have been systematically studied. The relevant mechanisms have been proposed and some phenomena in the literature have been reasonably explained.

This work was supported by the National Natural Science Foundation of China (No. 51372178) and the Natural Science Foundation for Distinguished Young Scholars of Hubei Province of China (No. 2013CFA021).

Open Access

This article is licensed under a [Creative Commons Attribution 4.0 International License](https://creativecommons.org/licenses/by/4.0/).

© The Author(s) 2017

Molecular Insights into Electrical Double Layers in Graphene-Based Supercapacitors

Sheng Bi,¹ Guang Feng,^{1,*} Song Li,¹ Nina Balke,² Peter T. Cummings,³ Rui Qiao,⁴ Alexei A. Kornyshev⁵

¹State Key Laboratory of Coal Combustion, Huazhong University of Science and Technology, Wuhan, Hubei 430074 China

²Center for Nanophase Materials Sciences, Oak Ridge National Laboratory, Oak Ridge, TN 37831, USA

³Department of Chemical and Biomolecular Engineering, Vanderbilt University, Nashville, TN 37235, USA

⁴Department of Mechanical Engineering, Virginia Tech, Blacksburg, Virginia 24061, USA

⁵Department of Chemistry, Imperial College London, SW7 2AZ London, UK

Corresponding Author. Email: gfeng@hust.edu.cn

Received: 30 May 2017, Accepted: 18 June 2017, Published Online: 12 October 2017

Citation Information: Sheng Bi, Guang Feng, Song Li, Nina Balke, Peter T. Cummings, Rui Qiao, Alexei A. Kornyshev, *Nano-Micro Conference, 2017, 1, 01022*
doi: [10.11605/cp.nmc2017.01022](https://doi.org/10.11605/cp.nmc2017.01022)

Abstract

Recently nano-structural carbons have become the most widely used electrode materials in supercapacitor community, because of their high specific surface area, good electrical conductivity, chemical stability in a variety of electrolytes, and relatively low cost. In particular, graphene-based carbons are emerging as an auspicious candidate due to the unique feature of graphene. Among electrolytes used for supercapacitors, ionic liquids (ILs) have been becoming a promising class of them, owing to their exceptionally wide electrochemical stability window, excellent thermal stability, non-volatility and relatively inert nature. Despite considerable work on supercapacitor with graphene-based carbon as electrodes, the details of what happens under nano-confinement, including pores, still require in-depth exploration especially for IL electrolytes.

We studied the interfacial phenomena occurring between ILs and graphene-based electrodes in supercapacitors, using the combined molecular dynamics (MD) simulation by modeling ILs-based EDLs at planar, cylindrical, spherical electrode surfaces and inside electrode pores at nano/micro-scale. This talk would include:

1) MD modeling on ILs-based EDLs at open surfaces (e.g., planar, cylindrical, spherical, with defects, etc.) [1-2] and the integration with experiments (e.g., atomic force microscopy, AFM) [3-4], which would focus on the EDL structure and its influence from ion size, ion type, applied potential, electrode curvature, etc.

2) MD modeling on ILs-based porous carbon supercapacitors [5-7], which would embody the pore size effects on capacitance, the ion dynamics under porous confinement, and pore expansion during charging.

3) The anatomy of electrosorption for water in ionic liquids at electrified interfaces [8], which would show, for the first time, the work on the adsorption of water on electrode surfaces in contact with humid ILs.

References

[1] G. Feng; S. Li; W. Zhao; P. T. Cummings, Microstructure of room temperature ionic liquids at stepped graphite electrodes. *AIChE Journal*. 61, 3022-3028 (2015). doi:[10.1002/aic.14927](https://doi.org/10.1002/aic.14927)

[2] G. Feng; D. E. Jiang; P. T. Cummings, Curvature Effect on the Capacitance of Electric Double Layers at Ionic Liquid/Onion-Like Carbon Interfaces. *Journal of Chemical Theory and Computation*. 8, 1058-1063 (2012). doi:[10.1021/ct200914j](https://doi.org/10.1021/ct200914j)

[3] J. M. Black; D. Walters; A. Labuda; G. Feng; P. C. Hillesheim; S. Dai; P. T. Cummings; S. V. Kalinin; R. Proksch; N. Balke, Bias-dependent molecular-level structure of electrical double layer in ionic liquid on graphite. *Nano Letters*. 13, 5954-5960 (2013). doi:[10.1021/nl4031083](https://doi.org/10.1021/nl4031083)

[4] J. M. Black; M. Baris Okatan; G. Feng; P. T. Cummings; S. V. Kalinin; N. Balke, Topological defects in electric double layers of ionic liquids at carbon interfaces. *Nano Energy*. 15, 737-745 (2015). doi:[10.1016/j.nanoen.2015.05.037](https://doi.org/10.1016/j.nanoen.2015.05.037)

[5] G. Feng; P. T. Cummings, Supercapacitor capacitance exhibits oscillatory behavior as a function of nanopore size. *The Journal of Physical Chemistry Letters*. 2, 2859-2864 (2011). doi:[10.1021/jz201312e](https://doi.org/10.1021/jz201312e)

[6] G. Feng; S. Li; V. Presser; P. T. Cummings, Molecular Insights into Carbon Supercapacitors Based on Room-Temperature Ionic Liquids. *The Journal of Physical Chemistry Letters*. 4, 3367-3376 (2013). doi:[10.1021/jz4014163](https://doi.org/10.1021/jz4014163)

[7] J. M. Black; G. Feng; P. F. Fulvio; P. C. Hillesheim; S. Dai; Y. Gogotsi; P. T. Cummings; S. V. Kalinin; N. Balke, Strain-Based In

Situ Study of Anion and Cation Insertion into Porous Carbon Electrodes with Different Pore Sizes. *Advanced Energy Materials*. 4, 1300683 (2014). doi:[10.1002/aenm.201300683](https://doi.org/10.1002/aenm.201300683)

[8] G. Feng; X. Jiang; R. Qiao; A. A. Kornyshev, Water in Ionic Liquids at Electrified Interfaces: The Anatomy of Electrosorption. *ACS Nano*. 8, 11685-11694 (2014). doi:[10.1021/nm505017c](https://doi.org/10.1021/nm505017c)

Open Access

This article is licensed under a [Creative Commons Attribution 4.0 International License](https://creativecommons.org/licenses/by/4.0/).

© The Author(s) 2017

Controllable Synthesis of N-Doped and Dually Doped Mesoporous Carbons for Adsorption and Catalysis Applications

Zhangxiong Wu,* Zhi Chen, Xingmin Gao, Zhujun Zhang

School of Chemical and Environmental Engineering, College of Chemistry, Chemical Engineering and Materials Science, Soochow University, NO. 199, Ren-Ai Road, Suzhou Industrial Park, Suzhou, Jiangsu 215123, China

Corresponding Author. Email: zhangwu@suda.edu.cn

Received: 05 June 2017, Accepted: 18 June 2017, Published Online: 13 October 2017

Citation Information: Zhangxiong Wu, Zhi Chen, Xingmin Gao, Zhujun Zhang, *Nano-Micro Conference*, 2017, 1, 01023 doi: 10.11605/cp.nmc2017.01023

Abstract

Mesoporous carbon materials are being in vogue because of their intriguing properties and wide potentials. Doping of heteroatoms, especially N, in carbons have attracted enormous interests owing to its capability in enhancing or expanding their applicability in separation, energy conversion and catalysis. In addition, N-doping can further boost dually doped carbons, such as with S and metal as the second dopant. Such a dual doping could possibly optimize material property and maximize performance through synergistic effects. In this talk, several synthetic methods, such as post modification [1-2], one-step solvent-free nano-confining synthesis [3-4] and spray-drying-assisted assembly [5], for the synthesis of heteroatom (singly or dually) porous carbon materials with different porosities and structures will be introduced and discussed. Furthermore, the controllable synthesis of metal/heteroatom dually doped mesoporous carbons with desirable fascinating properties will be introduced. The demo-applications of these materials in typical adsorption, such as arsenic removal and CO₂ capture, and typical catalysis, such as oxygen reduction, biodiesel production and dehydrogenation/hydrogenation coupling reactions, will be presented and their structure-performance correlations will be discussed.

References

- [1] Z. Wu; W. Li; P.A. Webley; D. Zhao, General and Controllable Synthesis of Novel Mesoporous Magnetic Iron Oxide@Carbon Encapsulates for Efficient Arsenic Removal. *Advanced Materials*. 24, 485-491 (2012). doi:10.1002/adma.201103789
- [2] Z. Wu; P.A. Webley; D. Zhao, Post-enrichment of nitrogen in soft-templated ordered mesoporous carbon materials for highly efficient phenol removal and CO₂ capture. *Journal of Materials Chemistry*. 22, 11379-11389 (2012). doi:10.1039/C2JM16183D
- [3] X. Gao; Z. Chen; Y. Yao; M. Zhou; Y. Liu; J. Wang; W.D. Wu; X.D. Chen; Z. Wu; D. Zhao, Direct Heating Amino Acids with Silica: A Universal Solvent-Free Assembly Approach to Highly Nitrogen-Doped Mesoporous Carbon Materials. *Advanced Functional Materials*. 26, 6649-6661 (2016). doi:10.1002/adfm.201601640
- [4] Z. Chen; X. Gao; X. Wei; X. Wang; Y. Li; T. Wu; J. Guo; Q. Gu; W.D. Wu; X.D. Chen; Z. Wu; D. Zhao, Directly anchoring Fe₃C nanoclusters and FeN_x sites in ordered mesoporous nitrogen-doped graphitic carbons to boost electrocatalytic oxygen reduction. *Carbon*. 121, 143-153 (2017). doi:10.1016/j.carbon.2017.05.078
- [5] Z. Wu; W.D. Wu; W. Liu; C. Selomulya; X.D. Chen; D. Zhao, A General "Surface-Locking" Approach toward Fast Assembly and Processing of Large-Sized, Ordered, Mesoporous Carbon Microspheres. *Angewandte Chemie International Edition*. 52, 13764-13768 (2013). doi:10.1002/anie.201307608

Open Access

This article is licensed under a [Creative Commons Attribution 4.0 International License](https://creativecommons.org/licenses/by/4.0/).

© The Author(s) 2017

Growth of TMDC Nanostructures by Chemical Vapor Deposition

Toshihiro Shimada,* Mengting Weng, Takashi Yanase, Sho Watanabe, Fumiya Uehara, Taro Nagahama

Division of Applied Chemistry, Hokkaido University, Kita-ku, Sapporo 060-8628, Hokkaido, Japan

Corresponding Author. Email: shimadat@eng.hokudai.ac.jp

Received: 31 May 2017, Accepted: 17 June 2017, Published Online: 14 October 2017

Citation Information: Toshihiro Shimada, Mengting Weng, Takashi Yanase, Sho Watanabe, Fumiya Uehara, Taro Nagahama, *Nano-Micro Conference, 2017, 1, 01024* doi: 10.11605/cp.nmc2017.01024

Abstract

Chemical vapor deposition (CVD) is a simple but powerful technique to synthesize thin films of various materials. It can also be used to synthesize nano-structured materials if it is used with nano-structured templates or catalysts. We have developed separate flow CVD system to make multilayered transition metal dichalcogenides (TMDCs) or doped layers [1,2]. We used the apparatus to make nanocomposite between carbon nanotube and MoS₂ that was applied to photovoltaic applications (Figure 1) [3]. We also describe the search for the catalysts to make TMDC nanostructures.

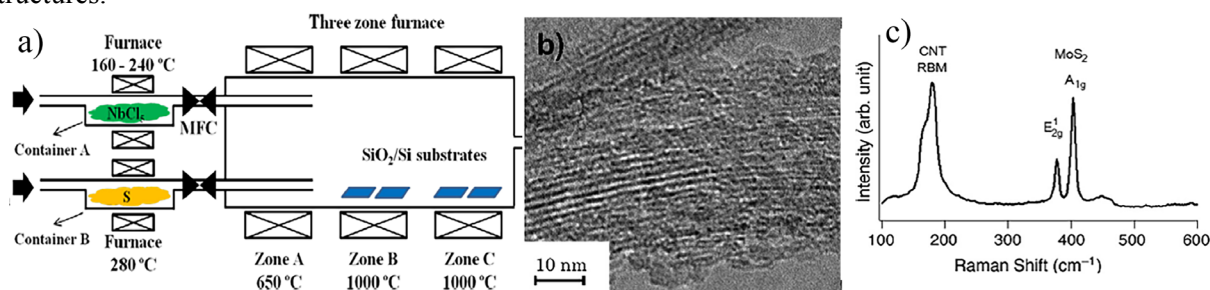


Figure 1. (a) Separate flow CVD [1,2] (b) TEM image and (c) Raman spectrum of MoS₂ nano flakes grown on carbon nanotube bundles [3].

References

- [1] T. Yanase; S. Watanabe; M. Weng; T. Nagahama; T. Shimada, Chemical vapor deposition of MoS₂: Insight into the growth mechanism by separated gas flow experiments. *Journal of Nanoscience and Nanotechnology*. 16, 3223-3227 (2016). doi:10.1166/jnn.2016.12313
- [2] T. Yanase; S. Watanabe; M. Weng; M. Wakeshima; Y. Hinatsu; T. Nagahama; T. Shimada, Chemical Vapor Deposition of NbS₂ from a Chloride Source with H₂ Flow: Orientation Control of Ultrathin Crystals Directly Grown on SiO₂/Si Substrate and Charge Wave Transition. *Crystal Growth & Design*. 16, 4467-4472 (2016). doi:10.1021/acs.cgd.6b00601
- [3] I. Jeon; D. Kutsuzawa; Y. Hashimoto; T. Yanase; T. Nagahama; T. Shimada; Y. Matsuo, Multilayered MoS₂ Nanoflakes Bound to Carbon Nanotubes as Electron Acceptors in Bulk Heterojunction Inverted Organic Solar Cells. *Organic Electronics*. 17, 275-280 (2015). doi:10.1016/j.orgel.2014.12.025

Open Access

This article is licensed under a [Creative Commons Attribution 4.0 International License](https://creativecommons.org/licenses/by/4.0/).

© The Author(s) 2017

Electrocatalytic hydrogen evolution reaction of MX₂ and MX₂ heterostructures

Yanfeng Zhang*

Department of Materials Science and Engineering, College of Engineering, Peking University, Beijing 100871, China

Corresponding Author. Email: yanfengzhang@pku.edu.cn

Received: 02 June 2017, Accepted: 16 June 2017, Published Online: 14 October 2017

Citation Information: Yanfeng Zhang, Nano-Micro Conference, 2017, 1, 01025 doi: 10.11605/cp.nmc.2017.01025

Abstract

Advanced materials for electrocatalytic and photoelectrochemical water splitting are central to the area of renewable energy. Recently, two dimensional layered materials of MX₂ (M: Mo, W; X: S, Se, etc.) have emerged as a new kind of catalysts for such applications. Our group have reported the direct synthesis of high-quality, domain size tunable, strictly monolayer MoS₂ flakes on commercially available Au foils by a chemical vapor deposition (CVD) method. The nano-sized triangular MoS₂ flakes on Au foils are proven to be excellent electrocatalysts for hydrogen evolution reaction (HER), featured by a rather low Tafel slope (61 mV/dec) and a relative high exchange current density (38.1 μA/cm²). The excellent electron coupling between MoS₂ and Au foils is considered to account for the extraordinary HER activity [1]. Furthermore, via a facile all-CVD approach, we have also demonstrated the direct growth of monolayer MoS₂ on graphene (MoS₂/Gr) over Au foils [2,3]. A dramatic decrease of the bandgap from ~2.20 to ~0.30 eV was detected at the domain edge of MoS₂ within a lateral distance of ~6 nm, as evidenced by STM/STS observations. The edges of monolayer MoS₂ nano-sheets were thus served as narrow-gap quantum wires, which can greatly facilitate the electrocatalytic property of MoS₂ in HER [4]. Meanwhile, we also synthesized either MoS₂/WS₂ or WS₂/MoS₂ vertical heterostructures on Au foils by a growth-temperature-mediated, selective two-step CVD strategy. Relative enhancement or reduction in the photocatalytic activities were observed for MoS₂/WS₂ and WS₂/MoS₂ in HER under illumination, respectively. This is explained from the type-II band alignment of the MoS₂/WS₂ stack that enables effective electron-hole separation and fast electron transfer kinetics, as well as directional electron flow from electrode to catalytically active sites [5]. The abovementioned efforts are expected to establish the internal relationship between the metallic edge states of MoS₂ and its HER performances, as well as the advantage of MX₂/MX₂ vertical stacks in photocatalytic HER applications.

References

- [1] J. P. Shi; D. L. Ma; G.-F. Han; Y. Zhang; Q. Q. Ji; T. Gao; J. Y. Sun; X. J. Song; C. Li; Y. S. Zhang; X.-Y. Lang; Y. F. Zhang; Z. F. Liu, Controllable Growth and Transfer of Monolayer MoS₂ on Au Foils and Its Potential Application in Hydrogen Evolution Reaction. ACS Nano. 8, 10196–10204 (2014). doi:10.1021/nn503211t
- [2] J. P. Shi; M. X. Liu; J. X. Wen; X. B. Ren; X. B. Zhou; Q. Q. Ji; D. L. Ma; Y. Zhang; C. H. Jin; H. J. Chen; S. Z. Deng; N. S. Xu; Z. F. Liu; Y. F. Zhang, All Chemical Vapor Deposition Synthesis and Intrinsic Bandgap Observation of MoS₂/Graphene Heterostructures. Advanced Materials. 27, 7086–7092 (2015). doi:10.1002/adma.201503342
- [3] J. P. Shi; Q. Q. Ji; Z. F. Liu; Y. F. Zhang, Recent Advances in Controlling Syntheses and Energy Related Applications of MX₂ and MX₂/Graphene Heterostructures. Advanced Energy Materials. 6, 1600459 (2016). doi:10.1002/aenm.201600459
- [4] J. P. Shi; X. B. Zhou; G.-F. Han; M. X. Liu; D. L. Ma; J. Y. Sun; C. Li; Q. Q. Ji; Y. Zhang; X. J. Song; X.-Y. Lang; Q. Jiang; Z. F. Liu; Y. F. Zhang, Narrow-Gap Quantum Wires Arising from the Edges of Monolayer MoS₂ Synthesized on Graphene. Advanced Materials Interfaces. 3, 1600332 (2016). doi:10.1002/admi.201600332
- [5] J. P. Shi; R. Tong; X. B. Zhou; Y. Gong; Z. P. Zhang; Q. Q. Ji; Y. Zhang; Q. Y. Fang; L. Gu; X. N. Wang; Z. F. Liu; Y. F. Zhang, Temperature-Mediated Selective Growth of MoS₂/WS₂ and WS₂/MoS₂ Vertical Stacks on Au Foils for Direct Photocatalytic Applications. Advanced Materials. 28, 10664–10672 (2016). doi:10.1002/adma.201603174

Open Access

This article is licensed under a [Creative Commons Attribution 4.0 International License](https://creativecommons.org/licenses/by/4.0/).

© The Author(s) 2017

Application of transition-metal dichalcogenides beyond general electronics

Yijin Zhang*

Max Planck Institute for Solid State Research, Heisenbergstr. 1, 70569 Stuttgart, Germany

Corresponding Author. Email: Y.Zhang@fkf.mpg.de

Received: 28 May 2017, Accepted: 18 June 2017, Published Online: 15 October 2017

Citation Information: Yijin Zhang, *Nano-Micro Conference*, 2017, 1, 01026 doi: 10.11605/cp.nmc2017.01026

Abstract

Transition-metal dichalcogenides (TMDs) are novel layered materials for various kind of application. In particular, those formed in hexagonal prismatic structure (Figure 1a) with group-VIB transition-metal are semiconductors in nature and show good transistor performance and strong light-matter interaction. However, the potential application of group-VIB TMDs is not only limited to such general electronics and optics, but also covers next-generation electronics of spintronics and valleytronics including the coupling to the optical polarization (Figure 1b) [1]. Owing to the lack of the inversion centre in the individual layer, the six conduction band minima and valence band maxima at the edge of the hexagonal Brillouin zone split into two groups, creating a valley degree of freedom. Optical interband transition at these high symmetry points are further coupled to the helicity of light. In addition, the heavy transition-metal elements leads to a large spin-orbit interaction and a consequent spin splitting.

Here, I will report our recent research aiming at next-generation electronics, including optoelectronic device utilizing valley degree of freedom [2,3] and the fundamental investigation of the spin relaxation in TMDs [4].

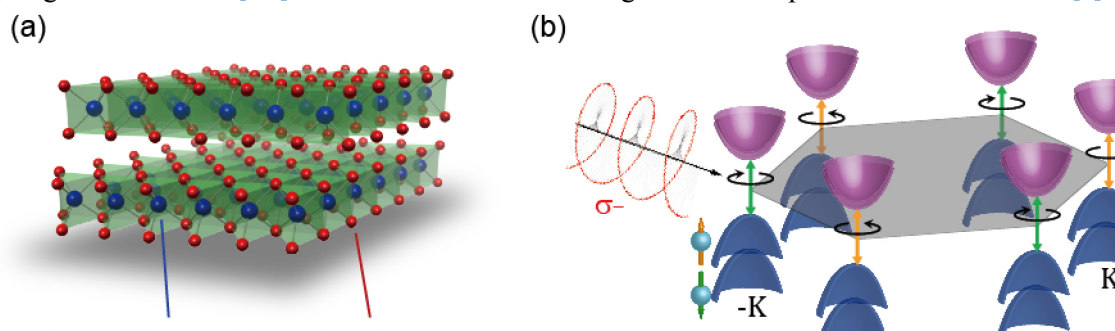


Figure 1. Crystal structure (a) and band structure (b) of group-VIB transition-metal dichalcogenides.

References

- [1] D. Xiao; G. B. Liu; W. X. Feng; X. D. Xu; W. Yao, Coupled spin and valley physics in monolayer MoS₂ and other group-VI dichalcogenides. *Physical Review Letters*. 108, 196802 (2012). doi:[10.1103/PhysRevLett.108.196802](https://doi.org/10.1103/PhysRevLett.108.196802)
- [2] Y. J. Zhang; T. Oka; R. Suzuki; J. T. Ye; Y. Iwasa, Electrically Switchable Chiral Light-Emitting Transistor. *Science*. 344, 725-728 (2014). doi:[10.1126/science.1251329](https://doi.org/10.1126/science.1251329)
- [3] M. Onga; Y. J. Zhang; R. Suzuki; Y. Iwasa, High circular polarization in electroluminescence from MoSe₂. *Applied Physics Letters*. 108, 073107 (2016). doi:[10.1063/1.4942367](https://doi.org/10.1063/1.4942367)
- [4] Y. J. Zhang; W. Shi; J. T. Ye; R. Suzuki; Y. Iwasa, Robustly protected carrier spin relaxation in electrostatically doped transition-metal dichalcogenides. *Physical Review B*. 95, 205302 (2017). doi:[10.1103/PhysRevB.95.205302](https://doi.org/10.1103/PhysRevB.95.205302)

Open Access

This article is licensed under a [Creative Commons Attribution 4.0 International License](https://creativecommons.org/licenses/by/4.0/).

© The Author(s) 2017

Prelithiated Si nanoparticles-carbon nanotubes composite anodes for Li-ion batteries

Kang Yao,^{1,2,3} Richard Liang,^{1,3,6} Jim P. Zheng^{1,2,4,5*}

¹Materials Science & Engineering,

²Aero-propulsion, Mechatronics and Energy Center,

³High-Performance Materials Institute,

⁴Center for Advanced Power Systems, Florida State University,

⁵Department of Electrical & Computer Engineering,

⁶Department of Industrial and Manufacturing Engineering,

Florida A&M University-Florida State University, Tallahassee, FL 32310, USA

Corresponding Author. Email: zheng@eng.famu.fsu.edu

Received: 11 May 2017, Accepted: 17 June 2017, Published Online: 15 October 2017

Citation Information: Kang Yao, Richard Liang, Jim P. Zheng, *Nano-Micro Conference*, 2017, 1, 01027 doi: 10.11605/cp.nmc2017.01027

Abstract

Freestanding flexible Si nanoparticles-multi-walled carbon nanotubes (SiNPs-MWNTs) composite paper anodes for Li-ion batteries (LIBs) have been prepared using a combination of ultra-sonication and pressure filtration. No conductive additive, binder or metal current collector is used. The SiNPs-MWNTs composite electrode material achieves first cycle specific discharge and charge capacities of 2298 and 1492 mAh/g, respectively. To address the first cycle irreversibility, stabilized Li metal powder (SLMP) has been utilized to pre-lithiate the composite anodes. As a result, the first cycle irreversible capacity loss is reduced from 806 to 28 mAh/g and the first cycle coulombic efficiency is increased from 65% to 98%. The relationship between different SLMP loadings and cell performance has been established to understand the pre-lithiation process of SLMP and to optimize the construction of Si-based cells. A cell containing the pre-lithiated anode is able to deliver charge capacity over 800 mAh/g without undergoing the initial discharge process, which enables the exploration of novel cathode materials.

It was also found out the SiNPs-MWNTs electrode with 3:2 Si/MWNT ratio exhibits the optimal balance between the high capacity of SiNPs and the high electrical conductivity and structural stabilization quality of MWNTs, leading to a high rate capability, high specific capacity, and cycle life surpassing the conventional slurry-cast SiNPs electrode using binder and Cu current collector. The reversible capacity is 1866 mAh/g (based on the total composite weight, the same below) at current density of 100 mA/g. After 100 cycles, the electrode retains capacity of 1170 mAh/g at 100 mA/g and 750 mAh/g at 500 mA/g. The superior performance is believed to be due to the cooperative or even synergistic effect achieved by the optimal combination. Furthermore, the freestanding feature of our electrode eliminates the non-active mass, which is promising for enhanced capacity and energy density of Li-ion cells.

Open Access

This article is licensed under a [Creative Commons Attribution 4.0 International License](https://creativecommons.org/licenses/by/4.0/).

© The Author(s) 2017

Investigating structure and stress evolution in Si anode using in situ high pressure technique and Raman microscopy

Zhidan Zeng*

Center for High Pressure Science and Technology Advanced Research (HPSTAR), Bldg 6, 1690 Cailun Road, Shanghai 201203, China

Corresponding Author. Email: zengzd@hpstar.ac.cn

Received: 22 May 2017, Accepted: 18 June 2017, Published Online: 15 October 2017

Citation Information: Zhidan Zeng, Nano-Micro Conference, 2017, 1, 01028 doi: 10.11605/cp.nmc2017.01028

Abstract

Silicon is widely regarded as one of the most promising anode materials for next-generation lithium-ion batteries, making Li-Si an important energy storage system. During Li insertion into Si, stress of gigapascal level is introduced accompanied by a volume expansion up to 280%, alters properties of materials, and leads to mechanical failure of Si anodes.

$\text{Li}_{15}\text{Si}_4$ (alpha- $\text{Li}_{15}\text{Si}_4$, space group: I-43d), the only crystalline phase that forms during lithiation of the Si anode in lithium-ion batteries, was found to undergo a structural transition to a new phase (beta- $\text{Li}_{15}\text{Si}_4$) at approximately 7 GPa (see Figure 1). Ab initio evolutionary metadynamics calculations suggest beta- $\text{Li}_{15}\text{Si}_4$ has an orthorhombic structure with an Fdd2 space group. This new beta- $\text{Li}_{15}\text{Si}_4$ has substantially larger elastic moduli compared with alpha- $\text{Li}_{15}\text{Si}_4$, and has good electrical conductivity. As a result, beta- $\text{Li}_{15}\text{Si}_4$ has superior resistance to deformation and fracture under stress. The theoretical volume expansion of Si would decrease 25% if it transformed to beta- $\text{Li}_{15}\text{Si}_4$, instead of alpha- $\text{Li}_{15}\text{Si}_4$, during lithiation. In addition, the fact that beta- $\text{Li}_{15}\text{Si}_4$ can be recovered back to ambient pressure, provides opportunities to further investigate its properties and potential applications [1].

Nanostructured Si are important materials to address mechanical stress issues in batteries although their stress were only calculated and no experimental data are available. Using in situ Raman microscopy to monitor the shift of the first-order Raman peak of Si, we were able to measure for the first time the lithiation-induced stress in Si nanoparticles. The shift of Raman peak of Si under hydrostatic stress was calibrated via an in situ high pressure Raman experiment. We observed a transition in the stress in Si core of nanoparticles during lithiation, from tensile to compressive (see Figure 2). At the beginning of lithiation, the reduction of the native oxide surface layer of the Si particle results in a tensile stress of approximately 0.2 GPa in Si. During the formation of amorphous Li_xSi in the outer layer of the nanoparticles, an increasing compressive stress up to 0.3 GPa is introduced to the Si core. This evolving stress explains the cracks that developed in the amorphous Li_xSi layer during lithiation of the Si nanoparticles, and is also consistent with modeling results. These results improve our understanding of lithiation-induced stress in nanostructured Si anodes, and provide valuable information for their theoretical study and future design [2].

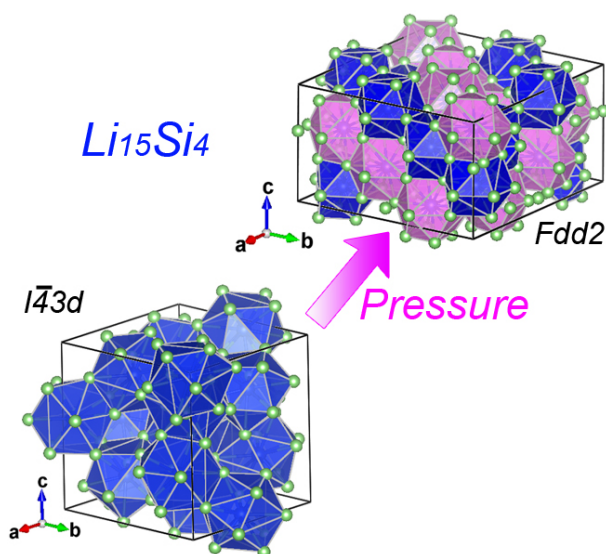


Figure 1. The atomic structure of alpha- $\text{Li}_{15}\text{Si}_4$ (lower left) and beta- $\text{Li}_{15}\text{Si}_4$ (upper right). Each silicon atom is surrounded by lithium atoms (green spheres) with the coordination number of 12 (shown in blue polyhedra) or 13 (shown in pink polyhedra).

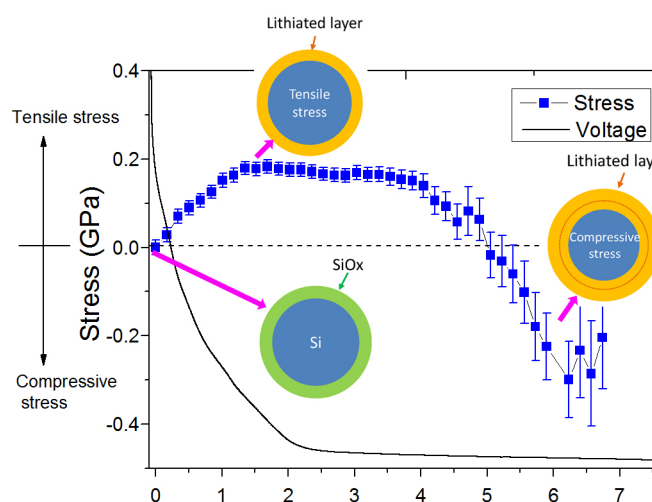


Figure 2. The stress in Si nanoparticles (left y-axis) and the potential of the half cell versus Li^+/Li (right y-axis) as a function of lithiation duration.

References

- [1] Zhidan Zeng; Qingfeng Zeng; Nian Liu; Artem R. Oganov; Qiaoshi Zeng; Yi Cui; Wendy L. Mao, A novel phase of $\text{Li}_{15}\text{Si}_4$ synthesized under pressure. *Advanced Energy Materials*. 5, 1500214 (2015). doi:[10.1002/aenm.201500214](https://doi.org/10.1002/aenm.201500214)
- [2] Zhidan Zeng; Nian Liu; Qiaoshi Zeng; Seok Woo Lee; Wendy L. Mao; Yi Cui, In situ measurement of lithiation-induced stress in silicon nanoparticles using micro-Raman spectroscopy. *Nano Energy*. 22, 105-110 (2016). doi:[10.1016/j.nanoen.2016.02.005](https://doi.org/10.1016/j.nanoen.2016.02.005)

Open Access

This article is licensed under a [Creative Commons Attribution 4.0 International License](https://creativecommons.org/licenses/by/4.0/).

© The Author(s) 2017

Silicon-based anode materials for high capacity lithium ion batteries

Junying Zhang, Chuanbo Li*

State Key Laboratory on Integrated Optoelectronics, Institute of Semiconductors, Chinese Academy of Sciences, Beijing 100083, China
Corresponding Author. Email: cbli@semi.ac.cn

Received: 05 June 2017, Accepted: 19 June 2017, Published Online: 16 October 2017

Citation Information: Junying Zhang, Chuanbo Li, *Nano-Micro Conference*, 2017, 1, 01029 doi: 10.11605/cp.nmc2017.01029

Abstract

Developing an anode material with high-energy capacity is crucial to improve the performance of rechargeable batteries. Si is an important anode candidate because of its large lithium storage capacity (4200 mAhg^{-1} , about 10 times higher than graphite, 372 mAhg^{-1}), low lithium alloying/dealloying potential, long discharge plateau, and abundance. However, the huge volume expansion/shrinkage of Si particles during charge/discharge cycles results in the pulverization of electrode structure and causes considerable capacity decay. The lack of electronic contacts between Si particles or between active coating materials and current collectors reduces its capacity. Many investigations have been carried out to accommodate this severe volume expansion including novel nanostructured Si, such as Si wires, Si tubes, porous thin films, and nest-like Si nanospheres, and multiphase composites with active Si and other active/inactive phases. However, the nano-sized Si particles would agglomerate during cycling which will decrease the cycling performance, due to high electrochemical activity. In this presentation, micro-sized polycrystalline Si particles have reduced agglomeration effect compared to nano-sized ones. We find that the electrochemical performances can be improved greatly by introducing proper binder to protect the electrode from cracking and using suitable conductive agent to provide an efficient conductive channel. By introducing nano-porous structures through chemical etching, the huge volume expansion can be effectively relieved by maintaining the complete structure of Si particles during charge/discharge cycles. Moreover, combined with carbon coating which is attractive owing to the conductive and ductile features of carbon, the conductivity can be improved and the volume expansion/shrinkage of Si can be further decreased. Developing nano-porous structure combining with pyrolyzed polyacrylonitrile could form a novel composite electrode. The electrochemical performance can be considerably improved with a conductive carbon network and nano-porous structure together with carbon layer accommodate the volume expansion/shrinkage during charge/discharge cycles.

Open Access

This article is licensed under a [Creative Commons Attribution 4.0 International License](https://creativecommons.org/licenses/by/4.0/).

© The Author(s) 2017

Efficient Solar-Rechargeable Lithium Ion Battery Energy Storage

Qiquan Qiao*

Centre for Advanced Photovoltaics, Electrical Engineering and Computer Science Department, South Dakota State University, Brookings, SD 57007, USA

Corresponding Author. Email: Qiquan.Qiao@sdstate.edu

Received: 11 June 2017, Accepted: 19 June 2017, Published Online: 19 October 2017

Citation Information: Qiquan Qiao, *Nano-Micro Conference*, 2017, 1, 01030 doi: 10.11605/cp.nmc2017.01030

Abstract

Use of energy storage devices such as lithium ion batteries (LIBs) can help to mitigate the problem of intermittent photovoltaic (PV) power to achieve higher PV penetration into the electric grid. Also, the benefit of deployment of electric vehicles for energy sustainable future seems rather irrelevant unless they are charged using electricity generated from renewables. In addition, large scale practical applications of battery based electric vehicles is still challenging because of the inflexibility it has with the charging stations. All these issues can be addressed by use of solar cells as a viable energy source to charge lithium ion batteries. Here we demonstrate simple, efficient and cost effective photo-charging design approach where the use of promising low cost solar cells such as perovskite solar cell or dye sensitized solar cell with the help of DC-DC power conversion can efficiently charge a $\text{Li}_4\text{Ti}_5\text{O}_{12}$ - LiCoO_2 LIB.

Open Access

This article is licensed under a [Creative Commons Attribution 4.0 International License](https://creativecommons.org/licenses/by/4.0/).

© The Author(s) 2017

High performances flexible energy storage devices

Bin Wang*

Institute of Chemical Materials, China Academy of Engineering Physics, No.596 Yinhe Road, Chengdu, Sichuan, China
 Corresponding Author. Email: binwang@caep.cn

Received: 31 May 2017, Accepted: 17 June 2017, Published Online: 19 October 2017

Citation Information: Bin Wang, Nano-Micro Conference, 2017, 1, 01031 doi: 10.11605/cp.nmc2017.01031

Abstract

In this work, the flexible fiber-shaped supercapacitors have been fabricated by using the conductive polymers and graphene as the electrodes. The prepared fiber-shaped electrodes show good mechanical properties and excellent electrochemical performances. They can be easily knotted, twisted and woven into different shapes without sacrificing their electrochemical properties [1-2].

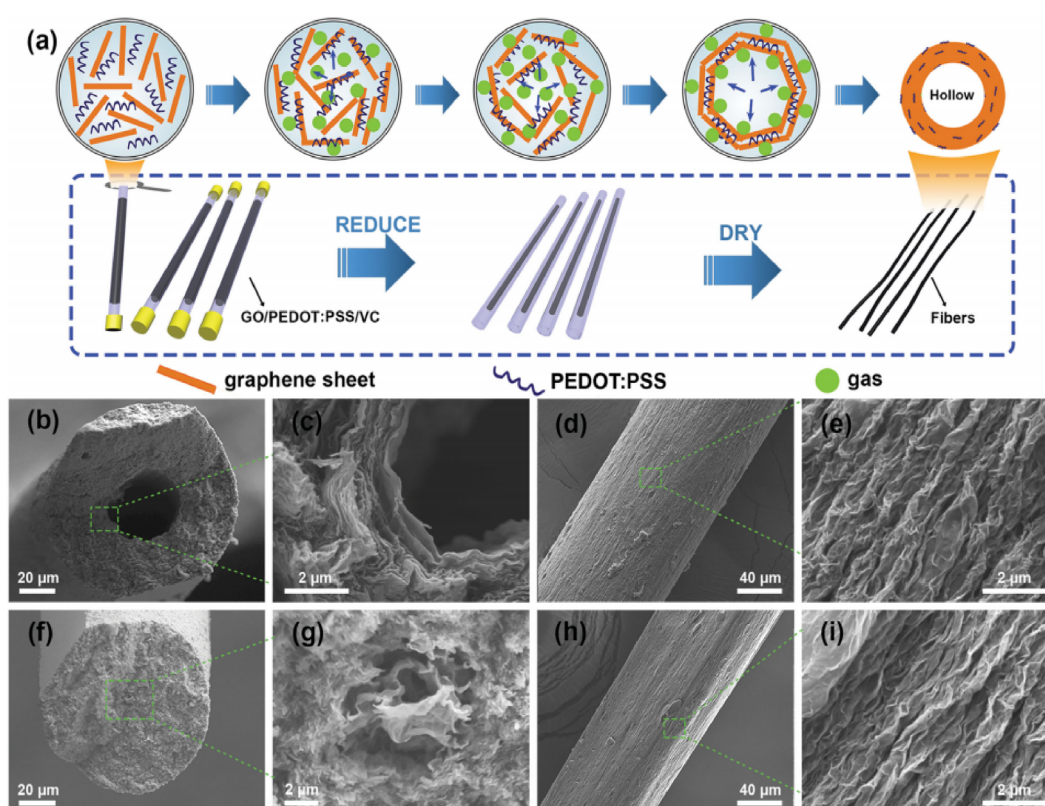


Figure 1. Schematic illustration and the SEM images of HCFs and formation of hollow structures.

References

- [1] Guoxing Qu; Jianli Cheng; Xiaodong Li; Demao Yuan; Peining Chen; Xuli Chen; Bin Wang; Huisheng Peng, A fiber supercapacitor with high energy density based on hollow graphene/conducting polymer fiber electrode. *Advanced Materials*. 28, 3646-3652 (2016). doi:10.1002/adma.201600689
- [2] Bin Wang; Chuangang Hua; Liming Dai, Functionalized carbon nanotubes and graphene-based materials for energy storage. *Chemical Communications*. 52, 14350-14360 (2016). doi:10.1039/C6CC05581H

Open Access

This article is licensed under a [Creative Commons Attribution 4.0 International License](https://creativecommons.org/licenses/by/4.0/).

© The Author(s) 2017

High Temperature Flexible Supercapacitors Using Graphene Electrodes

Ho Seok Park*

School of Chemical Engineering & Samsung Advanced Institute for Health Science & Technology (SAIHST), Sungkyunkwan University (SKKU), Suwon 440-746, Republic of Korea

Corresponding Author. Email: phs0727@skku.edu

Received: 16 May 2017, Accepted: 16 June 2017, Published Online: 20 October 2017

Citation Information: Ho Seok Park, Nano-Micro Conference, 2017, 1, 01032 doi: 10.11605/cp.nmc2017.01032

Abstract

With increasing demand for high performance energy storage systems, the feasibility of reliable and functional energy storage devices that well operates under extreme conditions is of prime importance for expanding applicative fields as well as for understanding materials' intrinsic and extrinsic properties and device physics. Our group has been investigating the control in the physical structure and chemical composition of 2D graphenes and beyond for ultracapacitive energy storage devices under limited circumstances, where conditions are classified into thermodynamic (e.g. pressure, volume and temperature) and kinetic (e.g. high rate and frequency) variables. We also studied a fundamental foundation via in-situ spectroscopic techniques to understand charge storage phenomenon of new materials and devices occurring on a nanoscale under various circumstances. In this talk, I will introduce high temperature operating, flexible supercapacitors based on graphene electrodes that can efficiently deliver electrical energy under electrochemical, mechanical and thermal stresses [1-4]. In order to achieve high performance supercapacitor devices under thermal, mechanical and electrochemical stresses, the micro- and macroscopic structures and chemical compositions of graphenes are delicately controlled by chemical modification. A new generation of flexible supercapacitors, with the long-term durability and outstanding electrochemical properties, were realized, showing a high position of the Ragone plot, even under severe conditions.

References

- [1] B. G. Choi; J. Hong; W. H. Hong; P. T. Hammond, Facilitated Ion Transport in All-Solid-State Flexible Supercapacitors. ACS Nano. 5, 7205-7213 (2011). doi:10.1021/nn202020w
- [2] B. C. Kim; J. Y. Hong; G. G. Wallace; H. S. Park, Recent Progress in Flexible Electrochemical Capacitors: Electrode Materials, Device Configuration, and Functions. Advanced Energy Materials. 5, 1500959 (2015). doi:10.1002/aenm.201500959
- [3] S. K. Kim; H. J. Kim; J. C. Lee; P. V. Braun; H. S. Park, Extremely Durable, Flexible Supercapacitors with Greatly Improved Performance at High Temperatures. ACS Nano. 9, 8569-8577 (2015). doi:10.1021/acsnano.5b03732
- [4] J. Y. Hong; B. M. Bak; J. J. Wie; J. Kong; H. S. Park, Reversibly Compressible, Highly Elastic, and Durable Graphene Aerogels for Energy Storage Devices under Limiting Conditions. Advanced Functional Materials. 25, 1053-1062 (2015). doi:10.1002/adfm.201403273

Open Access

This article is licensed under a [Creative Commons Attribution 4.0 International License](https://creativecommons.org/licenses/by/4.0/).

© The Author(s) 2017

Laser direct writing of high-performance micro-supercapacitors on graphene oxide and polymer films

Jinguang Cai,^{1*} Akira Watanabe^{2*}

¹Institute of Materials, China Academy of Engineering Physics, Jianguo 621908, Sichuan, PR China

²Institute of Multidisciplinary Research for Advanced Materials, Tohoku University, 2-1-1, Katahira, Sendai, 980-8577, Japan
Corresponding Author. Email: Jinguang Cai, caijinguang@foxmail.com; Akira Watanabe, watanabe@tagen.tohoku.ac.jp

Received: 17 May 2017, Accepted: 17 June 2017, Published Online: 20 October 2017

Citation Information: Jinguang Cai, Akira Watanabe, *Nano-Micro Conference*, 2017, 1, 01033 doi: 10.11605/cp.nmc2017.01033

Abstract

The rapid development of portable miniaturized electronics has improved the research demand for compact energy storage components with high energy and power densities. In recent several years, a new type on-chip energy storage unit, which is called micro-supercapacitor (MSC) with two interdigitated electrodes in the same plane, has attracted much research attention, because MSCs possess not only the advantages of the supercapacitors, such as high power densities, robust cycle performance, pollution-free operation, and maintenance-free features, but also the small size, light weight, and flexibility, as well as the simplified packaging processes and compatibility to the integrated circuits. However, the materials and fabrication methods should be cost-effective, scalable, and compatible with current electronic industries. Carbon materials, especially graphene, which possess high specific surface areas, electrochemical stability, high conductivity, and high mechanical tolerance, can meet the requirement for energy storage unit in flexible wearable devices. Laser induced carbonization from polymers and laser induced reduction of graphene oxide have been reported for the preparation of MSCs due to the high power at the focused area. Compared to the commonly used printing and lithographic techniques, laser direct writing is a non-contact fast single-step fabrication technique with no need for masks, post-processing, and complex clean environments. Moreover, the laser direct writing method has the potential to be integrated to current product lines for commercial use. Therefore, it is necessary and important to study the preparation of high-performance micro-supercapacitors on graphene oxide or polymer films by laser direct writing technique.

In this paper, we will introduce our recent studies on the laser direct writing of high-performance micro-supercapacitors on polyimide and graphene oxide films, which consists of the following several parts: the preparation of carbon MSCs by laser direct writing on polyimide films in air using a continuous-wave blue-violet semiconductor laser (Figure 1) [1]; the improvement of the carbon MSCs by laser direct writing in Ar [2]; the carbon/Au MSC with high-rate charge-discharge capacitive performance [3]; and electrolyte-free high-performance reduced graphene oxide (RGO)-GO-RGO MSCs prepared by laser direct writing on graphene oxide films (Figure 2) [4].

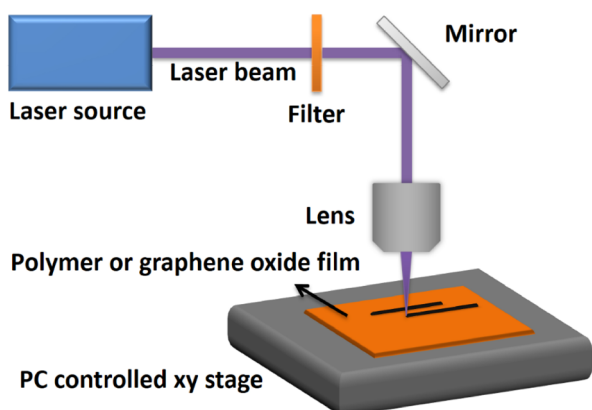


Figure 1. Schematic illustration of the laser direct writing system.

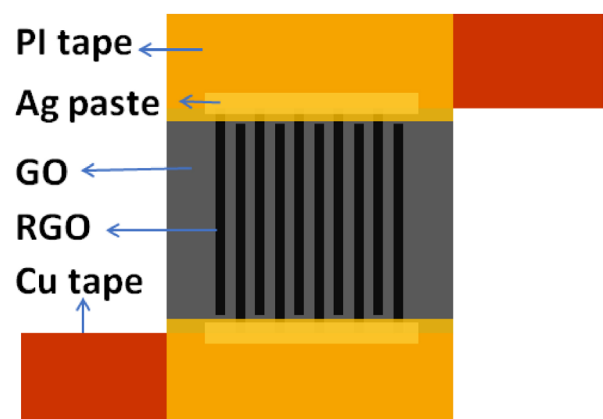


Figure 2. Schematic illustrating of a MSC device obtained by laser direct writing. Ag paste was used to make good connection between Cu tape electrodes and RGO lines.

References

- [1] J. Cai; C. Lv; A. Watanabe, Cost-effective fabrication of high-performance flexible all-solid-state carbon micro-supercapacitors by blue-violet laser direct writing and further surface treatment. *Journal of Materials Chemistry A*. 4, 1671 (2016). doi:10.1039/c5ta09450j
- [2] J. Cai; C. Lv; A. Watanabe, Laser direct writing of high-perfor-

- mance flexible all-solid-state carbon micro-supercapacitors for an on-chip self-powered photodetection system. *Nano Energy*. 30, 790 (2016). doi:10.1016/j.nanoen.2016.09.017
- [3] J. Cai; C. Lv; A. Watanabe, Laser direct writing of carbon/Au composite electrodes for high-performance micro-supercapacitors. *Proceedings SPIE 10092, Laser-based Micro- and Nanoprocessing*

XI. 100920P (2017). doi:[10.1117/12.2251151](https://doi.org/10.1117/12.2251151)

[4] J. Cai; C. Lv; A. Watanabe, Laser direct writing micro-supercapacitors from graphene oxide films. IEEE 16th International Conference on Nanotechnology (IEEE-NANO) in Sendai, Japan, 2016. doi:[10.1109/NANO.2016.7751433](https://doi.org/10.1109/NANO.2016.7751433)

Open Access

This article is licensed under a [Creative Commons Attribution 4.0 International License](https://creativecommons.org/licenses/by/4.0/).

© The Author(s) 2017

Rational Design of Novel Carbon Catalysts for Clean Energy Conversion and Storage

Zhenghang Zhao, Zhenhai Xia*

University of North Texas, 3940 North Elm St., Denton, TX 76203, USA

Corresponding Author. Email: Zhenhai.xia@unt.edu

Received: 01 June 2017, Accepted: 17 June 2017, Published Online: 20 October 2017

Citation Information: Zhenghang Zhao, Zhenhai Xia, *Nano-Micro Conference, 2017, 1, 01034* doi: 10.11605/cp.nmc.2017.01034

Abstract

In fuel cells and metal-air batteries, there are critical chemical reactions: oxygen reduction reaction (ORR), and oxygen evolution reaction (OER), respectively. These reactions, however, are sluggish and require noble metals (e.g., platinum) or their oxides as catalysts. The scarcity and high cost of noble metals have hampered the commercial applications of these technologies [1]. Therefore, it is necessary to search for alternative materials to replace Pt. Carbon nanomaterials, such as carbon nanotubes (CNTs) and graphene, are appealing as an alternative for metal-free catalytic applications because of their structures and excellent properties. Although the superior catalytic capabilities of heteroatom-doped carbon nanomaterials for ORR have been demonstrated, trial-and-error approaches are still used to date for the development of highly-efficient catalysts. To rationally design a catalyst, it is critical to correlate intrinsic material characteristics with catalytic activities. Through first-principles calculations, we have identified a material property that serves as the activity descriptor for both ORR and OER, and established a volcano relationship between the descriptor and the catalytic activities of the carbon-based nanomaterials [2]. The design principles can be used as a guidance to develop various new carbon-based materials for clean energy conversion and storage.

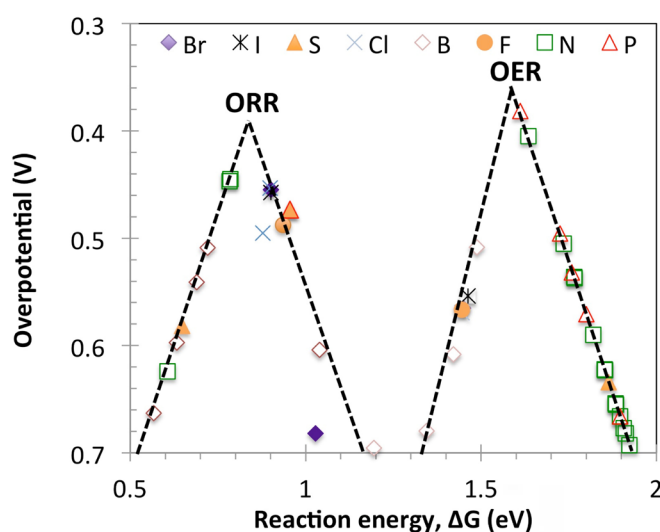


Figure 1. Volcano relationships between the descriptor and the catalytic activities of the carbon-based nanomaterials.

References

- [1] C. Sealy, The problem with platinum. *Materials Today*. 11, 65-68 (2008). doi:10.1016/S1369-7021(08)70254-2
- [2] Z. Zhao; M. Li; L. Zhang; L. Dai; Z. Xia, Design Principles for Heteroatom-doped Carbon Nanomaterials as Highly-efficient Catalysts for Fuel Cells and Metal-air Batteries, *Advanced Materials*. 27, 6834-6840 (2015). doi:10.1002/adma.201503211

Open Access

This article is licensed under a [Creative Commons Attribution 4.0 International License](https://creativecommons.org/licenses/by/4.0/).

© The Author(s) 2017

Low Dimensional Materials Used for Lithium/Sodium ion Battery Anode

Gaoxiang Wu, Xiaodan Li, Jiewei Chen, Yanjiao Guo, Bi Luo, Bing Jiang, Lihua Chu, Meicheng Li*

State Key Laboratory of Alternate Electrical Power System with Renewable Energy Sources, School of Renewable Energy, North China Electric Power University, Beinong Road 2, Beijing 102206, China

Corresponding Author. Email: mcli@ncepu.edu.cn

Received: 05 June 2017, Accepted: 19 June 2017, Published Online: 21 October 2017

Citation Information: Gaoxiang Wu, Xiaodan Li, Jiewei Chen, Yanjiao Guo, Bi Luo, Bing Jiang, Lihua Chu, Meicheng Li, *Nano-Micro Conference*, 2017, 1, 01035 doi: [10.11605/ep.nmc2017.01035](https://doi.org/10.11605/ep.nmc2017.01035)

Abstract

The exploitation of high-performance lithium ion batteries is an effective way to promote the practicality of electric vehicles and the large scale development of renewable energy. We have designed and used a low temperature solution approach which is simple, low cost, scalable to synthesize $Zn_2GeO_4/g-C_3N_4$ hybrid structure. Furthermore the synergistic effect on their lithium storage has been discussed. The $Zn_2GeO_4/g-C_3N_4$ hybrids exhibited highly reversible capacity of 1370 mA h g^{-1} at 200 mA g^{-1} after 140 cycles and excellent rate capability of 950 mA h g^{-1} at 2000 mA g^{-1} . On the other hand, molybdenum sulfide, one of the transition metal sulfides, has been considered as a hopeful anode material, because of the small volume change ($\sim 103\%$) and the high theoretical capacity ($669\sim 1675 \text{ mA h g}^{-1}$). In order to improve the electrochemical properties of molybdenum sulfide, we have designed and prepared $TiO_2@MoS_2$ core-shell structure. This composite structure provides a plenty of surface active sites for rapid transportation of lithium ions and orderly path for electrons. As a result, the electrochemical performance of $TiO_2@MoS_2$ is much higher than that of molybdenum sulfide as well as titanium dioxide. In addition, transition metal oxides also have been attracted widespread attention, because of its versatile nanostructures, high theoretical capacity and small volume change. We have synthesized 3D NiO microsphere architecture assembled from porous nanosheets via easy hydrothermal method. The advantage of large specific surface area endows the as-prepared 3D NiO microspheres with a good performance of stable and high reversible discharge capacity up to 820 mA h g^{-1} even after 100 cycles at a current density of 100 mA g^{-1} , and good rate capability of 634 mA h g^{-1} at a high current density of 1 A g^{-1} .

References

- [1] Xiaodan Li; Gaoxiang Wu; Xin Liu; Wei Li; Meicheng Li, Orderly integration of porous $TiO_2(B)$ nanosheets into bunched hierarchical structure for high-rate and ultralong-lifespan lithium-ion batteries. *Nano Energy*. 31, 1-8 (2017). doi:[10.1016/j.nanoen.2016.11.002](https://doi.org/10.1016/j.nanoen.2016.11.002)
- [2] Xiaodan Li; Gaoxiang Wu; Jiewei Chen; Meicheng Li; Wei Li; Tianyue Wang; Bing Jiang; Yue He; Liqiang Mai, Low-crystallinity molybdenum sulfide nanosheets assembled on carbon nanotubes for long-life lithium storage: Unusual electrochemical behaviors and ascending capacities. *Applied Surface Science*. 392, 297-304 (2017). doi:[10.1016/j.apsusc.2016.09.055](https://doi.org/10.1016/j.apsusc.2016.09.055)
- [3] Lihua Chu; Meicheng Li; Yu Wang; Xiaodan Li; Zipei Wan; Shangyi Dou; Yue Chu, Multishelled NiO Hollow Spheres Decorated by Graphene Nanosheets as Anodes for Lithium-Ion Batteries with Improved Reversible Capacity and Cycling Stability. *Journal of Nanomaterials*. 2016, 4901847 (2016). doi:[10.1155/2016/4901847](https://doi.org/10.1155/2016/4901847)
- [4] Xiaodan Li; Yi Feng; Meicheng Li; Wei Li; Hao Wei; Dandan Song, Smart Hybrids of Zn_2GeO_4 Nanoparticles and Ultrathin $g-C_3N_4$ Layers: Synergistic Lithium Storage and Excellent Electrochemical Performance. *Advanced Functional Materials*. 25 6858-6866 (2015). doi:[10.1002/adfm.201502938](https://doi.org/10.1002/adfm.201502938)
- [5] Xiaodan Li; Wei Li; Meicheng Li; Peng Cui; Dehong Chen; Thomas Gengenbach; Lihua Chu; Huiyuan Liu; Guangsheng Song, Glucose-assisted synthesis of the hierarchical TiO_2 nanowire@ MoS_2 nanosheet nanocomposite and its synergistic lithium storage performance. *Journal of Materials Chemistry A*. 3, 2762-2769 (2015). doi:[10.1039/C4TA05249H](https://doi.org/10.1039/C4TA05249H)
- [6] Peng Cui; Bixia Xie; Xiaodan Li; Meicheng Li; Yaoyao Li; Yu Wang; Zhuohai Liu; Xin Liu; Jing Huang; Dandan Song; Joseph Michel Mbengue, Anatase/ TiO_2 -B hybrid microspheres constructed from ultrathin nanosheets: facile synthesis and application for fast lithium ion storage. *CrystEngComm*. 17, 7930-7937 (2015).

doi:[10.1039/C5CE01600B](https://doi.org/10.1039/C5CE01600B)

[7] Lihua Chu; Meicheng Li; Xiaodan Li; Yu Wang; Zipei Wan; Shangyi Dou; Dandan Song; Yingfeng Li; Bing Jiang, High performance NiO microsphere anode assembled from porous nanosheets for lithium-ion batteries. *RSC Advances*. 5, 49765-49770 (2015). doi:[10.1039/C5RA05659D](https://doi.org/10.1039/C5RA05659D)

Open Access

This article is licensed under a [Creative Commons Attribution 4.0 International License](https://creativecommons.org/licenses/by/4.0/).

© The Author(s) 2017

Functionalized graphene with both physical and chemical adsorptions of charges for high-performance supercapacitors

Jinzhang Liu,* Yi Zhao

School of Materials Science and Engineering, Beihang University, Beijing 100191, China

Corresponding Author. Email: ljz78@buaa.edu.cn

Received: 26 May 2017, Accepted: 17 June 2017, Published Online: 24 October 2017

Citation Information: Jinzhang liu, Yi Zhao, Nano-Micro Conference, 2017, 1, 01036 doi: 10.11605/cp.nmc2017.01036

Abstract

Carbon-based supercapacitor is also called electric double-layer capacitor that store energy via physical adsorption and desorption of ions from the electrolyte. Pseudocapacitors based on metal oxides or conductive polymers store energy via a redox process and generally have higher specific capacitance compared to the EDL type. Graphene has been regarded as an ideal candidate for supercapacitor applications, while the specific capacitance achieved so far in the lab, normally 200-300 F/g, is much lower than its theoretical value of 550 F/g. In order to enhance the charge storage capacity of graphene, we functionalized reduced graphene oxide by N-doping and adsorption of small molecules of hydrolyzed polyimide (PI). In N-doped graphene, the N-O bonds are responsible for the enhanced capacitance owing to their pseudo capacitive property [1]. Further, we found that the hydrolysis of PI can release small molecules into water solution, and these aromatic molecules adsorbed onto graphene via π - π interaction have a significant effect in increasing the capacitance. With merely 3% weight increase after adsorption, the specific capacitance is about 40% increased. High capacitance over 420 F/g can be easily achieved from the functionalized graphene electrode in H_2SO_4 aqueous electrolyte, even the electrode has high mass loading around 5 mg/cm^2 . In Li_2SO_4 aqueous electrolyte that can extend the operation voltage window to 1.6 V, the specific capacitance also remains high around 400 F.

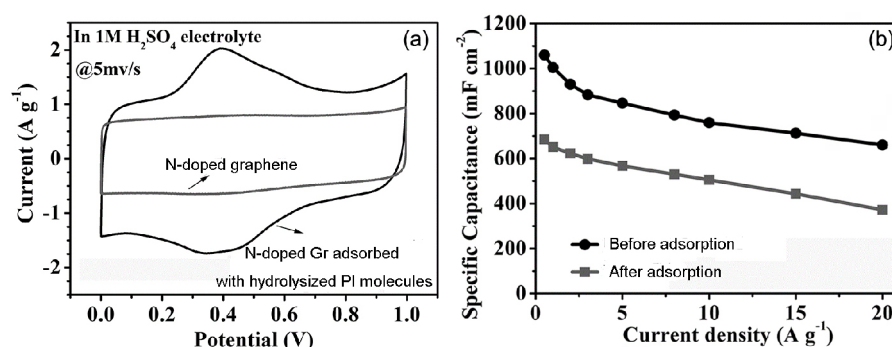


Figure 1. (a) Comparison to the electrochemical performance of N-doped graphene electrode before and after adsorption of hydrolyzed PI molecules. (a) CV curves. (b) Capacitance Vs. discharging current density in galvanostatic CD measurement.

References

- [1] T. Lin; I.-W. Chen; F. Liu; C. Yang; H. Bi; F. Xu; F. Huang. Nitrogen-doped mesoporous carbon of extraordinary capacitance for electrochemical energy storage. *Science*. 350, 1508-1513 (2015). doi:10.1126/science.aab3798

Open Access

This article is licensed under a [Creative Commons Attribution 4.0 International License](https://creativecommons.org/licenses/by/4.0/).

© The Author(s) 2017

How to improve the hydrogen storage of graphene based systems?

Santhanamoorthi Nachimuthu, Jyh-Chiang Jiang*

Department of Chemical Engineering, National Taiwan University of Science and Technology, Taipei 106, Taiwan

Corresponding Author. Email: jcjiang@mail.ntust.edu.tw

Received: 24 May 2017, Accepted: 16 June 2017, Published Online: 25 October 2017

Citation Information: Santhanamoorthi Nachimuthu, Jyh-Chiang Jiang, *Nano-Micro Conference, 2017, 1, 01037* doi: 10.11605/cp.nmc2017.01037

Abstract

In the last two decades, the significant efforts have been made to develop alternative energy sources instead of fossil fuels because of increasing CO₂ emissions and the environmental impacts. Besides; hydrogen has been concerned to be an ideal clean energy carrier among the other renewable energy sources because of its environmental friendliness. However, some challenges have to be addressed before hydrogen will become a conventional and commonly available energy carrier. Carbon-based materials such as graphene and carbon nanotubes have been designed for hydrogen storage due to their large surface area, light weight, and tunable properties. Recently, we proposed a new strategy in which we considered three pure transition metal (TM) atoms or/and a combination of two TM atoms and one alkali earth metal atom (AEM) with high, medium and low hydrogen adsorption energies. These different metal atoms are used to decorate the Boron doped graphene sheet (BDG) and investigated their performance towards hydrogen storage capacity through spillover mechanism using first-principles calculations. Our results indicate that the activation energies for H atom diffusion are much smaller, indicating that a fast H diffusion on this proposed surface can be achieved. These TM and AEM atoms decorated BDG surface can have the maximum hydrogen gravimetric capacity of 6.4% for double-sided adsorptions. To achieve higher gravimetric density, we also considered the Boron and Nitrogen co-doped graphene surface (BNDG) because B–N pair is isoelectronic to the C–C pair. However, controlling the binding strength of considered metal atoms with that of the BNDG surface is an important issue in the application of hydrogen storage. The recent studies have shown that the binding strength between the metal atom and the substrate can be controlled by means of applying an external electric field. Thus, the effects of the external electric field, as well as the effects of applying point charges on the designed medium towards its hydrogen storage capacity, will be discussed.

References

- [1] S. Nachimuthu; P-J. Lai; E. G. Leggesse; J. C. Jiang, A First Principles study on Boron-doped Graphene decorated by Ni-Ti-Mg atoms for Enhanced Hydrogen Storage Performance. *Scientific Reports*. 5, 16797 (2015). doi:[10.1038/srep16797](https://doi.org/10.1038/srep16797)
- [2] S. Nachimuthu; P-J. Lai; J. C. Jiang, Efficient hydrogen storage in boron doped graphene decorated by transition metals – A first-principles study. *Carbon*. 73, 132-140 (2014). doi:[10.1016/j.carbon.2014.02.048](https://doi.org/10.1016/j.carbon.2014.02.048)

Open Access

This article is licensed under a [Creative Commons Attribution 4.0 International License](https://creativecommons.org/licenses/by/4.0/).

© The Author(s) 2017

Ternary Nanostructured Photocatalysts for Photoelectrochemical Water Splitting

Meng Nan Chong,^{1,2*} Yi Wen Phuan¹

¹School of Engineering, Chemical Engineering Discipline, Monash University Malaysia, Jalan Lagoon, Selatan, Bandar Sunway, Selangor Darul Ehsan 47500 Malaysia

²Sustainable Water Alliance, Monash University Malaysia, Jalan Lagoon Selatan, Bandar Sunway, Selangor Darul Ehsan 47500 Malaysia
Corresponding Author. Email: Chong.Meng.Nan@monash.edu

Received: 11 May 2017, Accepted: 16 June 2017, Published Online: 25 October 2017

Citation Information: Meng Nan Chong, Yi Wen Phuan, *Nano-Micro Conference*, 2017, 1, 01038 doi: 10.11605/cp.nmc2017.01038

Abstract

The world's population is growing continuously and in close proportionality to the demand on fossil fuels, which may lead to its depletion in the coming decades. The ability to harness energy from renewable resources is highly desirable for sustainable energy economy. In recent years, photoelectrochemical (PEC) water splitting process based on Earth-abundant semiconductor photocatalysts has gained considerable research interests for resolving energy and environmental issues. The PEC water splitting that mimics the natural photosynthesis process can convert solar energy into storable form of hydrogen (H₂) energy, which is a good energy vector to meet the escalating energy demand. To date, however, almost all singular semiconductor photocatalysts used demonstrated poor PEC performance for solar-to-H₂ energy conversion. In this study, two different novel ternary nanostructured hematite-based photocatalysts of eRGO/C60/ α -Fe₂O₃ and eRGO/NiO/ α -Fe₂O₃ were synthesized, characterised and tested as photoanodes toward PEC water splitting application. The ternary nanostructured hematite-based photoanodes were characterised using FE-SEM, EDX, XRD, XPS, as well as Raman, UV-Vis and EIS spectroscopic methods. It was found that the ternary nanostructured photoanodes of eRGO/C60/ α -Fe₂O₃ and eRGO/NiO/ α -Fe₂O₃ showed 5-fold and 9-fold enhancement in current density and significant reduction in charge transfer resistance when compared to the pristine hematite photoanode. In this instance, the enhancement in PEC performance of ternary nanostructured eRGO/C60/ α -Fe₂O₃ photoanode was attributed to the electrons scavenging property of C60 as well as the highly conducting eRGO property that have mitigated the high interfacial recombination rate of photogenerated electron-hole pairs. Whilst for the ternary nanostructured eRGO/NiO/ α -Fe₂O₃ photoanode, eRGO transferred the electrons efficiently in the p-n heterojunction without causing substantial bulk recombination. Additionally, the internal electrostatic field in eRGO/NiO/ α -Fe₂O₃ could facilitate the effective separation of photogenerated electron-hole pairs so that more holes could participate in the water oxidation reaction instead of recombination process. It is anticipated that the fundamental understanding gained through this study is helpful to design and construct high-performance photoelectrodes for the application in PEC water splitting in the near future.

Open Access

This article is licensed under a [Creative Commons Attribution 4.0 International License](https://creativecommons.org/licenses/by/4.0/).

© The Author(s) 2017

Van der Waals Oxide Heteroepitaxy for Transparent and Flexible Electronics

Ying-Hao Chu*

National Chiao Tung University, Department of Materials Science & Engineering, 1001 University Road, Engineering Building 6, R318, Hsinchu 30010, Taiwan

Corresponding Author. Email: yhc@nctu.edu.tw

Received: 18 May 2017, Accepted: 17 June 2017, Published Online: 25 October 2017

Citation Information: Ying-Hao Chu, *Nano-Micro Conference, 2017, 1, 01039* doi: [10.11605/cp.nmc2017.01039](https://doi.org/10.11605/cp.nmc2017.01039)

Abstract

In the diligent pursuit of low-power consumption, multifunctional, and environmentally friendly electronics, more sophisticated requirements on functional materials are on demand. For example, flexible electronics represents a fast-developing field and has a great potential to impact our daily life. In building up flexible electronics, the materials with controllable conduction, transparency, and good flexibility are required. Recently, the discovery of free-standing 2D materials has created a revolution to this field. Pioneered by graphene, these new 2D materials exhibit abundant unusual physical phenomena that is undiscovered in bulk forms. In the meantime, it also possesses very high transparency to the visible light. However, the extensively studied pristine graphene naturally has no bandgap and become restricted in many field-effect based applications. Hence, looking for various types of new 2D materials has been a focal research direction nowadays. In this talk, we intend to take the same concept, but to integrate a family of functional materials in order to open new avenue to flexible electronics. Due to the interplay of lattice, charge, orbital, and spin degrees of freedom, correlated electrons in oxides generate a rich spectrum of competing phases and physical properties. However, a generic approach to build up flexible electronics based on functional oxides is yet to be developed. In this study, we use a 2D material as the substrate. And we take several functional oxides as model systems, including transparent conducting oxides, VO_2 , NiO , Fe_3O_4 , $\text{Pb}(\text{Zr,Ti})\text{O}_3$, and oxide nanocomposites, to demonstrate a pathway to build up functional oxides for transparent and flexible electronics.

Open Access

This article is licensed under a [Creative Commons Attribution 4.0 International License](https://creativecommons.org/licenses/by/4.0/).

© The Author(s) 2017

Nanowire-plasmonic photocatalysts and thermal emitters

Thang Duy Dao,^{1*} Tadaaki Nagao,^{1,2*} Kai Chen,¹ Shatoshi Ishii,¹ Gui Han¹

¹International Center for Materials Nanoarchitectonics (MANA), National Institute for Materials Science (NIMS), 1-1 Namiki, Tsukuba, Ibaraki 305-0044, Japan

²Condensed Matter Physics, Graduate School of Science, Hokkaido University, Kita 8, Nishi 5, Kita-ku, Sapporo 060-0810, Japan

Corresponding Author. Email: Thang Duy Dao, DAO.Duythang@nims.go.jp; Tadaaki Nagao, NAGAO.Tadaaki@nims.go.jp

Received: 12 June 2017, Accepted: 19 June 2017, Published Online: 25 October 2017

Citation Information: Thang Duy Dao, Tadaaki Nagao, Kai Chen, Shatoshi Ishii, Gui Han, Nano-Micro Conference, 2017, 1, 01040 doi: 10.11605/cp.nmc2017.01040

Abstract

Optical absorption enhancement using plasmonic structures enables a wide range of applications such as solar energy harvesting devices, light emitting devices and photothermal management. For example, in plasmonic photocatalysis, it has recently attracted great interest in enhancing photocatalytic efficiency not only by the plasmon-enhanced near field but also by the plasmon-enhanced hot-carrier injection, which could boost the visible response of wide bandgap photocatalysts [1]. Here we report measurements and simulations of the efficient sunlight-driven and visible-active photocatalysts composed of plasmonic metals and ZnO nanowire (NW) arrays fabricated via an all-wetchemical route (Figure 1a) [2]. Another application of plasmon-enhanced light absorption is the perfect absorber and thermal emitter [3]. It is found that with proper designs supported by the electromagnetic simulation, the plasmonic structures could exhibit near perfect absorption at desired resonant wavelengths, making them promising for a number of potential application such as thermal emitters (Figure 1b) [4], molecular sensors [5] and IR sensors [6].

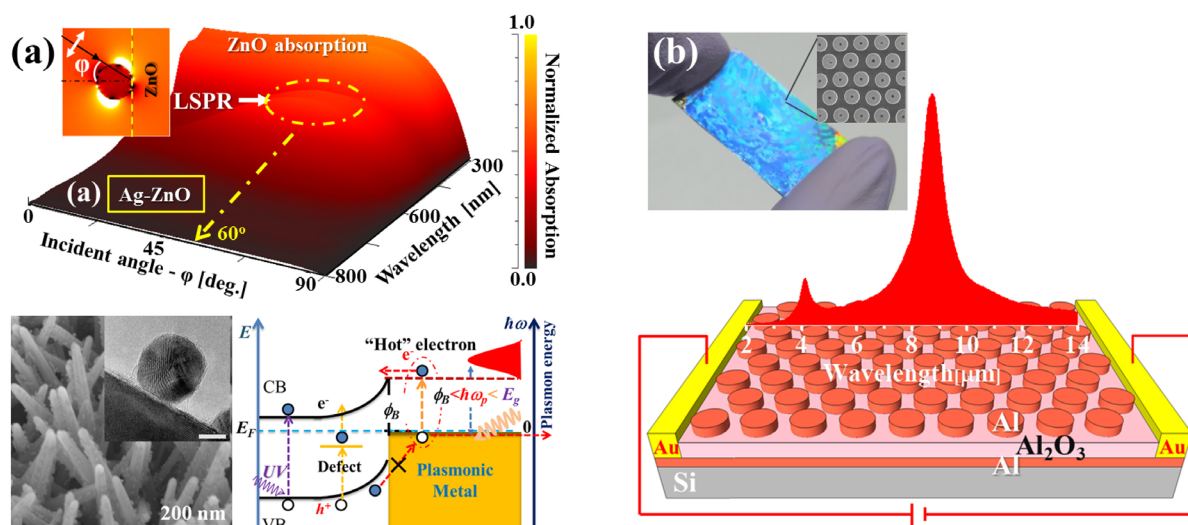


Figure 1. (a) Plasmon-mediated photocatalytic activity of ZnO NWs. (b) Plasmonic absorbers for thermal emitters.

References

- [1] M. L. Brongersma; N. J. Halas; P. Nordlander, Plasmon-induced hot carrier science and technology. *Nature Nanotechnology*. 10, 25-34 (2015). doi:10.1038/nnano.2014.311
- [2] T. D. Dao; G. Han; N. Arai; T. Nabatame; Y. Wada; C. V. Hoang; M. Aono; T. Nagao, Plasmon-mediated photocatalytic activity of wet-chemically prepared ZnO nanowire arrays. *Physical Chemistry Chemical Physics*. 17, 7395-7403 (2015). doi:10.1039/C4CP05843G
- [3] X. Liu; T. Tyler; T. Starr; A. F. Starr; N. M. Jokerst; W. J. Padilla, Taming the Blackbody with Infrared Metamaterials as Selective Thermal Emitters. *Physical Review Letters*. 107, 045901 (2011). doi:10.1103/PhysRevLett.107.045901
- [4] T. D. Dao; K. Chen; S. Ishii; A. Ohi; T. Nabatame; M. Kitajima; T. Nagao, Infrared Perfect Absorbers Fabricated by Colloidal Mask Etching of Al-Al₂O₃-Al Trilayers. *ACS Photonics*. 2, 964-970 (2015). doi:10.1021/acsp Photonics.5b00195
- [5] K. Chen; T. D. Dao; S. Ishii; M. Aono; T. Nagao, Infrared Aluminum Metamaterial Perfect Absorbers for Plasmon-Enhanced Infrared

Spectroscopy. *Advanced Functional Materials*. 25, 6637-6643 (2015). doi:10.1002/adfm.201501151

- [6] T. D. Dao; S. Ishii; T. Yokoyama; T. Sawada; R. P. Sugavaneshwar; K. Chen; Y. Wada; T. Nabatame; T. Nagao, Hole Array Perfect Absorbers for Spectrally Selective Midwavelength Infrared Pyroelectric Detectors. *ACS Photonics*. 3, 1271-1278 (2016). doi:10.1021/acsp Photonics.6b00249

Open Access

This article is licensed under a [Creative Commons Attribution 4.0 International License](https://creativecommons.org/licenses/by/4.0/).

© The Author(s) 2017

New Heterogeneous Photocatalysts Designed for Water Oxidation and CO₂ Reduction

Kazuhiko Maeda*

School of Science, Tokyo Institute of Technology, 2-12-1-NE-2 Ookayama, Meguro-ku, Tokyo

Corresponding Author. Email: maedak@chem.titech.ac.jp

Received: 17 May 2017, Accepted: 16 June 2017, Published Online: 26 October 2017

Citation Information: Kazuhiko Maeda, Nano-Micro Conference, 2017, 1, 01041 doi: 10.11605/cp.nmc2017.01041

Abstract

Water splitting and CO₂ fixation on heterogeneous photocatalysts are importance reactions from the viewpoint of solar-to-fuel energy conversion. To achieve these reactions, it is important to improve both bulk and surface properties of a photocatalyst so as to suppress electron-hole recombination and promote surface redox catalysis. In this presentation, recent progress on the development of new photocatalysts that are active for such artificial photosynthetic reactions will be given. In particular, surface modification techniques developed by our group to construct active sites and light-absorbing centers will be presented. For example, we developed a new powdered photocatalyst consisting of Co(OH)₂ and TiO₂ [1]. It is well known that TiO₂ is an active photocatalyst, but only works under UV irradiation. By contrast, the Co(OH)₂/TiO₂ hybrid photocatalyst is capable of absorbing visible light with wavelengths of up to 850 nm and oxidizing water into oxygen gas, even though it consists of only earth-abundant elements only. To our knowledge, this system provides the first demonstration of a photocatalytic material capable of water oxidation upon excitation by visible light up to such a long wavelength.

Open Access

This article is licensed under a [Creative Commons Attribution 4.0 International License](https://creativecommons.org/licenses/by/4.0/).

© The Author(s) 2017

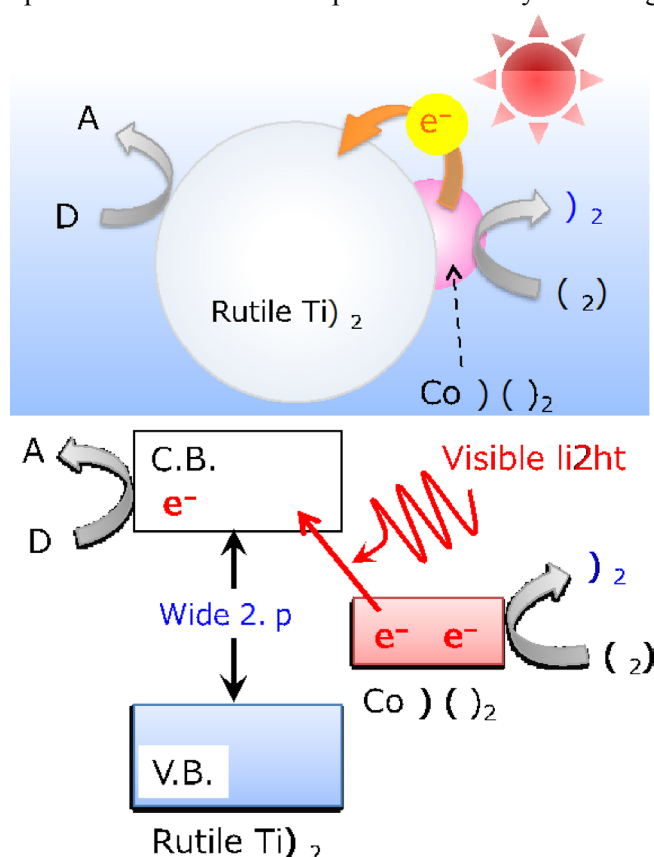


Figure 1. Visible-light-driven water oxidation using Co(OH)₂-modified rutile TiO₂.

References

- [1] K. Maeda; K. Ishimaki; Y. Tokunaga; D. Lu; M. Eguchi, Modification of Wide-Band-Gap Oxide Semiconductors with Cobalt Hydroxide Nanoclusters for Visible-Light Water Oxidation. *Angewandte Chemie International Edition*. 55, 8309-8313 (2016). doi:10.1002/anie.201602764

Photoelectrocatalytic Production of Solar Fuels from Water and CO₂

Hyunwoong Park*

School of Energy Engineering, Kyungpook National University, Daegu 41566, Republic of Korea

Corresponding Author. Email: hwp@knu.ac.kr

Received: 26 May 2017, Accepted: 16 June 2017, Published Online: 26 October 2017

Citation Information: Hyunwoong Park, *Nano-Micro Conference*, 2017, 1, 01042 doi: 10.11605/cp.nmc2017.01042

Abstract

There is renewed interest in the photocatalytic and photoelectrochemical conversion of CO₂ into value-added chemicals using various semiconductor particles and electrodes. Common CO₂ reduction products are C1 chemicals (CO, HCOOH, CH₃OH, and CH₄) in aqueous media, while the production of C2-C4 hydrocarbons (e.g., C₂H₆ and C₃H₈) has also been reported. A number of solar-active materials have been reported, but they still suffer from low selectivity, poor energy efficiency, and instability, while failing to drive simultaneous water oxidation. In this regard, p-type CuMO₂ (where M = Al³⁺ and Fe³⁺) is highly promising because of its unique structure; suitable bandgap energies; high conduction band level, which is sufficient for H₂ production and CO₂ reduction; and relative stability in aqueous solution. Unfortunately, the typical synthetic route for CuMO₂ is annealing a Cu(I) and M(III) salt mixture at high temperature, which inevitably results in irregular, coarse particles of several micrometers. Furthermore, the as-synthesized particles are difficult to fabricate into durable films on transparent conducting oxide (TCO) substrates because of the absence of particle-to-particle interaction. Even if they are fabricated, the films have less intimate and looser interparticle connections undergoing a significant charge recombination at the solid/solid interface. This difficulty in synthesizing CuMO₂ films has caused this material to be less studied despite its potential as a promising photocathode. With this in mind, we have attempted to synthesize high-efficiency CuMO₂ films on TCO substrates via electrochemical deposition. This talk presents our recent studies on the solar CO₂ conversion to value-added chemicals while using water as an electron donor in various photo-systems [1-11].

References

- [1] Sung Kyu Choi; Unseock Kang; Seunghoon Lee; Dong Jin Ham; Sang Min Ji; Hyunwoong Park, Sn-Coupled p-Si Nanowire Arrays for Solar Formate Production from CO₂. *Advanced Energy Materials*. 4, 1301614 (2014). doi:10.1002/aenm.201301614
- [2] Hyunwoong Park; Hsin-Hung Ou; Agustin J. Colussi; Michael R. Hoffmann, Artificial Photosynthesis of C1-C3 Hydrocarbons from Water and CO₂ on Titanate Nanotubes Decorated with Nanoparticle Elemental Copper and CdS Quantum Dots. *Journal of Physical Chemistry A*. 119, 4658-4666 (2015). doi:10.1021/jp511329d
- [3] Unseock Kang; Sung Kyu Choi; Dong Jin Ham; Sang Min Ji; Wonyong Choi; Dong Suk Han; Ahmed Abdel-Wahab; Hyunwoong Park, Photosynthesis of formate from CO₂ and water at 1% energy efficiency via copper iron oxide catalysis. *Energy & Environmental Science*. 8, 2638-2643 (2015). doi:10.1039/C5EE01410G
- [4] Hyunwoong Park; Hsin-Hung Ou; Unseock Kang; Jina Choi; Michael R. Hoffmann, Photocatalytic conversion of carbon dioxide to methane on TiO₂/CdS in aqueous isopropanol solution. *Catalysis Today*. 266, 153-159 (2016). doi:10.1016/j.cattod.2015.09.017
- [5] Narayan Chandra Deb Nath; Seung Yo Choi; Hye Won Jeong; Jae-Joon Lee; Hyunwoong Park, Stand-alone photoconversion of carbon dioxide on copper oxide wire arrays powered by tungsten trioxide/dye-sensitized solar cell dual absorbers. *Nano Energy*. 25, 51-59 (2016). doi:10.1016/j.nanoen.2016.04.025
- [6] Hye Won Jeong; Weon-Sik Chae; Bokyung Song; Chang-Hee Cho; Seong-Ho Baek; Yiseul Park; Hyunwoong Park, Optical resonance and charge transfer behavior of patterned WO₃ microdisc arrays. *Energy & Environmental Science*. 9, 3143-3150 (2016). doi:10.1039/C6EE01003B
- [7] Sung Kyu Choi; Weon-Sik Chae; Bokyung Song; Chang-Hee Cho; Jina Choi; Dong Suk Han; Wonyong Choi; Hyunwoong Park, Photoelectrochemical hydrogen production on silicon microwire arrays overlaid with ultrathin titanium nitride. *Journal of Materials Chemistry A*. 4, 14008-14016 (2016). doi:10.1039/C6TA05200B
- [8] Tae Hwa Jeon; Alok D. Bokare; Dong Suk Han; Ahmed Abdel-Wahab; Hyunwoong Park; Wonyong Choi, Dual modification of hematite photoanode by Sn-doping and Nb₂O₅ layer for water oxidation. *Applied Catalysis B: Environmental*. 201, 591-599 (2017). doi:10.1016/j.apcatb.2016.08.059
- [9] Unseock Kang; Hyunwoong Park, A facile synthesis of CuFeO₂ and CuO composite photocatalyst films for the production of liquid formate from CO₂ and water over a month. *Journal of Materials Chemistry A*. 5, 2123 (2017). doi:10.1039/C6TA09378G
- [10] Seunghoon Lee; Unseock Kang; Guangxia Piao; Soonhyun Kim; Dong Suk Han; Hyunwoong Park, Homogeneous photoconversion of seawater uranium using copper and iron mixed-oxide semiconductor electrodes. *Applied Catalysis B: Environmental*. 207, 35-41 (2017). doi:10.1016/j.apcatb.2017.02.004
- [11] Hyunwoong Park; Hyoung-il Kim; Gun-hee Moon; Wonyong Choi, Photoinduced charge transfer processes in solar photocatalysis based on modified TiO₂. *Energy & Environmental Science*. 9, 411-433 (2016). doi:10.1039/C5EE02575C

Open Access

This article is licensed under a [Creative Commons Attribution 4.0 International License](https://creativecommons.org/licenses/by/4.0/).

© The Author(s) 2017

Photocatalytic elimination of organic chemicals and aerosol-associated influenza virus infectivity in the air

Kimiyasu Shiraki,^{1*} Hiroshi Yamada,¹ Yoshihiro Yoshida,¹ Ayumu Ohno,¹ Teruo Watanabe,² Takafumi Watanabe,² Hiroyuki Watanabe,² Hidemitsu Watanabe,² Masao Yamaguchi,² Fumio Tokuoka,³ Shigeatsu Hashimoto,⁴ Masakazu Kawamura,⁵ Norihisa Adachi⁵

¹Department of Virology, University of Toyama

²APS Japan Co., Ltd.

³Shonan Ceramics Corporation

⁴Department of Metabolism, Diabetes and Nephrology, Fukushima Medical University Aizu Medical Center

⁵TechnoPLAS Japan Co., Ltd. Japan

Corresponding Author. Email: kshiraki@med.u-toyama.ac.jp

Received: 31 May 2017, Accepted: 16 June 2017, Published Online: 26 October 2017

Citation Information: Kimiyasu Shiraki, Hiroshi Yamada, Yoshihiro Yoshida, Ayumu Ohno, Teruo Watanabe, Takafumi Watanabe, Hiroyuki Watanabe, Hidemitsu Watanabe, Masao Yamaguchi, Fumio Tokuoka, Shigeatsu Hashimoto, Masakazu Kawamura, Norihisa Adachi, Nano-Micro Conference, 2017, 1, 01043 doi: 10.11605/cp.nmc2017.01043

Abstract

The efficiency of photocatalysis depends on the surface area and materials, and we have prepared a nanosized-titanium dioxide (TiO₂)-coated ceramic irradiated by UV-LED lamps as a photocatalytic air cleaner. Ceramic filter system decomposed 80% of acetaldehyde and Particulate dioxins (40 pg/m³) and gaseous dioxins (16 pg/m³) were removed by 7.5 and 2.8 pg/m³ by passing through four TiO₂-coated ceramic (30 × 30 × 2 cm) under black-light, indicating about 80% of dioxin was decomposed by the photocatalysis. Ceramic was changed to aluminum plate and the efficiency was improved. The 90% of 5 ppm acetaldehyde (12.4 μmol/h) was decomposed and generated carbon dioxide (25.43 μmol/h; RC: 92.5% carbon dioxide conversion rate) efficiently and continuously for 200 min with the ratio of one acetaldehyde (12.40 μmol/h) to two carbon dioxide (25.43 μmol/h) at their molar ratios by being passed through the TiO₂-coated aluminum plate (5 × 10 × 1 cm) under black light, indicating complete decomposition of acetaldehyde with high efficiency. This photocatalysis system was applied for elimination of acetaldehyde and inactivation of influenza aerosol in a closed cubic space using aluminum plates. Acetaldehyde at 20 ppm in a cubic 1 m³ space was eliminated by 60 min at a half-life of 8 min. The aerosol-associated infectivity and the RNA genome of influenza virus produced by a nebulizer in a 779 liter cubic space were eliminated within 7 minutes but were detectable up to 28 minutes without the function of a photocatalytic air cleaner. Influenza virus was broken down by photocatalysis rather than being trapped by Hepafilter as intermediate breakdown products of influenza virus were observed. Thus, a photocatalytic air cleaner efficiently decomposed and eliminated organic chemicals, acetaldehyde, and aerosol-associated influenza virus infectivity and viral RNA, indicating a photocatalytic air cleaner functioned in the cleaning and detoxification of the air in the closed space for maintaining a safer environment.

Open Access

This article is licensed under a [Creative Commons Attribution 4.0](https://creativecommons.org/licenses/by/4.0/)

[International License](https://creativecommons.org/licenses/by/4.0/).

© The Author(s) 2017

Photocatalytic Degradation of Polybrominated Diphenyl Ethers on TiO₂-based composites

Nan Wang,^{1*} Lihua Zhu,¹ Ming Lei,² Heqing Tang^{2*}

¹Shenzhen Institute of Huazhong University of Science and Technology, 518000, Shenzhen, China

²College of Resources and Environmental Science, South-Central University for Nationalities, 430074, Wuhan, China

Corresponding Author. Email: Nan Wang, nwang@hust.edu.cn; Heqing Tang, tangheqing@mail.scuec.edu.cn

Received: 02 June 2017, Accepted: 18 June 2017, Published Online: 27 October 2017

Citation Information: Nan Wang, Lihua Zhu, Ming Lei, Heqing Tang, *Nano-Micro Conference, 2017, 1, 01044* doi: 10.11605/cp.nmc2017.01044

Abstract

Polybrominated diphenyl ethers (PBDEs) are widely used as flame retardants, and become a new class of global contaminants. Because PBDEs possess typical characteristics of persistent organic pollutants (POPs) like persistent, bioaccumulation, and biotoxicity, their elimination therefore attracts much attention of researchers.

The reductive debromination is a common strategy to treat PBDEs. Among various reductive methods, the photogenerated electron of TiO₂ is considered to be highly efficient to reduce decabromodiphenyl ether (BDE209) [1]. However, this leads to accumulation of brominated intermediates, but the debromination products with less bromine atoms are much more difficult to get further reductive debromination.

To promote the photocatalytic reductive debromination, we developed several TiO₂-based composites including reduced graphene oxide (RGO) loaded TiO₂ (RGO/TiO₂), Ag/TiO₂, and CuO/TiO₂ to reduce BDE209 and/or 2,2',4,4'-tetrabromodiphenyl ether (BDE47) [2-4]. These heterostructured photocatalysts have two beneficial roles: charge separation in space, and enhanced adsorption of PBDEs. Thus, the photocatalytic reduction of PBDEs was greatly improved. However, the complete debromination of PBDEs to diphenyl ether through the photocatalytic reduction process is rather difficult. For example, although all the added BDE47 was rapidly reduced, the debromination efficiency was still less than 50% over Ag/TiO₂ and CuO/TiO₂ [3,4]. This is because that the reduction of low-brominated PBDEs is rather difficult, due to their weak electron affinity.

Although most studies indicate that BDE209 is strongly resistant to oxidation, we firstly demonstrated that the h⁺/•OH-involved oxidative degradation of BDE209 took place slowly in the UV-irradiated TiO₂ aqueous dispersions [5]. We also noted that the oxidation of BDE209 is much slower than the following oxidation of the less-brominated organic intermediates. Since the highly brominated PBDEs are more easily reduced, and the lower brominated PBDEs become more susceptible to the oxidation, we then developed an effective “one-pot” photocatalytic system for driving concurrently the pre-reduction and consecutive oxidation of BDE47.

Acknowledgements

The authors acknowledge the financial supports from the National Natural Science Foundation (Grants No. 21477043), Shenzhen Knowledge Innovation Plan of Shenzhen City Technology Innovation Committee (No. JCYJ20150616144425374).

References

- [1] Sun C; Zhao D; Chen C; W. Ma; J. Zhao, TiO₂-mediated photocatalytic debromination of decabromodiphenyl ether: kinetics and intermediates. *Environmental Science & Technology*. 43, 157-162 (2009). doi:10.1021/es801929a
- [2] M. Lei; N. Wang; L. Zhu; C. Xie; H. Tang, A peculiar mechanism for the photocatalytic reduction of decabromodiphenyl ether over reduced graphene oxide-TiO₂ photocatalyst. *Chemical Engineering Journal*. 241, 207-215 (2014). doi:10.1016/j.cej.2013.12.032
- [3] M. Lei; N. Wang; L. Zhu; Q. Zhou; G. Nie; H. Tang, Photocatalytic reductive degradation of polybrominated diphenyl ethers on CuO/TiO₂ nanocomposites: A mechanism based on the switching of photocatalytic reduction potential being controlled by the valence state of copper. *Applied Catalysis B: Environmental*. 182, 414-423 (2016). doi:10.1016/j.apcatb.2015.09.031
- [4] M. Lei; N. Wang; L. Zhu; H. Tang, Peculiar and rapid photocatalytic degradation of tetrabromodiphenyl ethers over Ag/TiO₂ induced by interaction between silver nanoparticles and bromine atoms in the target. *Chemosphere*. 150, 536-544 (2016). doi:10.1016/j.chemosphere.2015.10.048
- [5] Huang A; M. Lei; N. Wang; L. Zhu; Y. Zhang; Z. Lin; D. Ying; H. Tang, Efficient oxidative debromination of decabromodiphenyl

ether by TiO₂-mediated photocatalysis in aqueous environment. *Environmental Science & Technology*. 47, 518-525 (2013). doi:10.1021/es302935e

Open Access

This article is licensed under a [Creative Commons Attribution 4.0 International License](https://creativecommons.org/licenses/by/4.0/).

© The Author(s) 2017

Nanostructured TiO₂ with oxygen vacancies for the decomposition of organics

Chiaki Terashima*

Photocatalysis International Research Center, Research Institute for Science & Technology, Tokyo University of Science, 2641 Yamazaki, Noda, Chiba 278-8510, Japan

Corresponding Author. Email: terashima@rs.tus.ac.jp

Received: 18 May 2017, Accepted: 17 June 2017, Published Online: 27 October 2017

Citation Information: Chiaki Terashima, *Nano-Micro Conference*, 2017, 1, 01045 doi: 10.11605/cp.nmc2017.01045

Abstract

Titanium dioxide (TiO₂) has been widely not only studied but also applied in industrial fields as photocatalyst because of its environmentally and economically advantages with high chemical stability, earth abundant and bio compatible properties. However, its large band-gap for the activity to only UV light region, and the high recombination rate of photogenerated electron and hole pairs have to be overcome to utilize effectively sunlight and to enhance the photocatalytic performance. Recent enormous efforts to overcome the above-mentioned drawbacks have resulted in the one-dimensional TiO₂ nanotubes, nanofibers and nanorods to suppress the carrier recombination, and/or the heterojunction structure of TiO₂ with another semiconductor to achieve larger separation of the photogenerated electron and hole, as well as the modification of TiO₂ nanoparticles with gold clusters to expand the light conversion from UV to visible and near-infrared region. Here, we report simple and effective modification of nano-sized TiO₂ materials by in-liquid plasma processing, which is a non-thermal plasma discharged in liquid. The present study focused to treat pristine TiO₂ nanoparticles by the discharge in water-based solution and to investigate the material properties as well as the photocatalytic activities for decomposing organics. As a result of plasma treatment, we found the incorporation of oxygen vacancies on the sub-surface of TiO₂ nanoparticles, and concluded that the origin of photocatalytic enhancement for acetaldehyde decomposition under fluorescent lamp attributed in the recombination suppression by the surface trap of oxygen vacancies near the nanoparticles surface.

Open Access

This article is licensed under a [Creative Commons Attribution 4.0 International License](https://creativecommons.org/licenses/by/4.0/).

© The Author(s) 2017

One-dimensional nanoarrays for solar cells

Hao Wang*

Faculty of Physics and Electronic Science, Hubei University, Wuhan 430062, PR China

Corresponding Author. Email: nanoguy@126.com

Received: 01 June 2017, Accepted: 19 June 2017, Published Online: 27 October 2017

Citation Information: Hao Wang, *Nano-Micro Conference, 2017, 1, 01046* doi: [10.11605/cp.nmc2017.01046](https://doi.org/10.11605/cp.nmc2017.01046)

Abstract

Various kinds of modifying methods towards ZnO and TiO₂ one-dimensional nanostructures such as nanorods and nanotubes have been carried out for their applications in Dye-sensitized solar cell (DSSC), perovskite solar cell (PSC) and photo detectors (PD). Core-sheath ZnO/CdTe and double-sheath ZnO/CdSe/CdTe nanocable arrays as effective photoanode have been developed for solar cells, which resulted in a saturated current as high as 14.3 mA/cm². Large area free-standing highly ordered TiO₂ nanotube arrays on the fluorine-doped tin oxide (FTO) conductive glass substrates have been successfully obtained to serve as photo-anodes of DSSCs. The certified photovoltaic conversion efficiency of TiO₂ nanoarrays based DSSCs is up to 10.3% by using N719 as Dye and I⁻/I₃⁻ as electrolyte. Perovskite solar cell with efficiency of up to 18.6% based on TiO₂ nanorod arrays is also presented. Self-powered broadband photodetectors based on CH₃NH₃PbI₃/ZnO nanorod arrays heterostructure have been achieved with high detectivity of 3.56 × 10¹⁴ cm Hz^{1/2} W⁻¹ and high responsivity of 24.3 A W⁻¹.

References

- [1] X.N. Wang; H.J. Zhu; Y.M. Xu; Hao Wang; Y. Tao; S.K. Hark; X.D. Xiao; Q. Li, Aligned ZnO/CdTe Core-Shell Nanocable Arrays on Indium Tin Oxide: Synthesis and Photoelectrochemical Properties. *ACS Nano*. 4, 3302-3308 (2010). doi:[10.1021/nn1001547](https://doi.org/10.1021/nn1001547)
- [2] Hao Wang; Tian Wang; Xina Wang; Rong Liu; Hanbin Wang; Yang Xu; Jun Zhang; Jinxia Duan, Double-shelled ZnO/CdSe/CdTe nanocable arrays for photovoltaic applications: microstructure evolution and interfacial energy alignment. *Journal of Materials Chemistry*. 22, 12532-12537 (2012). doi:[10.1039/C2JM32253F](https://doi.org/10.1039/C2JM32253F)
- [3] J. Zhang; S. Li; H. Ding; Q. Li; B. Wang; X. Wang; H. Wang, Transfer and assembly of large area TiO₂ nanotube arrays onto conductive glass for dye sensitized solar cells. *Journal of Power Sources*. 247, 807-812 (2014). doi:[10.1016/j.jpowsour.2013.08.124](https://doi.org/10.1016/j.jpowsour.2013.08.124)
- [4] Y. Xu; Y. Wang; J. Yu; B. Feng; H. Zhou; J. Zhang; J. Duan; X. Fan; P.A.V. Aken; P.D. Lund; H. Wang, Performance Improvement of Perovskite Solar Cells Based on PCBM-Modified ZnO-Nanorod Arrays. *IEEE Journal of Photovoltaics*. 6, 1530-1536 (2016). doi:[10.1109/JPHOTOV.2016.2600341](https://doi.org/10.1109/JPHOTOV.2016.2600341)
- [5] S. Kazim; M.K. Nazeeruddin; M. Grätzel; S. Ahmad, Perovskite as Light Harvester: A Game Changer in Photovoltaics. *Angewandte Chemie International Edition*. 53, 2812-2824 (2014). doi:[10.1002/anie.201308719](https://doi.org/10.1002/anie.201308719)
- [6] J. Zhang; Q. Li; S. Li; Y. Wang; C. Ye; P. Ruterana; H. Wang, An efficient photoanode consisting of TiO₂ nanoparticle-filled TiO₂ nanotube arrays for dye sensitized solar cells. *Journal of Power Sources*. 268, 941-949 (2014). doi:[10.1016/j.jpowsour.2014.06.139](https://doi.org/10.1016/j.jpowsour.2014.06.139)
- [7] H. Wang; B. Wang; J. Yu; Y. Hu; C. Xia; J. Zhang; R. Liu, Significant enhancement of power conversion efficiency for dye sensitized solar cell using 1D/3D network nanostructures as photoanodes. *Scientific Reports*. 5, 9305 (2015). doi:[10.1038/srep09305](https://doi.org/10.1038/srep09305)
- [8] J.C. Yu; X. Chen; Y. Wang; H. Zou; M.N. Xue; Y. Xu; Z.S. Li; C. Ye; J. Zhang; P. A. van Aken; P. Lund; H. Wang, A high-performance self-powered broadband photodetector based on a CH₃NH₃PbI₃ perovskite/ZnO nanorod array heterostructure. *Journal Of Materials Chemistry C*. 4, 7302-7308 (2016). doi:[10.1039/C6TC02097F](https://doi.org/10.1039/C6TC02097F)

Open Access

This article is licensed under a [Creative Commons Attribution 4.0 International License](https://creativecommons.org/licenses/by/4.0/).

© The Author(s) 2017

Facile Development of Nanostructured Photocatalysts for CO₂ Capture and Conversion

Wei-Ning Wang*

Department of Mechanical and Nuclear Engineering, Virginia Commonwealth University, 800 E. Leigh St., Richmond, Virginia, United States of America

Corresponding Author. Email: wnwang@vcu.edu

Received: 30 May 2017, Accepted: 17 June 2017, Published Online: 27 October 2017

Citation Information: Wei-Ning Wang, *Nano-Micro Conference*, 2017, 1, 01047 doi: [10.11605/cp.nmc2017.01047](https://doi.org/10.11605/cp.nmc2017.01047)

Abstract

The continuous reliance on fossil fuel-based energy is inevitable. Rational strategies to reduce carbon dioxide (CO₂) emissions are thus highly demanded. Developing efficient photocatalysts that can harness solar energy appears to be a promising methodology to capture and recycle CO₂ as a fuel feedstock. The conversion efficiency of the current photocatalysts, however, is generally very low due to various limiting factors, such as fast electron-hole recombination rates, narrow light absorption range, and backward reactions. Thus, developing strategies to overcome the above limitations is an important task in this field.

Here we present several strategies through controlled synthesis to address the aforementioned limitations toward enhancing the overall CO₂ conversion efficiency. Examples of novel photocatalysts being explored include mesoporous nanocomposite particles (i.e., Cu-TiO₂-SiO₂) [1,2], 1D structured Pt-TiO₂ thin films [3], CuO-ZnO heterojunction nanowires [4], and crumpled graphene-based nanoballs [5,6]. Systematic materials characterization and photocatalysis analysis of the materials, by electron microscopy, X-ray diffraction, gas chromatography, X-ray photoelectron spectroscopy, in-situ diffuse reflectance infrared Fourier transform spectroscopy, and femtosecond time-resolved transient absorption spectroscopy, aid in understanding the quantitative CO₂ photoreduction pathways and the correlations between materials properties and CO₂ photoreduction performance.

References

- [1] W.N. Wang; J. Park; P. Biswas, Rapid synthesis of nanostructured Cu-TiO₂-SiO₂ composites for CO₂ photoreduction by evaporation driven self-assembly. *Catalysis Science & Technology*. 1, 593-600 (2011). doi:[10.1039/C0CY00091D](https://doi.org/10.1039/C0CY00091D)
- [2] Y. Li; W.N. Wang; Z.L. Zhan; M.H. Woo; C.Y. Wu; P. Biswas, Photocatalytic reduction of CO₂ with H₂O on mesoporous silica supported Cu/TiO₂ catalysts. *Applied Catalysis B: Environmental*. 100, 386-392 (2010). doi:[10.1016/j.apcatb.2010.08.015](https://doi.org/10.1016/j.apcatb.2010.08.015)
- [3] Wei-Ning Wang; Woo-Jin An; Balavinayagam Ramalingam; Somik Mukherjee; Dariusz M. Niedzwiedzki; Shubhra Gangopadhyay; Pratim Biswas, Size and structure matter: enhanced CO₂ photoreduction efficiency by size-resolved ultrafine Pt nanoparticles on TiO₂ single crystals. *Journal of the American Chemical Society*. 134, 11276-11281 (2012). doi:[10.1021/ja304075b](https://doi.org/10.1021/ja304075b)
- [4] Wei-Ning Wang; Fei Wu; Yoon Myung; Dariusz M. Niedzwiedzki; Hyung Soon Im; Jeunghee Park; Parag Banerjee; Pratim Biswas, Surface engineered CuO nanowires with ZnO islands for CO₂ photoreduction. *ACS Applied Materials & Interfaces*. 7, 5685-5692 (2015). doi:[10.1021/am508590j](https://doi.org/10.1021/am508590j)
- [5] W. N. Wang; Y. Jiang; J. Fortner; P. Biswas, Nanostructured graphene-titanium dioxide composites synthesized by a single-step aerosol process for photoreduction of carbon dioxide. *Environmental Engineering Science*. 31, 428 (2014). doi:[10.1089/ees.2013.0473](https://doi.org/10.1089/ees.2013.0473)
- [6] Y. Nie; W. N. Wang; Y. Jiang; J. Fortner; P. Biswas, Crumpled reduced graphene oxide-amine-titanium dioxide nanocomposites for simultaneous carbon dioxide adsorption and photoreduction. *Catalysis Science & Technology*. 6, 6187-6196 (2016). doi:[10.1039/C6CY00828C](https://doi.org/10.1039/C6CY00828C)

Open Access

This article is licensed under a [Creative Commons Attribution 4.0 International License](https://creativecommons.org/licenses/by/4.0/).

© The Author(s) 2017

Highly Concentrated CO Evolution for Photocatalytic Conversion of CO₂ by H₂O as an Electron Donor

Kentaro Teramura,^{1,2*} Kazutaka Hori,¹ Yosuke Terao,¹ Hiroyuki Tatsumi,¹ Zeai Huang,¹ Shoji Iguchi,¹ Zheng Wang,¹ Hiroyuki Asakura,^{1,2} Saburo Hosokawa,^{1,2} Tsunehiro Tanaka^{1,2}

¹Department of Molecular Engineering, Graduate School of Engineering, Kyoto University, Kyotodaigaku Katsura, Nishikyo-ku, Kyoto 615-8510, Japan

²Elements Strategy Initiative for Catalysts & Batteries (ESICB), Kyoto University, Kyotodaigaku Katsura, Nishikyo-ku, Kyoto 615-8520, Japan

Corresponding Author. Email: teramura@moleng.kyoto-u.ac.jp

Received: 17 May 2017, Accepted: 16 June 2017, Published Online: 27 October 2017

Citation Information: Kentaro Teramura, Kazutaka Hori, Yosuke Terao, Hiroyuki Tatsumi, Zeai Huang, Shoji Iguchi, Zheng Wang, Hiroyuki Asakura, Saburo Hosokawa, Tsunehiro Tanaka, *Nano-Micro Conference, 2017, 1, 01048* doi: [10.11605/cp.nmc2017.01048](https://doi.org/10.11605/cp.nmc2017.01048)

Abstract

The reduction in human-induced emissions of CO₂ from automobiles, factories, power stations etc., over the next 15 years is currently one of the most important issues facing the planet. We should therefore attempt to develop industrial processes using CO₂ as a feedstock in order to build a sustainable society in the near future. Linear CO₂ molecules adsorbed on the surface of the solid bases are converted into unique structures, such as bicarbonate and carbonate species possessing lattice oxygen atoms. We believe that the process involves the capture and distortion of CO₂ upon adsorption on a solid base through activation by photoirradiation. Unstable CO₂ species adsorbed onto the surface can then be reduced by electrons with protons derived from H₂O (CO₂ + 2e⁻ + 2H⁺ → CO + H₂O). These days, we succeeded in designing highly selective photocatalytic conversion of CO₂ by H₂O as the electron donor, by the simultaneous use of an inhibitor of the production of H₂ and a material for CO₂ capture and storage, such as ZnGa₂O₄/Ga₂O₃ [1,2], La₂Ti₂O₇ [3], SrO/Ta₂O₅ [4], ZnGa₂O₄ [5] and ZnTa₂O₆ [6], and Sr₂KTa₅O₁₅ [7] with the modification of Ag cocatalyst. An isotope experiment using ¹³CO₂ and mass spectrometry clarified that the carbon source of the evolved CO is not the residual carbon species on the photocatalyst surface, but the CO₂ introduced in the gas phase. In addition, stoichiometric amounts of O₂ evolved were generated together with CO.

References

- [1] Kentaro Teramura; Zheng Wang; Saburo Hosokawa; Yoshihisa Sakata; Tsunehiro Tanaka, A Doping Technique that Suppresses Undesirable H₂ Evolution Derived from Overall Water Splitting in the Highly Selective Photocatalytic Conversion of CO₂ in and by Water. *Chemistry - A European Journal*. 20, 9906-9909 (2014). doi:[10.1002/chem.201402242](https://doi.org/10.1002/chem.201402242)
- [2] Zheng Wang; Kentaro Teramura; Zeai Huang; Saburo Hosokawa; Yoshihisa Sakata; Tsunehiro Tanaka, Tuning the selectivity toward CO evolution in the photocatalytic conversion of CO₂ with H₂O through the modification of Ag-loaded Ga₂O₃ with a ZnGa₂O₄ layer. *Catalysis Science & Technology*. 6, 1025-1032 (2016). doi:[10.1039/C5CY01280E](https://doi.org/10.1039/C5CY01280E)
- [3] Zheng Wang; Kentaro Teramura; Saburo Hosokawa; Tsunehiro Tanaka, Photocatalytic conversion of CO₂ in water over Ag-modified La₂Ti₂O₇. *Applied Catalysis B: Environmental*. 163, 241-247 (2015). doi:[10.1016/j.apcatb.2014.07.052](https://doi.org/10.1016/j.apcatb.2014.07.052)
- [4] Teramura Kentaro; Tatsumi Hiroyuki; Wang Zheng; Hosokawa Saburo; Tanaka Tsunehiro, Photocatalytic Conversion of CO₂ by H₂O over Ag-Loaded SrO-Modified Ta₂O₅. *Bulletin of the Chemical Society of Japan*. 88, 431-437 (2015). doi:[10.1246/bcsj.20140385](https://doi.org/10.1246/bcsj.20140385)
- [5] Zheng Wang; Kentaro Teramura; Saburo Hosokawa; Tsunehiro Tanaka, Highly efficient photocatalytic conversion of CO₂ into solid CO using H₂O as a reductant over Ag-modified ZnGa₂O₄. *Journal of Materials Chemistry A*. 3, 11313-11319 (2015). doi:[10.1039/C5T-A01697E](https://doi.org/10.1039/C5T-A01697E)
- [6] Shoji Iguchi; Kentaro Teramura; Saburo Hosokawa and Tsunehiro Tanaka, A ZnTa₂O₆ photocatalyst synthesized via solid state reaction for conversion of CO₂ into CO in water. *Catalysis Science & Technology*. 6, 4978-4985 (2016). doi:[10.1039/C6CY00271D](https://doi.org/10.1039/C6CY00271D)
- [7] Zeai Huang; Kentaro Teramura; Saburo Hosokawa; Tsunehiro Tanaka, Fabrication of well-shaped Sr₂KTa₅O₁₅ nanorods with a

tetragonal tungsten bronze structure by a flux method for artificial photosynthesis. *Applied Catalysis B: Environmental*. 199, 272-281 (2016). doi:[10.1016/j.apcatb.2016.06.039](https://doi.org/10.1016/j.apcatb.2016.06.039)

Open Access

This article is licensed under a [Creative Commons Attribution 4.0 International License](https://creativecommons.org/licenses/by/4.0/).

© The Author(s) 2017

Highly efficient visible-light-driven BiVO₄-based Photoelectrode Materials

Tengjiao Niu, Jijuan He, Qizhao Wang*

College of Chemistry and Chemical Engineering, Northwest Normal University, Lanzhou, China
Corresponding Author. Email: qizhaosjtu@gmail.com

Received: 14 June 2017, Accepted: 19 June 2017, Published Online: 28 October 2017

Citation Information: Tengjiao Niu, Jijuan He, Qizhao Wang, *Nano-Micro Conference*, 2017, 1, 01049 doi: 10.11605/cp.nmc2017.01049

Abstract

BiVO₄ is an excellent visible-light-driven photocatalyst that can split water into O₂ for its more positive valence band than that of O₂/H₂O, whereas its positive conduction band makes it difficult to directly generate H₂ from H₂O. But using the PEC, BiVO₄ can become a promising candidate as photoanode for hydrogen evolution performance. In our group, the leaf-like structure BiVO₄ photoelectrodes were prepared by electrochemical deposition, in which Zn²⁺ ions were introduced as a direct agent to control the morphology and size of Bi nanoparticles [1]. NiFe₂O₄ and CoFe₂O₄ nanoparticles were loading on the surface of BiVO₄ to construct heterojunction. The heterojunctions can effectively prevent carriers from recombining and accelerate the separation of electrons and holes [2]. Besides, Bi/BiVO₄ [3] and FeF₂/BiVO₄ can enhanced PEC hydrogen evolution performance.

References

[1] Wanhong He; Ruirui Wang; Chen Zhou; Junjiao Yang; Feng Li; Xu Xiang, Controlling the Structure and Photoelectrochemical Performance of BiVO₄ Photoanodes Prepared from Electrodeposited Bismuth Precursors: Effect of Zinc Ions as Directing Agent. *Industrial & Engineering Chemistry Research*. 54, 10723-10730 (2015). doi:10.1021/acs.iecr.5b02460

[2] Qizhao Wang; Jijuan He; Yanbiao Shi; Shuling Zhang; Tengjiao Niu; Houde She; Yingpu Bi; Ziqiang Lei, Synthesis of MFe₂O₄ (M = Ni, Co)/BiVO₄ film for photoelectrochemical hydrogen production activity. *Applied Catalysis B: Environmental*. 214, 158-167 (2017). doi:10.1016/j.apcatb.2017.05.044

[3] Qizhao Wang; Jijuan He; Yanbiao Shi; Shuling Zhang; Tengjiao Niu; Houde She; Yingpu Bi, Designing non-noble/semiconductor Bi/BiVO₄ photoelectrode for the enhanced photoelectrochemical performance. *Chemical Engineering Journal*. 326, 411-418 (2017). doi:10.1016/j.cej.2017.05.171

Open Access

This article is licensed under a [Creative Commons Attribution 4.0 International License](https://creativecommons.org/licenses/by/4.0/).

© The Author(s) 2017

Nano Photocatalytic Materials Design Toward Small Molecular Hydrocarbons Oxidation

Zhiguo Yi*

Fujian Institute of Research on the Structure of Matter, Chinese Academy of Sciences, Fuzhou 350002, China

Corresponding Author. Email: zhiguo@fjirsm.ac.cn

Received: 11 May 2017, Accepted: 16 June 2017, Published Online: 28 October 2017

Citation Information: Zhiguo Yi, *Nano-Micro Conference*, 2017, 1, 01050 doi: 10.11605/cp.nmc2017.01050

Abstract

The search for active catalysts that efficiently oxidize methane under ambient conditions remains a challenging task for both C1 utilization and atmospheric cleansing [1-6]. Here, we show that when the particle size of zinc oxide is reduced down to the nanoscale, it exhibits high activity for methane oxidation under simulated sunlight illumination, and nano silver decoration further enhances the photo-activity via the surface plasmon resonance. The high quantum yield of 8% at wavelengths <400 nm and over 0.1% at wavelengths ~470 nm achieved on the silver decorated zinc oxide nanostructures shows great promise for atmospheric methane oxidation. Moreover, the nano-particulate composites can efficiently photo-oxidize other small molecular hydrocarbons such as ethane, propane and ethylene, and in particular, can dehydrogenize methane to generate ethane, ethylene and so on. On the basis of the experimental results, a two-step photocatalytic reaction process is suggested to account for the methane photo-oxidation.

References

- [1] Xuxing Chen; Yunpeng Li; Xiaoyang Pan; David Cortie; Xintang Huang; Zhiguo Yi, Photocatalytic oxidation of methane over silver decorated zinc oxide nanocatalysts. *Nature Communications*. 7, 12273 (2016). doi:10.1038/ncomms12273
- [2] Xiaoyang Pan; Xuxing Chen; Zhiguo Yi, Photocatalytic oxidation of methane over SrCO₃ decorated SrTiO₃ nanocatalysts via a synergistic effect. *Physical Chemistry Chemical Physics*. 18, 31400-31409 (2016). doi:10.1039/C6CP04604E
- [3] Yunpeng Li; Yuanzhu Cai; Xuxing Chen; Xiaoyang Pan; Mingxue Yang; Zhiguo Yi, Photocatalytic oxidation of small molecule hydrocarbons over Pt/TiO₂ nanocatalysts. *RSC Advances*. 6, 2760-2767 (2016). doi:10.1039/C5RA22459D
- [4] Peiqing Long; Yaohong Zhang; Xuxing Chen; Zhiguo Yi, Fabrication of Y_xBi_{1-x}VO₄ solid solutions for efficient C₂H₄ photodegradation. *Journal of Materials Chemistry A*. 3, 4163-4169 (2015). doi:10.1039/C4TA05872K
- [5] Dan Wang; Xiaoyang Pan; Guangtao Wang; Zhiguo Yi, Improved propane photooxidation activities upon nano Cu₂O/TiO₂ heterojunction semiconductors at room temperature. *RSC Advances*. 5, 22038-22043 (2015). doi:10.1039/C4RA15215H
- [6] Xuxing Chen; Xintang Huang; Zhiguo Yi, Enhanced Ethylene Photodegradation Performance of g-C₃N₄-Ag₃PO₄ Composites with Direct Z-Scheme Configuration. *Chemistry - A European Journal*. 20, 17590-17596 (2014). doi:10.1002/chem.201404284

Open Access

This article is licensed under a [Creative Commons Attribution 4.0 International License](https://creativecommons.org/licenses/by/4.0/).

© The Author(s) 2017

TiO₂-C hybrid aerogel photocatalysts for methylene blue degradation

Xia Shao, Rui Zhang*

School of Materials Science and Engineering, Shanghai Institute of Technology, 100 Haiquan Road, Shanghai, China

Corresponding Author. Email: zhangrui@sit.edu.cn

Received: 01 June 2017, Accepted: 17 June 2017, Published Online: 28 October 2017

Citation Information: Xia Shao, Rui Zhang, *Nano-Micro Conference*, 2017, 1, 01051 doi: 10.11605/cp.nmc2017.01051

Abstract

TiO₂-C hybrid aerogels were prepared by one-pot sol-gel process in ethanol, followed by supercritical drying and carbonization, using TiCl₄ as TiO₂ precursor, resorcinol-furfural as carbon precursors, ethyl acetoacetate (EA) as a chelating agent and propylene epoxide (PO) as a gel initiator. Ce doping was performed by adding cerous nitrate into the solutions that form gels to modify the photocatalytic properties. Microstructures of samples were characterized by XRD, SEM, TEM, UV-Vis, Raman spectroscopy, nitrogen adsorption, mercury porosimetry, XPS and IR spectroscopy and the photocatalytic properties for methylene blue degradation were tested under UV and Vis light irradiation. Results showed that the porous textures of the hybrid aerogels were related to TiCl₄/resorcinol-furfural mass ratio, the molar ratios of EA/Ti and PO/Ti. The samples had large specific surface areas, high adsorption capacities for methylene blue, uniform distribution of TiO₂ nanoparticles as anatase in the amorphous carbon structure. The presence of the amorphous carbon inhibited both the growth of TiO₂ nanoparticles and their conversion from anatase to rutile phase. The adsorption of methylene blue followed the pseudo-second-order kinetics model and its degradation followed the first-order kinetics model. The maximum photocatalytic activity for methylene degradation was up to 4.23 times that of P25 for the TiO₂-C hybrid aerogels carbonized at 800 °C. A partial reduction of Ti⁴⁺ to Ti³⁺ was found for the samples carbonized at 900 °C, which improved significantly the catalytic activity under visible light. Methylene blue can be degraded under visible light within 60 min with the Ce-doped TiO₂-C hybrid aerogels or the undoped one carbonized at 900 °C. Adsorption coupled with photo excitation, reduced recombination rate of e/h pair, band gap narrowing by interaction of carbon with TiO₂, partial reduction of Ti⁴⁺ to Ti³⁺ during carbonization or Ce-doping, and the increased light utilization via scattering by macropores are responsible for the improved catalytic performance as compared with P25 photocatalyst from Degussa.

Open Access

This article is licensed under a [Creative Commons Attribution 4.0 International License](https://creativecommons.org/licenses/by/4.0/).

© The Author(s) 2017

Noble metal-free Metal Sulphides as Highly Efficient Visible Light Driven Photocatalysts for H₂ Production from H₂S

Ying Zhou,^{1,2*} Meng Dan,^{1,2} Arvind Prakash²

¹State Key Laboratory of Oil and Gas Reservoir Geology and Exploitation, Southwest Petroleum University

²The Center of New Energy Materials and Technology, School of Materials Science and Engineering, Southwest Petroleum University, Chengdu 610500, China

Corresponding Author. Email: yzhou@swpu.edu.cn

Received: 01 June 2017, Accepted: 17 June 2017, Published Online: 28 October 2017

Citation Information: Ying Zhou, Meng Dan, Arvind Prakash, Nano-Micro Conference, 2017, 1, 01052 doi: 10.11605/cp.nmc2017.01052

Abstract

Hydrogen sulfide is an extremely toxic gas which is generated from both nature and human factors. Recently, photocatalytic splitting of H₂S into H₂ and S has attracted great attention because hydrogen production and H₂S removal are simultaneously achieved. However, the deactivation of the photocatalysts and lack of suitable setup for photocleavage of H₂S to H₂ limit its wide application. Herein, we constructed a complete setup for H₂ production from H₂S. This setup has some functions including H₂S absorption, decomposition and product recovery. Simultaneously, a series of MnS/In₂S₃ composites were successfully fabricated by a solvothermal method. A maximum H₂ production rate of 8360 μmol g⁻¹ h⁻¹ can be achieved over MnS/In₂S₃_0.7 catalyst, and the corresponding QE of this sample is as high as 34.2% at 450 nm even in the absence of any noble-metal co-catalysts. Importantly, MnS/In₂S₃ composite displays a good stability and also anti-photocorrosion. Additionally, in order to further enhance visible-light photocatalytic H₂ production activity of MnS/In₂S₃, MnS/In₂S₃/CuS composites were prepared through solvothermal treatment. And a maximum H₂ production rate of 29252 μmol g⁻¹ h⁻¹ can be achieved over a MnS/In₂S₃/CuS with optimized composition, which is 3.5 times higher than that of MnS/In₂S₃_0.7, and this reveals that the addition of CuS can effectively increase the photocatalytic activity for splitting H₂S into H₂. All in all, suitable setup for photocatalytic splitting of H₂S and noble-metal free metal sulphides photocatalysts have great significance for photocleavage of H₂S to H₂.

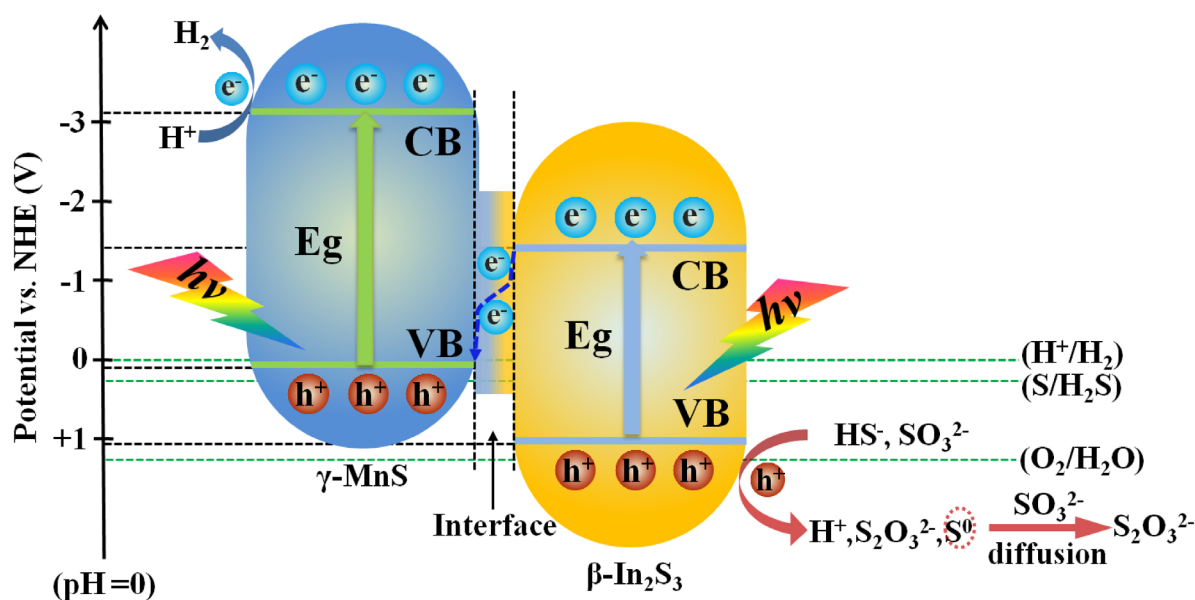


Figure 1. Photocatalytic process of splitting H₂S in 0.6 M Na₂SO₃/0.1 M Na₂S/3 M H₂S solution.

Open Access

This article is licensed under a [Creative Commons Attribution 4.0](https://creativecommons.org/licenses/by/4.0/)

[International License](https://creativecommons.org/licenses/by/4.0/).

© The Author(s) 2017

CO₂ Photocatalytic Reduction over TiO₂ Nanocrystals with Coexposed {001} and {101} Facets

Yongchun Zhao,* Zhuo Xiong, Ze Lei, Junying Zhang, Chuguang Zheng

State Key Laboratory of Coal Combustion, School of Energy and Power Engineering, Huazhong University of Science & Technology, 1037 Luoyu Road, Wuhan 430074, China

Corresponding Author. Email: yczhao@hust.edu.cn

Received: 01 June 2017, Accepted: 17 June 2017, Published Online: 28 October 2017

Citation Information: Yongchun Zhao, Zhuo Xiong, Ze Lei, Junying Zhang, Chuguang Zheng, Nano-Micro Conference, 2017, 1, 01053 doi: 10.11605/cp.nmc2017.01053

Abstract

CO₂ photocatalytic reduction with water is one of the most popular and challenging technologies to produce renewable energy. Engineering TiO₂ with coexposed {001} and {101} facets could enhance the conversion efficiency of CO₂ due to the effective separation of photogenerated charges caused by the formation of {001}/{101} surface heterojunction. However, faceted TiO₂ nanocrystals still suffers from low conversion efficiency and low selectivity for CO₂ reduction. Faceted TiO₂ nanocrystals were combined with graphene and metal nanoparticles respectively to improve the activity and selectivity of CO₂ photocatalytic reduction. The results show that the faceted TiO₂/graphene composites exhibited higher CO yield than that of pristine TiO₂ due to the formation of {001}/{101} surface heterojunction and supporting of graphene, which can effectively promote the spatial separation of photogenerated electrons and holes. Differing from graphene, Pt loading tended to promote the production of CH₄ and H₂ while Cu₂O suppressed H₂ evolution and exhibited lower CH₄ selectivity comparing with Pt. Furthermore, when Pt and Cu₂O were co-deposited on TiO₂ crystals, H₂ and CO production were both inhibited and CO₂ was selectively reduced to CH₄. Pt could not only capture photogenerated electrons but also increase the electrons density on the surface of TiO₂. Meanwhile, Cu₂O loading enhanced the CO₂ chemisorption on TiO₂ while inhibited that of water. As a result, Pt and Cu₂O co-deposited TiO₂ crystals exhibited high selectivity for CH₄ production.

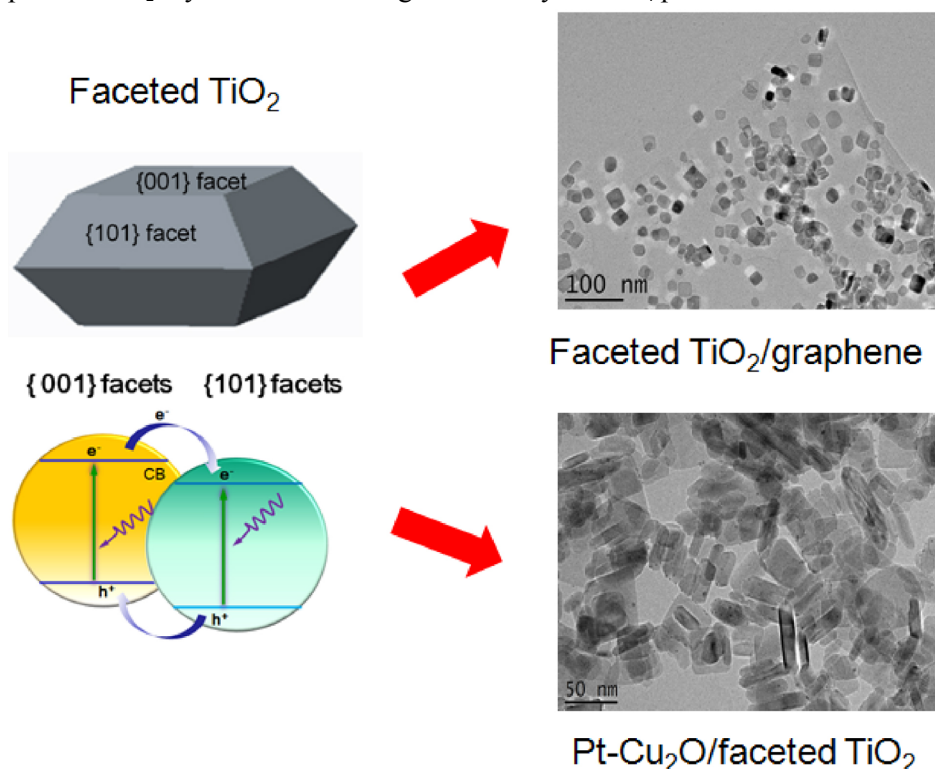


Figure 1. Schematic diagram of graphene and metal modified faceted TiO₂ nanocrystals.

Open Access

This article is licensed under a [Creative Commons Attribution 4.0 International License](https://creativecommons.org/licenses/by/4.0/).

© The Author(s) 2017

Albumin-mediated Gold/Platinum Nanocomposites for Dual Mode CT/MR Imaging Applications

Wenjing Zhao, Zhiming Wang, Zhongyun Chu, Nengqin Jia*

The Education Ministry Key Laboratory of Resource Chemistry and Shanghai Key Laboratory of Rare Earth Functional Materials, Department of Chemistry, College of Life and Environmental Sciences, Shanghai Normal University, 100 Guilin Road, Shanghai 200234, China
 Corresponding Author. Email: nqjia@shnu.edu.cn

Received: 01 June 2017, Accepted: 16 June 2017, Published Online: 29 October 2017

Citation Information: Wenjing Zhao, Zhiming Wang, Zhongyun Chu, Nengqin Jia, *Nano-Micro Conference, 2017, 1, 01054* doi: 10.11605/cp.nmc2017.01054

Abstract

Contrast agents play a vital role in the enhanced examination of biomedical imaging. However, traditional clinical small-molecule agents face a variety of drawbacks, such as low blood circulating time, difficult modification and potential toxic and side effects. Herein, a simple albumin directed fabrication of gold (Au) or platinum (Pt) nanoparticles was achieved for exploring the utilization in CT and MR imaging. Firstly, ultra-small nanoagents (Pt@BSA) with a mean core size of 2.1 nm were obtained through a facile one-pot synthesis by the reduction of chloroplatinic acid hexahydrate using bovine serum albumin (BSA) as the biotemplate under room temperature. It was demonstrated that the nanocrystals could serve as potential new and potent CT contrast agents, especially vital for in vivo imaging with prominent enhancement and metabolizable behaviours due to the combination of the higher X-ray attenuation property and prolonged imaging time [1]. Then gold nanoparticles (Au@BSA) were also prepared with BSA as a biotemplate following with conjugation of diatrizoic acid (DTA) for a potential CT imaging contrast agent (Au@BSA-DTA). The biomimetic material Au@BSA-DTA with double radiodense elements of Au and iodine displayed much stronger CT imaging effect compared with the traditional small molecule contrast agents [2]. Finally, a novel CT/MR contrast agent Au@BSA-Gd-DTPA was fabricated by modifying the as-prepared Au@BSA with diethylene triamine pentaacetic acid (DTPA), followed by the chelation of Gd (III) ions. For the CT phantoms, the formed nanocomplex showed an improved contrast in CT scanning than that of Au@BSA as well as small molecule iodine-based CT contrast agents, and for the T_1 -weighted MRI images, the nanoagents displayed a relatively higher r_1 relaxivity than that of the commercial MR contrast agents. Importantly, the above mentioned nanoagents exhibited not only good colloid stability and water dispersibility, but also satisfying low-cytotoxicity and hemocompatibility. In summary, we have constructed a series of novel biomaterials that can be used as contrast agents for both X-ray CT and MR phantoms, which paves the potential clinical applications in cancer early diagnosis.

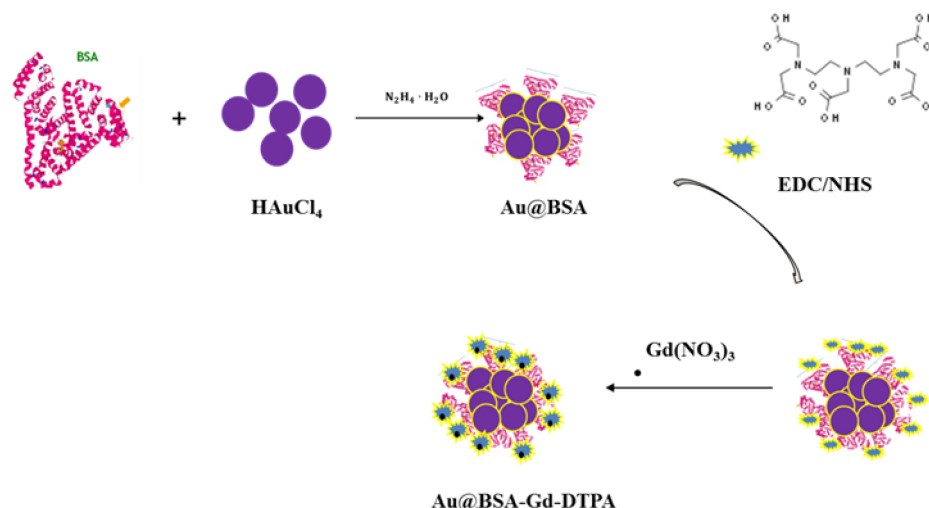


Figure 1. A schematic illustration of the preparation of the Au@BSA-Gd-DTPA.

References

- [1] Z. Wang; L. Chen; C. Huang; Y. Huang; N. Jia, Albumin-mediated platinum nanocrystals for in vivo enhanced computed tomography imaging. *Journal of Materials Chemistry B*. 5, 3498-3510 (2017). doi:10.1039/C7TB00561J
- [2] W. Zhao; Z. Wang; L. Chen; C. Huang; Y. Huang; N. Jia, A biomimetic Au@BSA-DTA nanocomposites-based contrast agent for computed tomography imaging. *Materials Science and Engineering:*

C. 78, 565-570 (2017). doi:10.1016/j.msec.2017.04.127

Open Access

This article is licensed under a [Creative Commons Attribution 4.0 International License](https://creativecommons.org/licenses/by/4.0/).

© The Author(s) 2017

Nanoparticles in Magnetic Resonance Imaging

Renhua Wu,^{1*} Zhiwei Shen,² Zhuozhi Dai³

Department of Medical Imaging, Shantou University Medical College, 22 Xinling Road, Shantou 515041, China
Corresponding Author. Email: rhwu@stu.edu.cn

Received: 28 May 2017, Accepted: 16 June 2017, Published Online: 29 October 2017

Citation Information: Renhua Wu, Zhiwei Shen, Zhuozhi Dai, Nano-Micro Conference, 2017, 1, 01055 doi: 10.11605/cp.nmc2017.01055

Abstract

Magnetic resonance imaging (MRI) provides crucial roles in diagnosis and treatment of human diseases. More and more new MRI techniques have been developed recently. Among them, chemical exchange saturation transfer (CEST) imaging (Figure 1) has shown its promising for noninvasive pH imaging and metabolic imaging [1]. Nanoparticles have also been studied widely in the field of magnetic resonance imaging, including disease detection and stem cell migration. For example, superparamagnetic iron oxide nanoparticles (SPIONs) have been intensively studied for their biomedical applications as T2 contrast agents in MRI. We collaborated with Zhang BL group [2] and found that compared with other nanoparticles, SPIONs exhibit highmagnetic responsivity which can reduce the amount of the contrast agents needed for calcium-responsive MRI, low cytotoxicity, higher biocompatibility and chemical stability. The assessment of changes in the extracellular calcium concentration by magnetic resonance imaging would be a valuable biomedical research tool to monitor brain neuronal activity. The nanoparticles, EGTA-SPIONs, have potential as smart contrast agents for Ca²⁺-sensitive MRI. We also collaborated with Bu WB group [3] and found that both T1-weighted imaging and in vivo pH mapping can be successfully acquired on the kidney and glioblastoma (GBM) of the mouse after intravenous injection of the T1/CEST NaGdF₄@PLL nanodots (NDs), demonstrating the feasibility of such an anatomical and functional dual-mode imaging technique on one magnetic resonance machine by the rational design of MRI contrast agents. Meanwhile, the PLL shell exhibits a sensitive CEST effect that depends on the pH value of the lesions. Attractively, these ultras-small nanoagents could be excreted through urine with negligible toxicity to body tissues, which has been demonstrated by the blood biochemistry, hematology, and tissue H&E staining analysis.

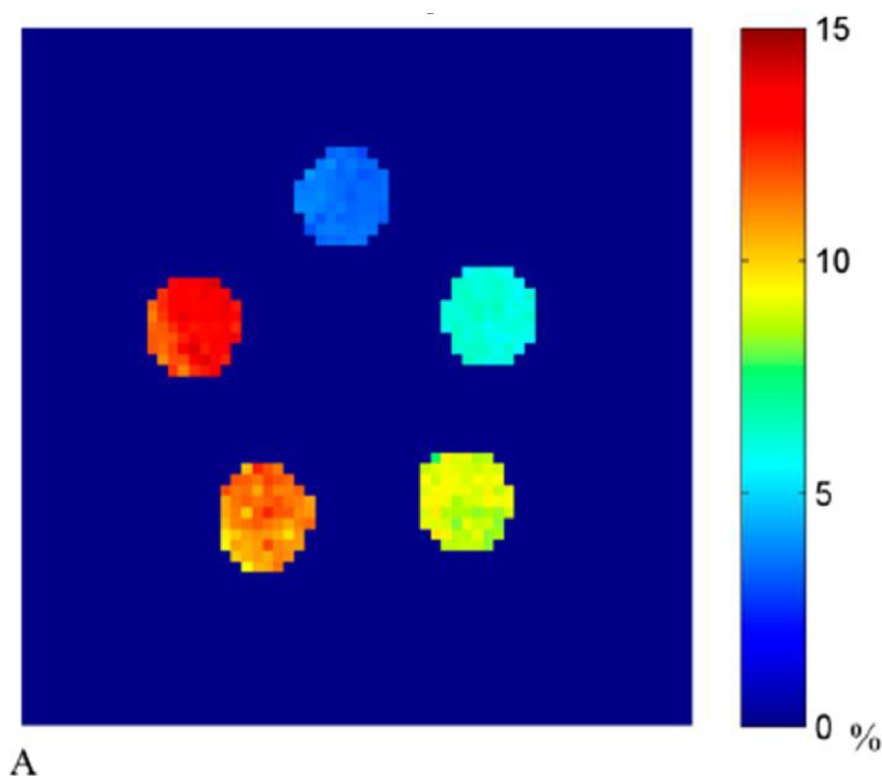


Figure 1. CEST images of creatine tubes of different concentrations.

References

[1] Xiangyong Tang; Zhuozhi Dai; Gang Xiao; Gen Yan; Zhiwei Shen; Tao Zhang; Guishan Zhang; Zerui Zhuang; Yuanyu Shen; Zhiyan Zhang; Wei Hu; Renhua Wu, Nuclear Overhauser Enhance-

ment-Mediated Magnetization Transfer Imaging in Glioma with Different Progression at 7 T. ACS Chemical Neuroscience. 8, 60-66 (2017). doi:10.1021/acscchemneuro.6b00173

[2] Pengfei Xu; Zhiwei Shen; Baolin Zhang; Jun Wang; Renhua Wu,

Synthesis and characterization of superparamagnetic iron oxide nanoparticles as calcium-responsive MRI contrast agents. *Applied Surface Science*. 389, 560-566 (2016). doi:[10.1016/j.apsusc.2016.07.160](https://doi.org/10.1016/j.apsusc.2016.07.160)

[3] Dalong Ni; Zhiwei Shen; Jiawen Zhang; Chen Zhang; Renhua Wu; Jianan Liu; Meizhi Yi; Jing Wang; Zhenwei Yao; Wenbo Bu; Jianlin Shi, Integrating Anatomic and Functional Dual-Mode Magnetic Resonance Imaging: Design and Applicability of a Bifunctional Contrast Agent. *ACS Nano*. 10, 3783-3790 (2016). doi:[10.1021/acs.nano.6b00462](https://doi.org/10.1021/acs.nano.6b00462)

Open Access

This article is licensed under a [Creative Commons Attribution 4.0 International License](https://creativecommons.org/licenses/by/4.0/).

© The Author(s) 2017

Proteins promote cancer nanotheranostics

Bingbo Zhang*

The Institute for Biomedical Engineering & Nano Science, Tongji University School of Medicine, Shanghai, 200443, China
Corresponding Author. Email: bingbozhang@tongji.edu.cn

Received: 17 May 2017, Accepted: 16 June 2017, Published Online: 29 October 2017

Citation Information: Bingbo Zhang, *Nano-Micro Conference*, 2017, 1, 01056 doi: 10.11605/cp.nmc2017.01056

Abstract

Utilizing molecular imaging probes can increase the detection rate and diagnosis accuracy of tumors. However, the non-specific adsorption of nanoprobe is seriously affecting the detection accuracy and sensitivity. Leveraging on the unique domains and amino acid sequences of bio-endogenous proteins, some specific tactics, including surface engineering of nanoparticles with proteins, and protein-mediated biomimetic synthesis of nanoprobe have been developed in a green chemistry fashion in our group [1-4]. This protein-mediated cancer nanotheranostic strategy is of great significance in reducing nonspecific adsorption of nanoprobe for in vitro diagnosis and in vivo applications. Capitalizing on this strategy, protein-coated nanoparticles with single-/dual- imaging modality were fabricated. Furthermore, therapeutical moieties can be imparted to the above structures in a one-pot manner for enhanced tumor theranostics. Particularly, the operating mechanisms of these reactions are preliminarily studied [5].

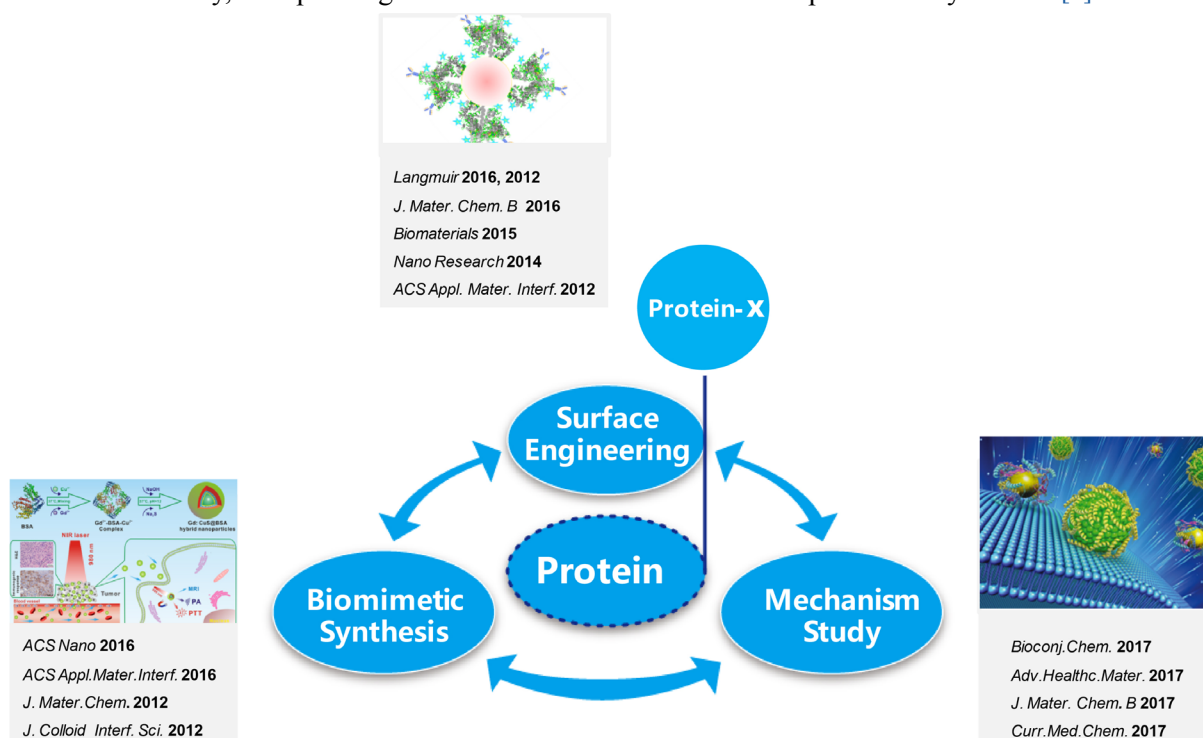


Figure 1. Protein-Mediated Biomimetic Tactics in Our Group.

References

- [1] W. Yang; W. Guo; W. Le; G. Lv; F. Zhang; L. Shi; X. Wang; J. Wang; S. Wang; J. Chang; B. Zhang, Albumin-Bioinspired Gd:CuS Nanotheranostic Agent for In Vivo Photoacoustic/Magnetic Resonance Imaging-Guided Tumor-Targeted Photothermal Therapy. *ACS Nano*. 10, 10245-10257 (2016). doi:10.1021/acsnano.6b05760
- [2] X. Xing; B. Zhang; X. Wang; F. Liu; D. Shi; Y. Cheng, An "imaging-biopsy" strategy for colorectal tumor reconfirmation by multi-purpose paramagnetic quantum dots. *Biomaterials*. 48, 16-25 (2015). doi:10.1016/j.biomaterials.2015.01.011
- [3] J. Zhang; G. Hao; C. Yao; J. Yu; J. Wang; W. Yang; C. Hu; B. Zhang, Albumin-Mediated Biomimetic Synthesis of Paramagnetic NIR Ag₂S QDs for Tiny Tumor Bimodal Targeted Imaging in Vivo. *ACS Applied Materials & Interfaces*. 8, 16612-16621 (2016). doi:10.1021/acsami.6b04738
- [4] B. Zhang; H. Jin; Y. Li; B. Chen; S. Liu; D. Shi, Bioinspired synthesis of gadolinium-based hybrid nanoparticles as MRI blood pool

contrast agents with high relaxivity. *Journal of Materials Chemistry*. 22, 14494-14501 (2012). doi:10.1039/C2JM30629H

- [5] B. Zhang; J. Wang; J. Yu; X. Fang; X. Wang; D. Shi, Site-specific Biomimetic Precision Chemistry of Bimodal Contrast Agent with Modular Peptides for Tumor-targeted Imaging. *Bioconjugate Chemistry*. 28, 330-335 (2017). doi:10.1021/acs.bioconjchem.6b00712

Open Access

This article is licensed under a [Creative Commons Attribution 4.0 International License](https://creativecommons.org/licenses/by/4.0/).

© The Author(s) 2017

Tracking of Stem Cells with Magnetic Resonance Imaging

Qun Zhao*

Bioimaging Research Center & Department of Physics, University of Georgia, Athens, GA., USA

Corresponding Author. Email: qzhao@physast.uga.edu

Received: 11 May 2017, Accepted: 16 June 2017, Published Online: 29 October 2017

Citation Information: Qun Zhao, *Nano-Micro Conference*, 2017, 1, 01057 doi: [10.11605/cp.nmc2017.01057](https://doi.org/10.11605/cp.nmc2017.01057)

Abstract

Recently various cell therapies have improved outcome of many diseases. A critical component of cell therapies is the ability to track the cells after transplantation. Monitoring a cell's survival, migration, differentiation, and integration within host tissue is crucial for assessing the safety and efficacy of cellular treatments. In this talk magnetic resonance imaging (MRI) based tracking of stem cells is presented, where cells labeled with superparamagnetic iron oxide (SPIO) nanoparticles can be tracked in a chicken embryo model up to 10 days post transplantation. Nevertheless, SPIO nanoparticles as a T_2^* contrast agent are usually associated with signal loss in MR images, leading to difficulties for cell tracking. To overcome this problem, a new imaging sequence, SWIFT with water and fat suppression, is introduced. Compared with other conventional pulse sequences, such as spin echo and gradient-recalled echo, the SWIFT approach enhances in vivo mapping of SPIO distribution in tissues, and improves detection sensitivity of SPIO nanoparticles.

Open Access

This article is licensed under a [Creative Commons Attribution 4.0](https://creativecommons.org/licenses/by/4.0/)

[International License](https://creativecommons.org/licenses/by/4.0/).

© The Author(s) 2017

Tuning solar absorbance and reflection of high-temperature solar spectrally selective surfaces

Feng Cao,^{1*} Qian Zhang,² Zhifeng Ren³

¹School of Science, Harbin Institute of Technology Shenzhen Graduate School, Shenzhen, 518055, China

²School of Materials Science and Engineering, Harbin Institute of Technology Shenzhen Graduate School, Shenzhen, 518055, China

³Department of Physics and TeSUH, University of Houston, Houston, TX 77204, USA

Corresponding Author. Email: caofeng@hit.edu.cn

Received: 24 May 2017, Accepted: 17 June 2017, Published Online: 29 October 2017

Citation Information: Feng Cao, Qian Zhang, Zhifeng Ren, *Nano-Micro Conference*, 2017, 1, 01058 doi: 10.11605/cp.nmc2017.01058

Abstract

Spectrally-selective solar absorbers are widely used in solar hot water and concentrating solar power (CSP) systems [1,2]. However, the performance at high temperatures (>450 °C) is still not satisfactory due to their high infrared (IR) emittance and long term thermal stability. Recent progress on cermet-based solar absorbers has shown promising temperature thermal stability and wavelength selectivity. Thus, here we explore W-Ni-Al₂O₃, W-Ni-YSZ (yttria-stabilized-zirconia) and W-Ni-SiO₂ cermet based spectrally selective surfaces for high-temperature solar absorber applications [3,4]. The developed multilayer selective surfaces are deposited on a polished stainless steel substrate comprising two sunlight absorbing cermet layers with different W-Ni volume fraction inside the dielectric matrix, one or two anti-reflection coatings (ARCs) and one tungsten IR reflection layer for reduced IR emittance and improved thermal stability.

Regarding the W-Ni-Al₂O₃ cermet based solar absorbers; we observed a detrimental change in the morphology, phase, and optical properties if the cermet layers are deposited on a stainless steel substrate with a thin nickel adhesion layer, which is due to the diffusion of iron atoms from the stainless steel into the cermet layer forming a FeWO₄ phase. A 100 nm thick tungsten layer can suppress the degradation of the optical properties at high temperatures and lowers the emittance relative to the stainless steel substrate, which improves the spectral selectivity of the solar absorber. We experimentally demonstrated a solar absorber with a solar absorptance of ~0.9 and total hemispherical emittance of ~0.15 at an operating temperature of 500 °C.

The fabricated W-Ni-YSZ cermet based solar absorbers are tested for their long term thermal stability at 600 °C. A distinct change in surface morphology of the solar absorbers with high oxygen deficiency in their YSZ-ARC layers, suggests to causing the degradation of the optical properties at high temperature. The oxygen deficiency can be effectively overcome through increasing the oxygen partial pressure during sputtering, which leads to a stable solar absorber with an experimentally demonstrated solar absorptance of ~0.91 and a total hemispherical emittance of ~0.13 at 500 °C.

We also developed a new kind of absorber that reflects a certain range of wavelength and absorbs the rest of the whole solar spectra [5]. The absorbed part is used for electrical power generation by steam engine and the reflected part is used for solar photovoltaic conversion. The thermal energy can be easily stored for later conversion to provide electrical power around the clock without worrying the Sun's night time.

References

- [1] C. E. Kennedy, Review of Mid to High Temperature Solar Selective Absorber Materials. National Renewable Energy Laboratory. 2002. doi:10.2172/15000706
- [2] F. Cao; K. McEnaney; G. Chen; Z. Ren, A review of cermet-based spectrally selective solar absorbers. *Energy & Environmental Science*. 7, 1615-1627 (2014). doi:10.1039/C3EE43825B
- [3] F. Cao; D. Kraemer; T. Y. Sun; Y. C. Lan; G. Chen; Z. F. Ren, Enhanced Thermal Stability of W-Ni-Al₂O₃ Cermet-based Spectrally Selective Solar Absorbers with W Infrared Reflector. *Advanced Energy Materials*. 5, 1401042 (2015). doi:10.1002/aenm.201401042
- [4] F. Cao; D. Kraemer; L. Tang; Y. Li; Alexander P. Litvinchuk; J. Bao; G. Chen; Z. F. Ren, A high-performance spectrally-selective solar absorber based on a yttria-stabilized zirconia cermet with high-temperature stability. *Energy & Environmental Science*. 8, 3040-3048 (2015). doi:10.1039/C5EE02066B
- [5] F. Cao; Y. Huang; L. Tang; T. Y. Sun; S. V. Boriskina; G. Chen; Z. F. Ren, Toward a High-Efficient Utilization of Solar Radiation by Quad-Band Solar Spectral Splitting. *Advanced Materials*. 28, 10659-

10663 (2016). doi:10.1002/adma.201603113

Open Access

This article is licensed under a [Creative Commons Attribution 4.0 International License](https://creativecommons.org/licenses/by/4.0/).

© The Author(s) 2017

Titanium Dioxide Films with Pure Anatase Phase Synthesized by Mist Chemical Vapour Deposition

Chaoyang Li,* Qiang Zhang, Lilin Xie

School of System Engineering, Kochi University of Technology, 185 Miyanokuchi Tosayamada cho Kami City, Kochi 782-8502, Japan

Corresponding Author. Email: li.chaoyang@kochi-tech.ac.jp

Received: 31 May 2017, Accepted: 16 June 2017, Published Online: 29 October 2017

Citation Information: Chaoyang Li, Qiang Zhang, Lilin Xie, Nano-Micro Conference, 2017, 1, 01059 doi: 10.11605/cp.nmc2017.01059

Abstract

Pure anatase structured TiO₂ films were successfully synthesized by a novel fine channel mist chemical vapour deposition which is a vacuum free, low temperature method [1]. The effects of TTIP concentration on the morphological, structural and optical properties of TiO₂ films were investigated. It was confirmed that anatase crystallinity of TiO₂ film increased with the increase of TTIP concentration. Figure 1 showed that XRD patterns of TiO₂ thin films which were synthesized with the different concentration of TTIP in ethanol varying from 0.025 to 0.4 mol/L. The high catalytic activity will be expected by using obtained stable anatase TiO₂ films.

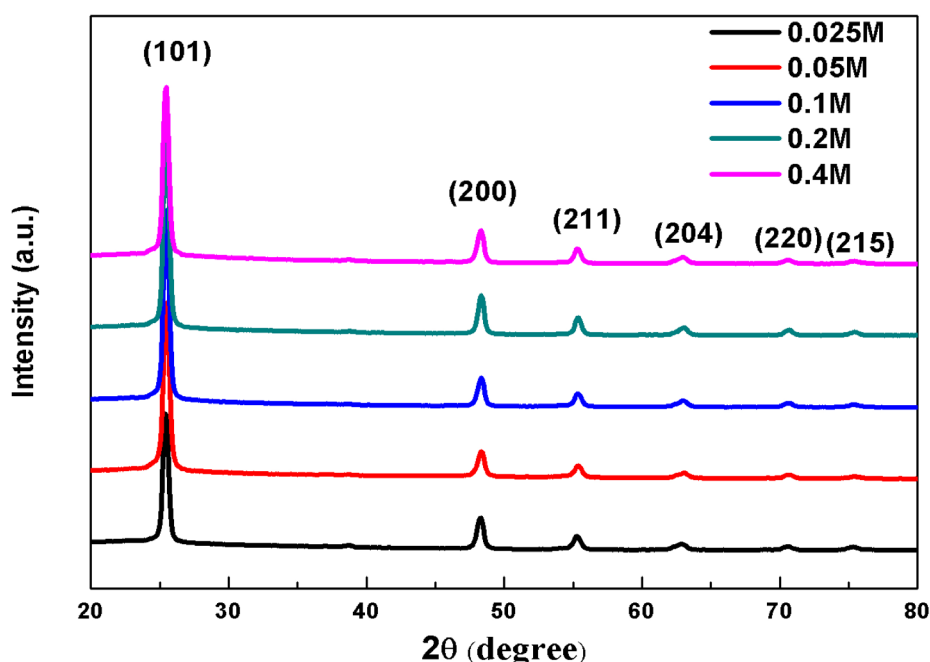


Figure 1. XRD patterns of TiO₂ films synthesized at TTIP concentration of 0.025, 0.05, 0.1, 0.2, and 0.4 mol/L.

References

- [1] T. Kawaharamura; S. Fujita, An approach for single crystalline zinc oxide thin films with fine channel mist chemical vapor deposition method. *Physica Status Solidi (c)*, 5, 3138-3140 (2008). doi:10.1002/pssc.200779305

Open Access

This article is licensed under a [Creative Commons Attribution 4.0 International License](https://creativecommons.org/licenses/by/4.0/).

© The Author(s) 2017

Broadband Optical Absorption Based on Plasmonic Nanostructures

Qiang Li,* Min Qiu

State Key Laboratory of Modern Optical Instrumentation, College of Optical Science and Engineering, Zhejiang University, Hangzhou 310027, China

Corresponding Author. Email: qiangli@zju.edu.cn

Received: 02 June 2017, Accepted: 18 June 2017, Published Online: 29 October 2017

Citation Information: Qiang Li, Min Qiu, *Nano-Micro Conference*, 2017, 1, 01060 doi: 10.11605/cp.nmc2017.01060

Abstract

Plasmonic metamaterial absorbers have garnered significant interest due to their unique ability to trap light beyond diffraction limit and potential applications in energy harvesting and information processing. Especially, the broadband absorbers show fascinating applications in photovoltaics and thermophotovoltaics, bolometers, thermal emitters, and photodetectors. In this talk, I will review our recent work on broadband optical absorption based on plasmonic based on ultra-thin metal-insulator-metal (MIM) plasmonic absorbers [1,2].

References

[1] W. Wang; Y.R. Qu; K. K. Du; S. A. Bai; J. Y. Tian; M. Y. Pan; H. Ye; M. Qiu; Q. Li, Broadband Optical Absorption Based on Single-sized Metal-dielectric-metal Plasmonic Nanostructures with High- ϵ'' Metals. *Applied Physics Letters*. 110, 101101 (2017). doi:10.1063/1.4977860

[2] X. X. Chen; H. M. Gong; S. W. Dai; D. Zhao; Y. Q. Yang; Q. Li; M. Qiu, Near-infrared broadband absorber with film-coupled multi-layer nanorods. *Optics Letters*. 38, 2247-2249 (2013). doi:10.1364/OL.38.002247

Open Access

This article is licensed under a [Creative Commons Attribution 4.0 International License](https://creativecommons.org/licenses/by/4.0/).

© The Author(s) 2017

One-Dimensional Nanomaterials for Energy Storage

Liqiang Mai,* Lin Xu

State Key Laboratory of Advanced Technology for Materials Synthesis and Processing, School of Materials Science and Engineering, Wuhan University of Technology, Wuhan, 430070, China

Corresponding Author. Email: mlq518@whut.edu.cn

Received: 26 May 2017, Accepted: 16 June 2017, Published Online: 29 October 2017

Citation Information: Liqiang Mai, Lin Xu, *Nano-Micro Conference*, 2017, 1, 01061 doi: 10.11605/cp.nmc2017.01061

Abstract

One-dimensional nanomaterials can offer large surface area, facile strain relaxation upon cycling and efficient electron transport pathway to achieve high electrochemical performance. Hence, nanowires have attracted increasing interest in energy related fields. We designed the single nanowire electrochemical device for in situ probing the direct relationship between electrical transport, structure, and electrochemical properties of the single nanowire electrode to understand intrinsic reason of capacity fading. The results show that during the electrochemical reaction, conductivity of the nanowire electrode decreased, which limits the cycle life of the devices [1]. We have fabricated hierarchical $\text{MnMoO}_4/\text{CoMoO}_4$ heterostructured nanowires by combining “oriented attachment” and “self-assembly” [2]. The asymmetric supercapacitors based on the hierarchical heterostructured nanowires show a high specific capacitance and good reversibility with a cycling efficiency of 98% after 1,000 cycles. Then, we designed the general synthesis of complex nanotubes by gradient electrospinning, including $\text{Li}_3\text{V}_2(\text{PO}_4)_3$, $\text{Na}_{0.7}\text{Fe}_{0.7}\text{Mn}_{0.3}\text{O}_2$ and Co_3O_4 mesoporous nanotubes, which exhibit ultrastable electrochemical performance when used in lithium-ion batteries, sodium-ion batteries and supercapacitors, respectively [3]. In addition, we have successfully fabricated a field-tuned hydrogen evolution reaction (HER) device with an individual MoS_2 nanosheet to explore the impact of field effect on catalysis [4]. We also constructed a new-type carbon coated $\text{K}_{0.7}\text{Fe}_{0.5}\text{Mn}_{0.5}\text{O}_2$ interconnected nanowires through a simply electrospinning method. The interconnected nanowires exhibit a discharge capacity of 101 mAh g^{-1} after 60 cycles, when measured as a cathode for K-ion batteries [5]. Our work presented here can inspire new thought in constructing novel one-dimensional structures and accelerate the development of energy storage applications.

Reference

- [1] L. Q. Mai; Y. J. Dong; L. Xu; C. H. Han, Single Nanowire Electrochemical Devices. *Nano Letters*. 10, 4273-4278 (2010). doi:10.1021/nl102845r
- [2] L. Q. Mai; F. Yang; Y. L. Zhao; X. Xu; L. Xu; Y. Z. Lou, Hierarchical $\text{MnMoO}_4/\text{CoMoO}_4$ heterostructured nanowires with enhanced supercapacitor performance. *Nature Communications*. 2, 381 (2011). doi:10.1038/ncomms1387
- [3] C. J. Niu; J. S. Meng; X. P. Wang; C. H. Han; M. Y. Yan; K. N. Zhao; X. M. Xu; W. H. Ren; Y. L. Zhao; L. Xu; Q. J. Zhang; D. Y. Zhao; L. Q. Mai, General synthesis of complex nanotubes by gradient electrospinning and controlled pyrolysis. *Nature Communications*. 6, 7402 (2015). doi:10.1038/ncomms8402
- [4] J. H. Wang; M. Y. Yan; K. N. Zhao; X. B. Liao; P. Y. Wang; X. L. Pan; W. Yang; L. Q. Mai, Field Effect Enhanced Hydrogen Evolution Reaction of MoS_2 Nanosheets. *Advanced Materials*. 29, 1604464 (2017). doi:10.1002/adma.201604464
- [5] X. P. Wang; X. M. Xu; C. J. Niu; J. S. Meng; M. Huang; X. Liu; Z. A. Liu; L. Q. Mai, Earth Abundant Fe/Mn-Based Layered Oxide Interconnected Nanowires for Advanced K-Ion Full Batteries. *Nano Letters*. 17, 544-550 (2017). doi:10.1021/acs.nanolett.6b04611

Open Access

This article is licensed under a [Creative Commons Attribution 4.0 International License](https://creativecommons.org/licenses/by/4.0/).

© The Author(s) 2017

Green Semiconductor Vertical-Cavity Surface-Emitting Lasers based on Quantum Dots

Baoping Zhang,* Yang Mei, Rongbin Xu, Zhiwei Zheng, Hao Long, Leiying Ying

Department of Electronic Engineering, Optoelectronics Engineering Research Center, Xiamen University, Xiamen, Fujian 361005, China

Corresponding Author. Email: bzhang@xmu.edu.cn

Received: 20 May 2017, Accepted: 10 June 2017, Published Online: 30 October 2017

Citation Information: Baoping Zhang, Yang Mei, Rongbin Xu, Zhiwei Zheng, Hao Long, Leiying Ying, Nano-Micro Conference, 2017, 1, 01062 doi: 10.11605/cp.nmc2017.01062

Abstract

Green VCSELs emitting in the spectral range from 491.8 nm to 565.7 nm, covering most of the ‘green gap’, are demonstrated. These devices are featured with low threshold current and CW lasing at room temperature. A few technologies such as laser liftoff of sapphire substrate, the removal of high-defect GaN buffer and Cu plating to increase the heat dissipation. Two dielectric DBRs were adopted as the cavity mirrors. The results presented here open up opportunities to design and fabricate semiconductor green lasers with excellent performance that may lead to wide-gamut, low consumption power and compact displays and projectors. The VCSELs could also be bonded on to Si for integration with other optoelectronic devices/circuits.

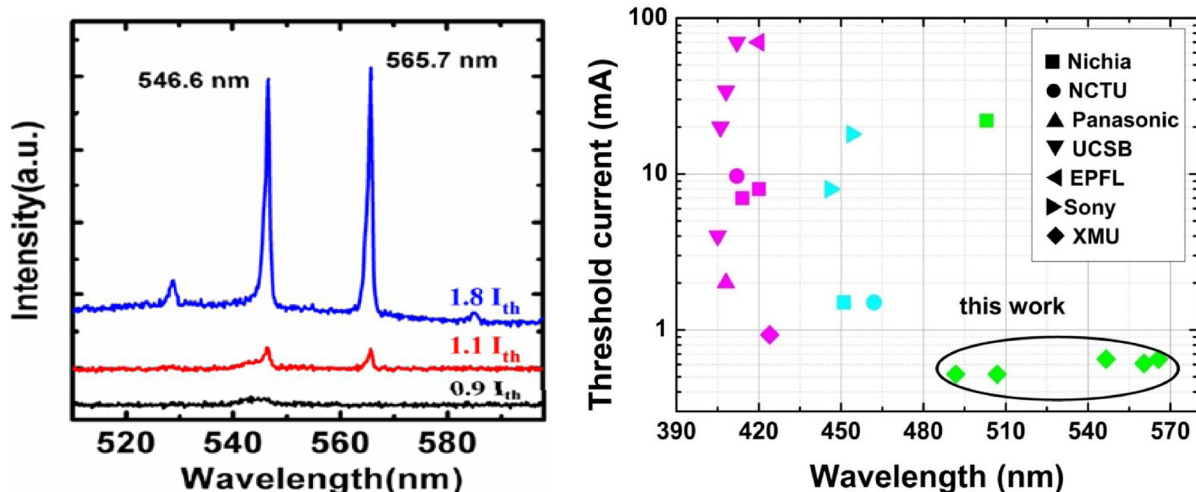


Figure 1. Lasing spectra (left) in this work and comparison (right) of threshold currents with literatures.

References

[1] Y. Mei; G. E. Weng; B. P. Zhang; J. P. Liu; W. Hofmann; L. Y. Ying; J. Y. Zhang; Z. C. Li; H. Yang; H. C. Kuo, Quantum dot vertical-cavity surface-emitting lasers covering the ‘green gap’. *Light: Science & Applications*. 6, e16199 (2017). doi:10.1038/lsa.2016.199

Open Access

This article is licensed under a [Creative Commons Attribution 4.0 International License](https://creativecommons.org/licenses/by/4.0/).

© The Author(s) 2017

Spin Texture And Spin Injection In A 3D Topological Insulator

W. M. Chen,^{1*} Y. Q. Huang,¹ I. A. Buyanova,¹ Y. X. Song,² S. M. Wang²

¹Department of Physics, Chemistry and Biology, Linköping University, S-581 83 Linköping, Sweden

²State Key Laboratory of Functional Materials for Informatics, CAS Center of Excellence for Superconducting Electronics, Shanghai Institute of Microsystem and Information Technology, Chinese Academy of Sciences, 865 Changning Road, Shanghai 200050, China

Corresponding Author. Email: wmc@ifm.liu.se

Received: 31 May 2017, Accepted: 12 June 2017, Published Online: 30 October 2017

Citation Information: W. M. Chen, Y. Q. Huang, I. A. Buyanova, Y. X. Song, S. M. Wang, *Nano-Micro Conference, 2017, 1, 01063* doi: 10.11605/cp.nmc2017.01063

Abstract

One of the most critical steps towards spin functionalized electronics and optoelectronics is to generate and manipulate spin current in a desirable way. In 3D topological insulators (TIs), a strong spin-orbit interaction and the time-reversal symmetry result in spin-momentum locking of the surface electrons, which leads to a unique surface spin texture and the prospect of generating directional and dissipationless spin current running across the surface that is promising for spintronic applications. However, the metallic nature that is often found to be inherent to many 3D TIs due to residual defects has unfortunately imposed a severe obstacle to controlling surface spin current. As a result, very little experimental work has been done so far on this issue. Moreover, since most of the early studies have been limited to Bi₂Se₃ - a prototypical TI with a rather weak hexagonal warping effect, the contribution of the out-of-plane spin texture to the photocurrent remains elusive so far. In this work, we show that, with circular polarized light, helicity driven photocurrent is obtained in another 3D TI Bi₂Te₃ that exhibits a stronger hexagonal warping effect. We find the helicity-dependent photocurrent to be sensitive to the incident angle of the light, which could be explained within the framework of the circular photo-galvanic effect (CPGE) by taking into account the spin texture of the topological surface state. By correlating the light incident angle and probing surface current directions, we are able to identify photocurrent components associated with the in-plane and out-of-plane spin texture of the TI and thereby directly uncover the impact of the out-of-plane spin texture on surface spin current promoted by the strong hexagonal warping effect. By exploring the out-of-plane spin texture, we demonstrate spin injection from GaAs to TI and its significant contribution to the surface current [1]. We further show that the spin current of TI can be manipulated by the precession of injected electron spins in an external magnetic field. These discoveries pave the way to not only intriguing new physics but also enriched spin functionalities by integrating TI with conventional semiconductors, such that spin-enabled optoelectronic devices may be fabricated in such hybrid structures.

References

[1] Y. Q. Huang; Y. X. Song; S. M. Wang; I.A. Buyanova; W. M. Chen, Spin injection and helicity control of surface spin photocurrent in a three dimensional topological insulator. *Nature Communications*. 8, 15401 (2017). doi:10.1038/ncomms15401

Open Access

This article is licensed under a [Creative Commons Attribution 4.0 International License](https://creativecommons.org/licenses/by/4.0/).

© The Author(s) 2017

Quantum phase transitions and order parameters of a topological insulator

Yan-Chao Li^{1,2,*}

¹College of Materials Science and Opto-Electronic Technology, University of Chinese Academy of Sciences, Beijing, 100049, China

²Beijing Computational Science Research Center, Beijing 100193, China

Corresponding Author. Email: ycli@ucas.ac.cn

Received: 15 May 2017, Accepted: 10 June 2017, Published Online: 30 October 2017

Citation Information: Yan-Chao Li, *Nano-Micro Conference*, 2017, 1, 01064 doi: 10.11605/cp.nmc2017.01064

Abstract

Using quantum entanglement, quantum coherence, and the reduced density matrix, we study the quantum phase transitions and propose order parameters for the phases of a topological insulator, specifically a spinless Su-Schrieffer-Heeger (SSH) model, and consider the effect of short-range interactions. All the derived order parameters and their possible corresponding quantum phases are verified by the entanglement entropy and electronic configuration analysis results. The order parameter appropriate to the topological regions is further proved by calculating the Berry phase under twisted boundary conditions. It is found that the topological nontrivial phase is robust to the introduction of repulsive intersite interactions and can appear in the topological trivial parameter region when appropriate interactions are added.

Open Access

This article is licensed under a [Creative Commons Attribution 4.0 International License](https://creativecommons.org/licenses/by/4.0/).

© The Author(s) 2017

Novel Topological Phase with a Zero Berry Curvature

Feng Liu,^{1*} Katsunori Wakabayashi^{1,2}

¹Department of Nanotechnology for Sustainable Energy, School of Science and Technology, Kwansai Gakuin University, Gakuen 2-1, Sanda 669-1337, Japan

²National Institute for Materials Science (NIMS), Namiki 1-1, Tsukuba 305-0044, Japan

Corresponding Author. Email: ruserzz@gmail.com

Received: 31 May 2017, Accepted: 12 June 2017, Published Online: 30 October 2017

Citation Information: Feng Liu, Katsunori Wakabayashi, *Nano-Micro Conference*, 2017, 1, 01065 doi: 10.11605/cp.nmc2017.01065

Abstract

Recalling the scenario of Aharonov-Bohm effect that electrons experience a phase shift induced by a magnetic vector potential in spite of a zero-magnetic field, we have a similar story in topological version to tell here, where the magnetic field and the magnetic vector potential are replaced by their geometric counterparts, Berry curvature and Berry connection, respectively.

Starting from a simple two-dimensional tight-binding model with two types of hopping, i.e. intercellular γ and intracellular hopping γ' based on square lattice, we show that nontrivial topological phase emerges when $|\gamma| < |\gamma'|$ under a zero Berry curvature. Our work offers a new way to design topological materials without Berry curvatures [1].

References

[1] F. Liu; K. Wakabayashi, Novel Topological Phase with a Zero Berry Curvature. *Physical Review Letters*. 118, 076803 (2017). doi:10.1103/PhysRevLett.118.076803

Open Access

This article is licensed under a [Creative Commons Attribution 4.0 International License](https://creativecommons.org/licenses/by/4.0/).

© The Author(s) 2017

Spin texture of flatten Dirac-cone surface state on W(110)

Koji Miyamoto,^{1*} Taichi Okuda,¹ Henry Wortelen,² Markus Donath²

¹Hiroshima Synchrotron Radiation Center, Hiroshima University, Kagamiyama 2-313, 7390046 Higashi-Hiroshima, Japan

²Physikalisches Institut, Westfälische Wilhelms-Universität Münster, Wilhelm-Klemm-Strasse 10, 28149 Münster, Germany

Corresponding Author. Email: kmiyamoto@hiroshima-u.ac.jp

Received: 18 May 2017, Accepted: 10 June 2017, Published Online: 31 October 2017

Citation Information: Koji Miyamoto, Taichi Okuda, Henry Wortelen, Markus Donath, Nano-Micro Conference, 2017, 1, 01066 doi: 10.11605/cp.nmc2017.01066

Abstract

Topological insulators and Rashba systems with spin-split energy band structure induced by strong spin-orbit interaction have attracted a great attention for the dissipationless spin current transport. The spin orientation of such spin-split state is locked with their crystal momentum and is strongly influenced by the symmetry of surface crystal. However, so-far, most of topological material and Rashba systems are sp-electrons system with C_{3v} point group symmetry [1].

Recently, we have reported spin polarized Dirac-cone surface state on W(110) with C_{2v} symmetry [2]. This surface state is formed by d-electrons and strongly influence by two-fold symmetry: the massless and massive band dispersion along $\overline{\Gamma\text{H}}$ and $\overline{\Gamma\text{N}}$. Moreover, by model Hamiltonian based on $\mathbf{k}\cdot\mathbf{p}$ theorem, it have been predicted that the spin-polarized flatten Dirac-cone surface state shows quasi-one dimensional spin texture as shown in Figure 1 [3]. However, there is no evidence for the spin texture on W(110).

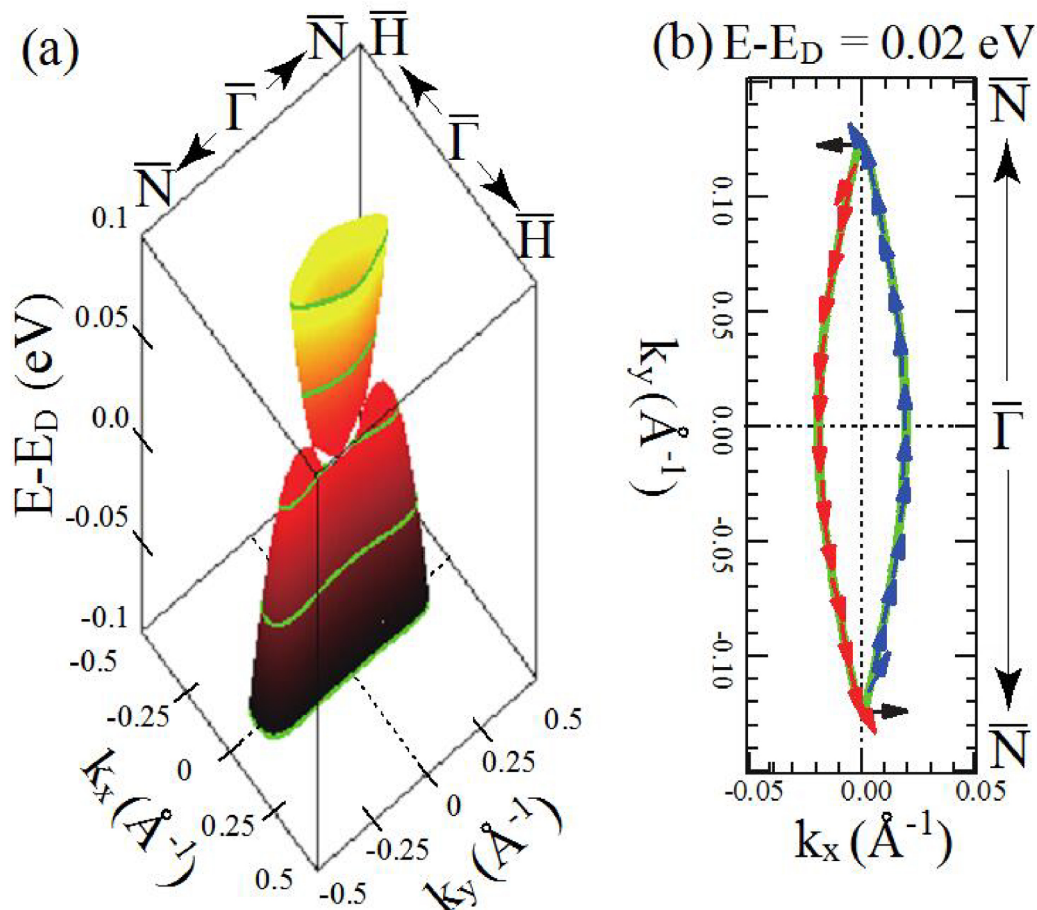


Figure 1. (a) Energy Contours of the surface state as function of k_x , k_y for energies around crossing point based on model calculation. (b) Spin texture for the constant-energy surface (solid line) at 0.02eV above crossing point. The in-plane spin components are shown as arrows.

In this presentation, we have clarified the spin texture of flatten Dirac-cone surface state on W(110) studied by spin- and angle-resolved photoemission spectroscopy. The observed spin texture is in good agreement with our predicted one. This research is the model case of d-electron –based surface state with C_{2v} symmetry. The finding opens a new avenue in the study of d-electrons-based spin texture with C_{2v} symmetry. If I have remaining time enough to talk another symmetry surface of tungsten, I will introduce you.

References

- [1] M. Z. Hasan; C. L. Kane, Colloquium: Topological insulators. *Reviews of Modern Physics*. 82, 3045 (2010). doi:[10.1103/RevModPhys.82.3045](https://doi.org/10.1103/RevModPhys.82.3045)
- [2] K. Miyamoto; A. Kimura; K. Kuroda; T. Okuda; K. Shimada; H. Namatame; M. Taniguchi; M. Donath, Spin-polarized Dirac-cone-like surface state with d character at W(110). *Physical Review Letters*. 108, 066808 (2012). doi:[10.1103/PhysRevLett.108.066808](https://doi.org/10.1103/PhysRevLett.108.066808)
- [3] K. Miyamoto; A. Kimura; T. Okuda; K. Shimada; H. Iwasawa; H. Hayashi; H. Namatame; M. Taniguchi; M. Donath, Massless or heavy due to two-fold symmetry: Surface-state electrons at W(110). *Physical Review B*. 86, 161411(R) (2012). doi:[10.1103/PhysRevB.86.161411](https://doi.org/10.1103/PhysRevB.86.161411)

Open Access

This article is licensed under a [Creative Commons Attribution 4.0 International License](https://creativecommons.org/licenses/by/4.0/).

© The Author(s) 2017

One-dimensional edge states with spin splitting in bismuth

A. Takayama,^{1*} T. Sato,² S. Souma,³ T. Oguchi,⁴ T. Takahashi^{2,3}

¹Department of Physics, The University of Tokyo, Bunkyo-ku 113-0033, Japan

²Department of Physics, Tohoku University, Sendai 980-8578, Japan

³WPI Research Center, Advanced Institute for Materials Research, Tohoku University, Sendai 980-8577, Japan

⁴Institute of Scientific and Industrial Research, Osaka University, Ibaraki, Osaka 567-0047, Japan

Corresponding Author. Email: a.takayama@surface.phys.s.u-tokyo.ac.jp

Received: 31 May 2017, Accepted: 12 June 2017, Published Online: 31 October 2017

Citation Information: A. Takayama, T. Sato, S. Souma, T. Oguchi, T. Takahashi, Nano-Micro Conference, 2017, 1, 01067 doi: 10.11605/cp.nmc2017.01067

Abstract

A two-dimensional (2D) system with strong spin-orbit coupling like a topological-insulator surface and semiconductor-heterostructure interface has provided a useful platform for realizing novel quantum phenomena applicable to advanced spintronic devices. 1 bilyer (BL) bismuth is theoretically predicted to be 2D topological insulator and have a spin-polarized state at edge [1,2]. However, it is not certain experimentally because to preparer a free-standing 1 BL bismuth is very difficult. Here we challenged to observe a spin-polarized electric state at edge by different approach. As observed by the atomic force microscopy (AFM) of our Bi thin film (Figure 1a), triangular-shaped bismuth BL islands with typically $\sim 0.1 \mu\text{m}$ edge length are formed on the top surface of the Bi thin film, and the edge of each island runs along the $\Gamma\bar{K}$ direction in the k space. And we have also observed the 1D band dispersion from the edge state of bismuth islands measured by ARPES. In this presentation, we show the result of ARPES and spin-resolved ARPES for bismuth thin film, and discuss the origin of the 1D spin-splitting band compared with our first-principles band-calculations.

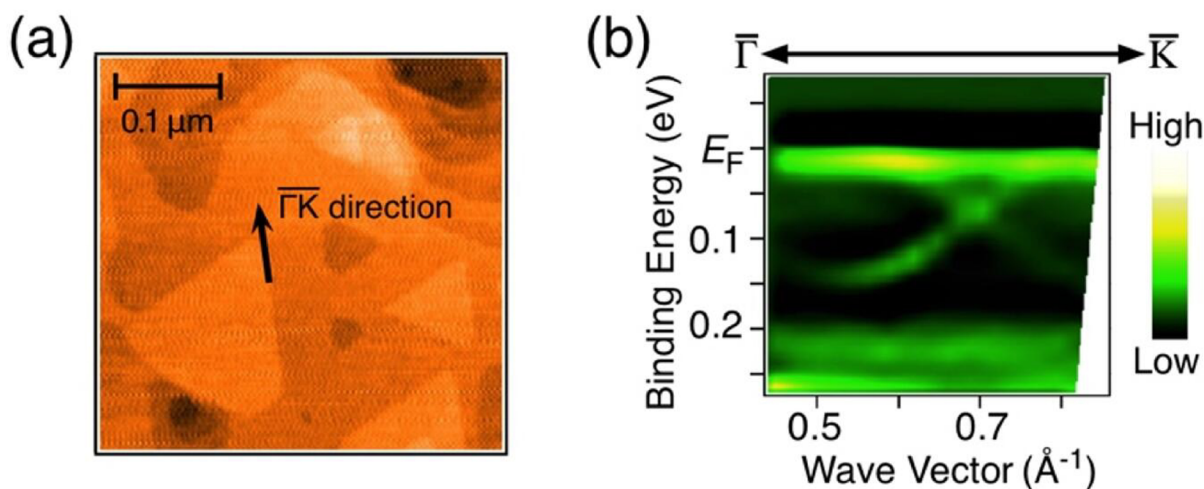


Figure 1. (a) AFM image measured at 300 K in Air and (b) Band dispersion near E_F along $\Gamma\bar{K}$ line measured at 30 K in UHV for a Bi thin film, respectively.

References

[1] S. Murakami, Quantum Spin Hall Effect and Enhanced Magnetic Response by Spin-Orbit Coupling. *Physical Review Letters*. 97, 236805 (2006). doi:10.1103/PhysRevLett.97.236805

[2] M. Wada; S. Murakami; F. Freimuth; G. Bihlmayer, Localized edge states in two-dimensional topological insulators: Ultrathin Bi films. *Physical Review B*. 83, 121310(R) (2011). doi:10.1103/PhysRevB.83.121310

Open Access

This article is licensed under a [Creative Commons Attribution 4.0 International License](https://creativecommons.org/licenses/by/4.0/).

© The Author(s) 2017

Magnetic Topological Insulators and Their Heterostructures

Xufeng Kou,^{1,2*} Lei Pan,² Qinglin He,² Yabin Fan,² Kang L. Wang^{2,3,4}

¹School of Information Science and Technology, ShanghaiTech University, Shanghai, China

²Department of Electrical Engineering, University of California, Los Angeles, USA

³Department of Physics, University of California, Los Angeles, USA

⁴Department of Materials Sciences and Engineering, University of California, Los Angeles, USA

Corresponding Author. Email: kxf2323@gmail.com

Received: 26 May 2017, Accepted: 10 June 2017, Published Online: 31 October 2017

Citation Information: Xufeng Kou, Lei Pan, Qinglin He, Yabin Fan, Kang L. Wang, *Nano-Micro Conference, 2017, 1, 01068* doi: [10.11605/cp.nmc2017.01068](https://doi.org/10.11605/cp.nmc2017.01068)

Abstract

When magnetic order is introduced into topological insulators (TIs), the time-reversal-symmetry is broken, and the non-trivial topological surface is driven into a new massive Dirac-fermions state. By adjusting the Fermi level position, quantum anomalous Hall effect (QAHE) emerges in the Cr-doped $(\text{BiSb})_2\text{Te}_3$ samples where dissipationless chiral edge conduction is realized in the macroscopic millimeter-size devices without the presence of an external magnetic field, and the stability of the dissipationless chiral edge conductance is well-maintained as the film thickness varies across the 2D hybridization limit. By further manipulating the topological surface gap, we realize the metal-to-insulator quantum phase transition in the system.

In addition to the uniform magnetic TIs, our recent work on several magnetic TI based heterostructures will be presented. First, in the TI/Cr-doped TI system, we demonstrate that the spin-orbit torque is highly efficient that the critical charge current density required for the magnetization switching is three orders of magnitude smaller than that of heavy metals. In addition, by constructing novel AFM/TI heterostructures, we realize emergent interfacial magnetic effects, which can be tailored through artificial structural engineering. Finally, by introducing additional superconductivity (SC), we observe the presence of the chiral Majorana edge mode in the QAHE-SC hybrid system. All these exotic magnetic TI-based phenomena will serve as fundamental steps to further explore the TRS-breaking TI systems.

Open Access

This article is licensed under a [Creative Commons Attribution 4.0 International License](https://creativecommons.org/licenses/by/4.0/).

© The Author(s) 2017

Charge-current induced spin polarization in BiSbTeSe₂ topological insulators

Fan Yang,^{1*} Subhamoy Ghatak,¹ A. A. Taskin,¹ Yoichi Ando,¹ Yuichiro Ando,² Masashi Shiraishi,² Kouji Segawa,³ Yasushi Kanai,³ Kazuhiko Matsumoto,³ Achim Rosch⁴

¹Institute of Physics II, University of Cologne, Zulpicher Strasse 77, 50937 Koeln, Germany

²Department of Electronic Science and Engineering, Kyoto University, Katsura, Nishikyo-ku, Kyoto 615-8510, Japan

³Institute of Scientific and Industrial Research, Osaka University, 8-1 Mihogaoka, Ibaraki, Osaka 567-0047, Japan

⁴Institute of Theoretical Physics, University of Cologne, Zulpicher Strasse 77, 50937 Koeln, Germany

Corresponding Author. Email: yang@ph2.uni-koeln.de

Received: 24 May 2017, Accepted: 08 June 2017, Published Online: 31 October 2017

Citation Information: Fan Yang, Subhamoy Ghatak, A. A. Taskin, Yoichi Ando, Yuichiro Ando, Masashi Shiraishi, Kouji Segawa, Yasushi Kanai, Kazuhiko Matsumoto, Achim Rosch, *Nano-Micro Conference*, 2017, 1, 01069 doi: 10.11605/cp.nmc2017.01069

Abstract

The surface states of 3D topological insulators (TIs) possess a helical spin texture in which the spin and momentum are perpendicularly locked to each other. Due to this spin-momentum locking, a net spin polarization can be induced by a charge current and vice versa. However, topological surface states are expected to give rise to only one type of spin polarization for a given current direction, which has been a limiting factor for spin manipulations. In this talk we report that in devices based on the bulk-insulating topological insulator BiSbTeSe₂, two different kinds of spin polarizations were observed in different devices: The spin polarization expected from the topological surface states was detected in a heavily electron-doped device, whereas the opposite polarization was reproducibly observed in devices with low carrier densities [1]. We propose that the latter type of spin polarization stems from topologically-trivial two-dimensional states with a large Rashba spin splitting, which are caused by a strong band bending at the surface of BiSbTeSe₂ beneath the ferromagnetic electrode used as a spin detector. This finding paves the way for realizing the “spin transistor” operation in future topological spintronic devices.

References

[1] F. Yang; S. Ghatak; A. A. Taskin; K. Segawa; Y. Ando; M. Shiraishi; Y. Kanai; K. Matsumoto; A. Rosch; Y. Ando, Switching of charge-current-induced spin polarization in the topological insulator BiSbTeSe₂. *Physical Review B*. 94, 075304 (2016). doi:[10.1103/PhysRevB.94.075304](https://doi.org/10.1103/PhysRevB.94.075304)

Open Access

This article is licensed under a [Creative Commons Attribution 4.0 International License](https://creativecommons.org/licenses/by/4.0/).

© The Author(s) 2017

Focusing and Separating Diamagnetic Microparticles with Multiphase Ferrofluids

Cheng Wang,* Ran Zhou

Department of Mechanical and Aerospace Engineering, Missouri University of Science and Technology, 400 W. 13th St., MO 65409, USA

Corresponding Author. Email: wancheng@mst.edu

Received: 29 May 2017, Accepted: 12 June 2017, Published Online: 31 October 2017

Citation Information: Cheng Wang, Ran Zhou, Nano-Micro Conference, 2017, 1, 01070 doi: 10.11605/cp.nmc.2017.01070

Abstract

Ferrofluids have demonstrated great potential for a variety of manipulations of diamagnetic (or non-magnetic) micro-particles/cells in microfluidics, including sorting, focusing, and enriching. By utilizing size-dependent magnetophoresis velocity, most of the existing techniques employ single phase ferrofluids to push particles towards channel walls. In this work, we demonstrate a novel strategy for focusing and separating diamagnetic micro-particles by using the laminar fluid interface of two co-flowing fluids -- a ferrofluid and a non-magnetic fluid [1]. As shown in Figure 1, next to the microfluidic channel, microscale magnets are fabricated to generate strong localized magnetic field gradients and forces. Due to the negative magnetophoresis force, diamagnetic particles suspended in the ferrofluid phase migrate across the ferrofluid stream at size-dependent velocities. Because of the low Reynolds number and high Peclet number associated with the flow, the fluid interface is sharp and stable. When the micro-particles migrate to the interface, they are accumulated near the interface, resulting in effective focusing and separation of particles. We investigated several factors that affect the focusing and separation efficiency, including susceptibility of the ferrofluid, distance between the microfluidic channel and microscale magnet, and width of the microfluidic channel. This concept can be extended to multiple fluid interfaces. As an example, complete separation of micro-particles was demonstrated by using a three-stream multiphase flow configuration.

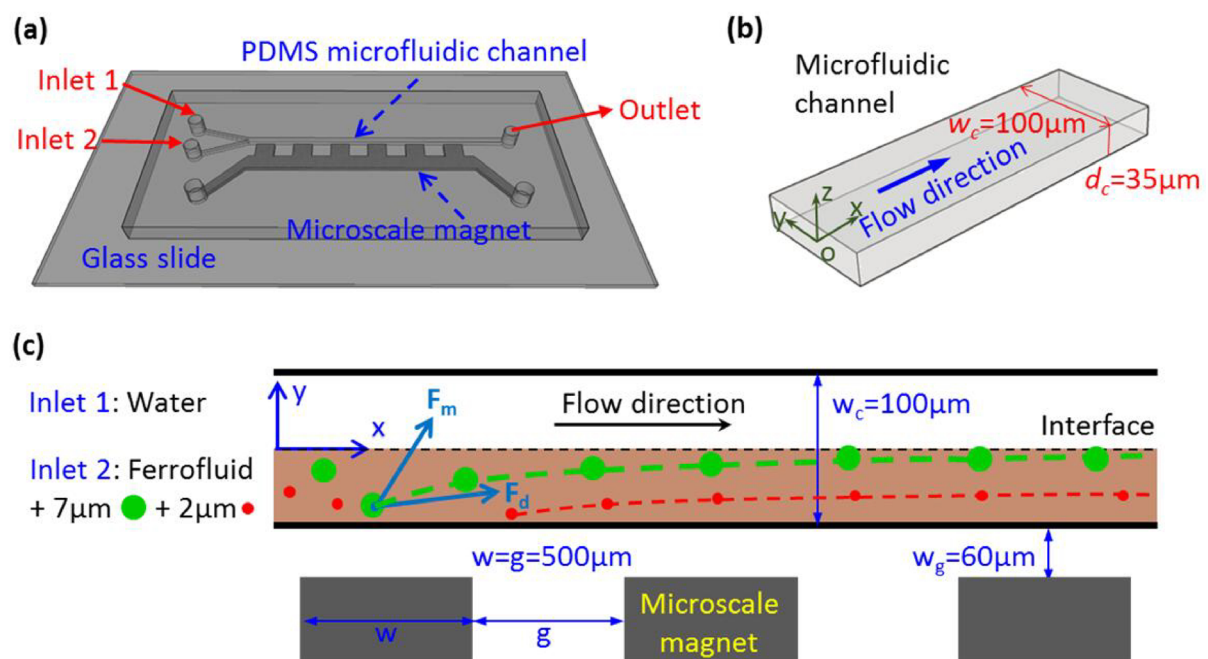


Figure 1. Overview of the device and principle of particle separation. (a) a two-inlet microchannel and microscale magnets; (b) dimensions of the main fluidic channel; (c) basic principle of particle movement in a ferrofluid.

References

[1] Ran Zhou; Cheng Wang, Multiphase ferrofluid flows for micro-particle focusing and separation. *Biomicrofluidics*. 10, 034101 (2016). doi:10.1063/1.4948656

Open Access

This article is licensed under a [Creative Commons Attribution 4.0 International License](https://creativecommons.org/licenses/by/4.0/).

© The Author(s) 2017

Porous carbon fibers for electromagnetic wave absorption

Chun Shan, Linchang Mao, Kang Fu, Guang Li*

State key laboratory for modification of chemical fibers and polymer materials, Donghua University, Shanghai, China

Corresponding Author. Email: lig@dhu.edu.cn

Received: 14 June 2017, Accepted: 18 June 2017, Published Online: 31 October 2017

Citation Information: Chun Shan, Linchang Mao, Kang Fu, Guang Li, *Nano-Micro Conference, 2017, 1, 01071* doi: 10.11605/cp.nmc2017.01071

Abstract

Modern warfare urgently needs radar stealth technology to meet the shelter requirements of weapons and equipment. In this paper, porous carbon fibers were developed as an efficient microwave absorbent filler to prepare microwave absorbing composites. Firstly, polyacrylonitrile (PAN) was used as carbon precursor polymer (CPP), while polymethyl methacrylate (PMMA) as thermally decomposed polymer (TDP). PAN/PMMA (70/30) blend fibers were prepared by a wet spinning of PAN/PMMA solutions. Secondly, Porous carbon fibers (PCF) were obtained through carbonization of the blend fibers. The molecular weight of PAN could be used to control the size of pores in PCF, that is, when the average molecular weight of PAN was 51,000 g/mol and 83,000 g/mol respectively, PCF with pores ranging 1-10 μ m in diameter (designated PCF-L); and the other one with pores with diameter in the range of 0.1-1 μ m (designated PCF-S) were obtained. The resultant porous fibers, PCF-L and PCF-S, were used as microwave absorbing fillers to mix with epoxy respectively, the composites containing 2-6 wt% of the filler were fabricated. It was found that PCF-S filled composites showed much better microwave absorption performance than that PCF-L filled one. The composite containing 6 wt% of PCF-S reached the lowest reflection loss of -32dB; and the reflection loss below -10 dB covered the whole X band. The change or destruction of the porous structure in PCF showed great effect on the microwave absorption properties, which demonstrate that the pores in PCF could make great contribution to the microwave absorption.

Open Access

This article is licensed under a [Creative Commons Attribution 4.0 International License](https://creativecommons.org/licenses/by/4.0/).

© The Author(s) 2017

Chiral modes of topological semimetals under magnetic field

Xiao-Xiao Zhang*

Department of Applied Physics, The University of Tokyo, 7-3-1 Hongo, Bunkyo-ku, Tokyo 113-8656, Japan

Corresponding Author. Email: zhang@appi.t.u-tokyo.ac.jp

Received: 03 June 2017, Accepted: 12 June 2017, Published Online: 31 October 2017

Citation Information: Xiao-Xiao Zhang, *Nano-Micro Conference*, 2017, 1, 01072 doi: 10.11605/cp.nmc2017.01072

Abstract

Topological Dirac/Weyl semimetals, two new quantum phases of matter, attract broad interests from both condensed matter and particle physicists [1-3]. A Dirac (Weyl) semimetal with degenerate (nondegenerate) linear touchings, dubbed as Dirac (Weyl) points, in the electronic band structure is protected by various crystal symmetries (topology) [4-12]. While a Weyl point bears a topological charge in terms of the momentum-space Berry gauge flux, a Dirac point is neutral since it consists of two Weyl points of the opposite topological charge [13]. In addition, the Dirac (Weyl) semimetal exhibits cusps (Fermi arcs) instead of the conventional Fermi ring at the boundary of the Brillouin zone. On the other hand, because of the Landau level formation under an external magnetic field, these band touchings gain to hold massless chiral one-dimensional channels rarely seen outside the discussion of fundamental particles. As a result of the famous chiral anomaly [14-21], the chiral magnetic effect [22-24] is realized in such systems and is observed as the negative magnetoresistance [25-28].

Here, we try to provide a natural but yet missing analysis of the chiral matter, Weyl semimetal, in terms of the powerful framework of Tomonaga-Luttinger liquid, which enables us to examine the correlation and localization effects largely enhanced in this system under a strong magnetic field. We found new features unique to the 1D channels such as the independent critical exponents for the Greens function and the resistivity, which can be directly compared with experiments of realistic materials. The ubiquitous presence of a large number of Weyl points is also taken into account.

Besides, we consider the Dirac semimetal in the form of a nanowire, i.e., new ingredient of confinement geometry is added to this conventional gapless topological semimetal. Once a magnetic field along the nanowire direction is further applied, there will occur a competition between the effects of the confinement and the magnetic field, which strongly affects how the band gap is opened in the system. Expectedly, the system at finite temperature will show distinct transport features as one turns on and gradually increases the external magnetic field.

There has been an increase of interest recently by the micro- or nano-technology community in considering topological materials emerged in the last decade, whose novel topological properties may bring about new possibilities in various applications. Based on these findings, we hope to clarify a few aspects from the viewpoint of either fundamental science or nano-micro engineering.

Acknowledgements

This work was supported by JSPS Grant-in-Aids for Scientific Research (No. 16J07545) from the Ministry of Education, Culture, Sports, Science and Technology (MEXT) of Japan.

References

- [1] Hermann Weyl, *Elektron und Gravitation. I. Zeitschrift für Physik*. 56, 330-352 (1929). doi:10.1007/BF01339504
- [2] B. Q. Lv; H. M. Weng; B. B. Fu; X. P. Wang; H. Miao; J. Ma; P. Richard; X. C. Huang; L. X. Zhao; G. F. Chen; Z. Fang; X. Dai; T. Qian; H. Ding, Experimental Discovery of Weyl Semimetal TaAs. *Physical Review X*. 5, 031013 (2015). doi:10.1103/PhysRevX.5.031013
- [3] S.-Y. Xu; I. Belopolski; N. Alidoust; M. Neupane; G. Bian; C. Zhang; R. Sankar; G. Chang; Z. Yuan; C.-C. Lee; S.-M. Huang; H. Zheng; J. Ma; D. S. Sanchez; B. Wang; A. Bansil; F. Chou; P. P. Shibayev; H. Lin; S. Jia; M. Z. Hasan, Discovery of a Weyl fermion semimetal and topological Fermi arcs. *Science*. 349, 613-617 (2015). doi:10.1126/science.aaa9297
- [4] O. Vafek; A. Vishwanath, Dirac Fermions in Solids: From High-Tc Cuprates and Graphene to Topological Insulators and Weyl Semimetals. *Annual Review of Condensed Matter Physics*. 5, 83-112 (2014). doi:10.1146/annurev-conmatphys-031113-133841
- [5] Y. Ren; Z. Qiao; Q. Niu, Topological phases in two-dimensional materials: a review. *Reports on Progress in Physics*. 79, 066501 (2016). doi:10.1088/0034-4885/79/6/066501
- [6] S. Murakami, Phase transition between the quantum spin Hall and insulator phases in 3D: emergence of a topological gapless phase. *New Journal of Physics*. 9, 356 (2007). doi:10.1088/1367-2630/9/9/356
- [7] X. Wan; A. M. Turner; A. Vishwanath; S. Y. Savrasov, Topological semimetal and Fermi-arc surface states in the electronic structure of pyrochlore iridates. *Physical Review B*. 83, 205101 (2011). doi:10.1103/PhysRevB.83.205101
- [8] Gábor B. Halász; Leon Balents, Time-reversal invariant realization of the Weyl semimetal phase. *Physical Review B*. 85, 035103 (2012). doi:10.1103/PhysRevB.85.035103
- [9] G. Xu; H. Weng; Z. Wang; X. Dai; Z. Fang, Chern Semimetal and the Quantized Anomalous Hall Effect in HgCr₂Se₄. *Physical Review Letters*. 107, 186806 (2011). doi:10.1103/PhysRevLett.107.186806
- [10] D. Bulmash; C.-X. Liu; X.-L. Qi, Prediction of a Weyl semimetal in Hg_{1-x-y}Cd_xMn_yTe. *Physical Review B*. 89, 081106 (2014). doi:10.1103/PhysRevB.89.081106
- [11] A. A. Burkov; L. Balents, Weyl Semimetal in a Topological Insulator Multilayer. *Physical Review Letters*. 107, 127205 (2011).

doi:[10.1103/PhysRevLett.107.127205](https://doi.org/10.1103/PhysRevLett.107.127205)

[12] A. A. Zyuzin; S. Wu; A. A. Burkov, Weyl semimetal with broken time reversal and inversion symmetries. *Physical Review B*. 85, 165110 (2012). doi:[10.1103/PhysRevB.85.165110](https://doi.org/10.1103/PhysRevB.85.165110)

[13] G. E. Volovik, *The Universe in a Helium Droplet* (International Series of Monographs on Physics), 1st ed. (Oxford University Press, 2009).

[14] S. L. Adler, Axial-Vector Vertex in Spinor Electrodynamics. *Physical Review Journals Archive*. 177, 2426 (1969). doi:[10.1103/PhysRev.177.2426](https://doi.org/10.1103/PhysRev.177.2426)

[15] J. S. Bell; R. Jackiw, A PCAC puzzle: $\pi^0 \rightarrow \gamma\gamma$ in the σ -model. *Il Nuovo Cimento A* (1965-1970). 60, 47-61 (1969). doi:[10.1007/BF02823296](https://doi.org/10.1007/BF02823296)

[16] H. Nielsen; M. Ninomiya, Absence of neutrinos on a lattice: (I). Proof by homotopy theory. *Nuclear Physics B*. 185, 20-40 (1981). doi:[10.1016/0550-3213\(81\)90361-8](https://doi.org/10.1016/0550-3213(81)90361-8)

[17] H. B. Nielsen; Masao Ninomiya, The Adler-Bell-Jackiw anomaly and Weyl fermions in a crystal. *Physics Letters B*. 130, 389-396 (1983). doi:[10.1016/0370-2693\(83\)91529-0](https://doi.org/10.1016/0370-2693(83)91529-0)

[18] C.-X. Liu; P. Ye; X.-L. Qi, Chiral gauge field and axial anomaly in a Weyl semimetal. *Physical Review B*. 87, 235306 (2013). doi:[10.1103/PhysRevB.87.235306](https://doi.org/10.1103/PhysRevB.87.235306)

[19] P. Hosur; X. Qi, Recent developments in transport phenomena in Weyl semimetals. *Comptes Rendus Physique*. 14, 857-870 (2013). doi:[10.1016/j.crhy.2013.10.010](https://doi.org/10.1016/j.crhy.2013.10.010)

[20] A. A. Zyuzin; A. A. Burkov, Topological response in Weyl semimetals and the chiral anomaly. *Physical Review B*. 86, 115133 (2012). doi:[10.1103/PhysRevB.86.115133](https://doi.org/10.1103/PhysRevB.86.115133)

[21] A. A. Burkov, Chiral anomaly and transport in Weyl metals. *Journal of Physics: Condensed Matter*. 27, 113201 (2015). doi:[10.1088/0953-8984/27/11/113201](https://doi.org/10.1088/0953-8984/27/11/113201)

[22] K. Fukushima; D. E. Kharzeev; H. J. Warringa, Chiral magnetic effect. *Physical Review D*. 78, 074033 (2008). doi:[10.1103/PhysRevD.78.074033](https://doi.org/10.1103/PhysRevD.78.074033)

[23] D. T. Son; B. Z. Spivak, Chiral anomaly and classical negative magnetoresistance of Weyl metals. *Physical Review B*. 88, 104412 (2013). doi:[10.1103/PhysRevB.88.104412](https://doi.org/10.1103/PhysRevB.88.104412)

[24] D. E. Kharzeev, The Chiral Magnetic Effect and anomaly-induced transport. *Progress in Particle and Nuclear Physics*. 75, 133-151 (2014). doi:[10.1016/j.pnpnp.2014.01.002](https://doi.org/10.1016/j.pnpnp.2014.01.002)

[25] J. Xiong; S. K. Kushwaha; T. Liang; J. W. Krizan; M. Hirschberger; W. Wang; R. J. Cava; N. P. Ong, Evidence for the chiral anomaly in the Dirac semimetal Na_3Bi . *Science*. 350, 413-416 (2015). doi:[10.1126/science.aac6089](https://doi.org/10.1126/science.aac6089)

[26] Qiang Li; Dmitri E. Kharzeev; Cheng Zhang; Yuan Huang; I. Pletikosić; A. V. Fedorov; R. D. Zhong; J. A. Schneeloch; G. D. Gu; T. Valla, Chiral magnetic effect in ZrTe_5 . *Nature Physics*. 12, 550-554 (2016). doi:[10.1038/nphys3648](https://doi.org/10.1038/nphys3648)

[27] X. Huang; L. Zhao; Y. Long; P. Wang; D. Chen; Z. Yang; H. Liang; M. Xue; H. Weng; Z. Fang; X. Dai; G. Chen, Observation of the Chiral-Anomaly-Induced Negative Magnetoresistance in 3D Weyl Semimetal TaAs. *Physical Review X*. 5, 031023 (2015). doi:[10.1103/PhysRevX.5.031023](https://doi.org/10.1103/PhysRevX.5.031023)

[28] C. Shekhar; A. K. Nayak; Y. Sun; M. Schmidt; M. Nicklas; I. Leermakers; U. Zeitler; Y. Skourski; J. Wosnitza; Z. Liu; Y. Chen; W. Schnelle; H. Borrmann; Y. Grin; C. Felser; B. Yan, Extremely large magnetoresistance and ultrahigh mobility in the topological Weyl semimetal candidate NbP. *Nature Physics*. 11, 645-649 (2015). doi:[10.1038/nphys3372](https://doi.org/10.1038/nphys3372)

Open Access

This article is licensed under a [Creative Commons Attribution 4.0 International License](https://creativecommons.org/licenses/by/4.0/).

© The Author(s) 2017

Novel Self-powered UV-Visible Photodetector with Fast Response and High Photosensitivity Employing Fe:TiO₂/n-Si Heterojunction

Lin Sun,^{1*} Chunrui Wang,^{1*} Tao Ji^{2,3}

¹Department of Applied Physics and state key laboratory for modification of chemical fibers and polymer materials, Donghua University, 2999 Renmin Rd North, Songjiang District, Shanghai, China

²State Key Laboratory for Modification of Chemical Fibers and Polymer Materials, College of Materials Science and Engineering, Donghua University, 2999 Renmin Rd North, Songjiang District, Shanghai, China

³School of Fundamental Studies, Shanghai University of Engineering Science, 333 Long Teng Road, Songjiang District, Shanghai, China
Corresponding Author. Email: Lin Sun, suns@mail.dhu.edu.cn; Chunrui Wang, crwang@dhu.edu.cn

Received: 31 May 2017, Accepted: 13 June 2017, Published Online: 31 October 2017

Citation Information: Lin Sun, Chunrui Wang, Tao Ji, Nano-Micro Conference, 2017, 1, 01073 doi: 10.11605/cp.nmc2017.01073

Abstract

A UV-Visible photodetector employing heterojunction between the Fe:TiO₂ and Si was fabricated via a facile solution process. The existence of built-in electric field between TiO₂ and Si help facilitate the separation of photogenerated electron-hole pairs and regulate the electron transport. Under zero bias, the device exhibited high responsivity of 46 mA/W (350 nm) and 60 mA/W (600 nm) with a 0.5 mw·cm⁻² light irradiation. At a small reverse bias of -0.5V, the quantum efficiency of the heterojunction rise up beyond 100% with a broad wavelength range. The exploring of Fe:TiO₂/n-Si heterojunction photodetector demonstrates an ultrasensitive (on/off ratio up to 10³), fast (rise/decay time of <10/15 ms), and broad-band (UV-visible) photodetection with no or low external energy supply. Such novel photodetector with Fe:TiO₂/n-Si Heterojunction might be potentially useful for relative applications with weak-signal fast detection in UV-visible band.

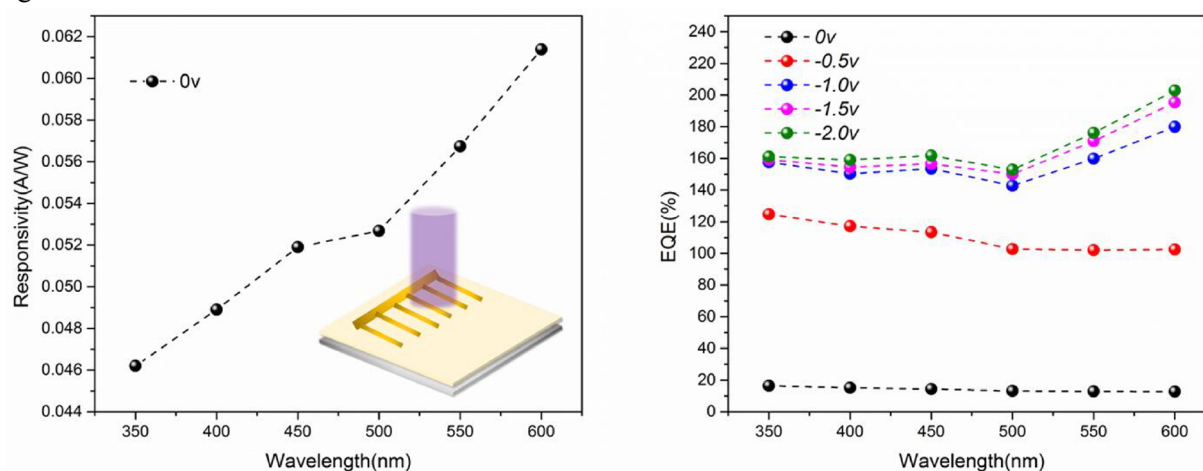


Figure 1. Responsivity and EQE of Fe:TiO₂/n-Si heterojunction under each bias in UV-visible band.

References

- [1] Tao Ji; Qian Liu; Rujia Zou; Yangang Sun; Kaibing Xu; Liwen Sang; Meiyong Liao; Yasuo Koide; Li Yu; Junqing Hu, An Interface Engineered Multicolor Photodetector Based on n-Si(111)/TiO₂ Nanorod Array Heterojunction. *Advanced Functional Materials*. 26, 1400-1410 (2016). doi:[10.1002/adfm.201504464](https://doi.org/10.1002/adfm.201504464)
- [2] Tao Ji; Ze Cui; Wenlong Zhang; Yunjiu Cao; Yongfang Zhang; Shu-ang He; Mingdong Xu; Yangang Sun; Rujia Zou; Junqing Hu, UV and visible light synergetic photodegradation using rutile TiO₂ nanorod arrays based on a p-n Junction. *Dalton Transactions*. 46, 4296-4302 (2-17). doi:[10.1039/C7DT00261K](https://doi.org/10.1039/C7DT00261K)

Open Access

This article is licensed under a [Creative Commons Attribution 4.0 International License](https://creativecommons.org/licenses/by/4.0/).

© The Author(s) 2017

Gram-scale production of nanoporous graphene by Mg-thermoreduction of CS₂ for electrochemical energy storage

Lu Sun, Jinzhang Liu, Yan Li*

School of Materials Science and Engineering, Beihang University, Beijing 100191, China

Corresponding Author. Email: liyan@buaa.edu.cn

Received: 31 May 2017, Accepted: 13 June 2017, Published Online: 16 November 2017

Citation Information: Lu Sun, Jinzhang Liu, Yan Li, *Nano-Micro Conference*, 2017, 1, 01074 doi: 10.11605/cp.nmc2017.01074

Abstract

Mass production of porous carbon at low cost for supercapacitor applications is highly desired. Herein, for the first time we report a novel method to grow porous 3D graphene by using Mg to reduce CS₂ vapor. In a tube furnace the mixture of Mg and NaCl powders are heated at 570 °C and reacted with CS₂ vapor carried by an Ar flow. The Mg powder can be about 95% consumed and the weight of resultant carbon nanomaterial is in gram scale after one experiment. This 3D graphene product with specific surface area of 980 cm²/g is processed into electrodes for electrochemical test, showing a specific capacitance of 212 F/g at 1 A/g in H₂SO₄ aqueous electrolyte. Besides, the electrode is continuously charged/discharged at 5 A/g for 10,000 cycles and its capacitance remains 98.5% of the original value.

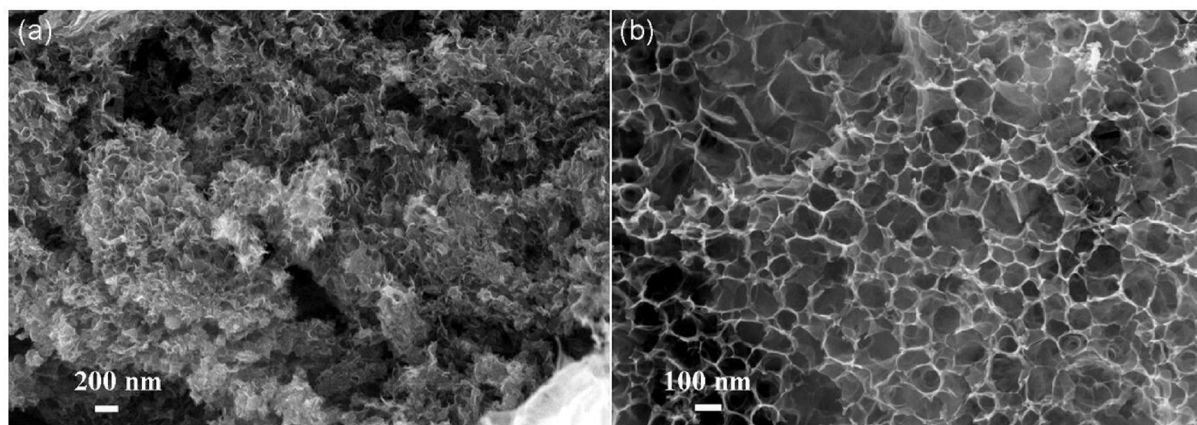


Figure 1. (a) and (b) SEM images of the 3D graphene product at low and high magnifications.

Open Access

This article is licensed under a [Creative Commons Attribution 4.0 International License](https://creativecommons.org/licenses/by/4.0/).

© The Author(s) 2017

Enhanced electrochemical energy storage of N-doped graphene by adsorbing molecules of hydrolyzed polyimide

Yi Zhao, Jinzhang Liu*

School of Materials Science and Engineering, Beihang University, Beijing 100191, China

Corresponding Author. Email: ljz78@buaa.edu.cn

Received: 28 May 2017, Accepted: 12 June 2017, Published Online: 16 November 2017

Citation Information: Yi Zhao, Jinzhang Liu, *Nano-Micro Conference*, 2017, 1, 01075 doi: 10.11605/cp.nmc2017.01075

Abstract

A novel approach for increasing the specific capacitance of graphene-based supercapacitors is reported. In this work, Kapton, which is polyimide (PI) film widely used in industry, is used as the starting material to functionalize graphene. Hydrolysis of PI in alkalic solution released small aromatic molecules containing pyrrolic nitrogen that can be dissolved in water and easily adsorbed onto graphene sheets via π - π interaction (Figure 1). These small molecules store charge via a redox process, endowing graphene with pseudocapacitance and increasing the specific capacitance. N-doped graphene films are obtained by hydrothermally reducing solid composite films consisting of graphene oxide, ammonium acetate, and salt. These films are firstly used as electrodes to make symmetric supercapacitors with H_2SO_4 aqueous electrolyte as electrolyte, and show specific capacitances around 310 F/g. After the adsorption of hydrolyzed PI molecules, the weight of graphene film is $\sim 3\%$ increased, and the specific capacitance was remarkable increased up to 467 F/g. Notably, the areal specific capacitance is in the scale of 1.2 F/cm^2 . When using the Li_2SO_4 aqueous electrolyte that can extend the potential window to 1.5 V, the device also remains high specific capacitance around 445 F/g, and exhibits high energy densities up to 35 Wh/Kg. Our devices not only deliver excellent capacitive performances in aqueous electrolyte (89% capacitance retention at 20 A/g and 85% capacitance retention over 5 000 cycles), but also exhibit extraordinary mechanical flexibility. This novel strategy by adsorbing small molecules from hydrolyzed PI provides a promising route towards high-performance supercapacitors.

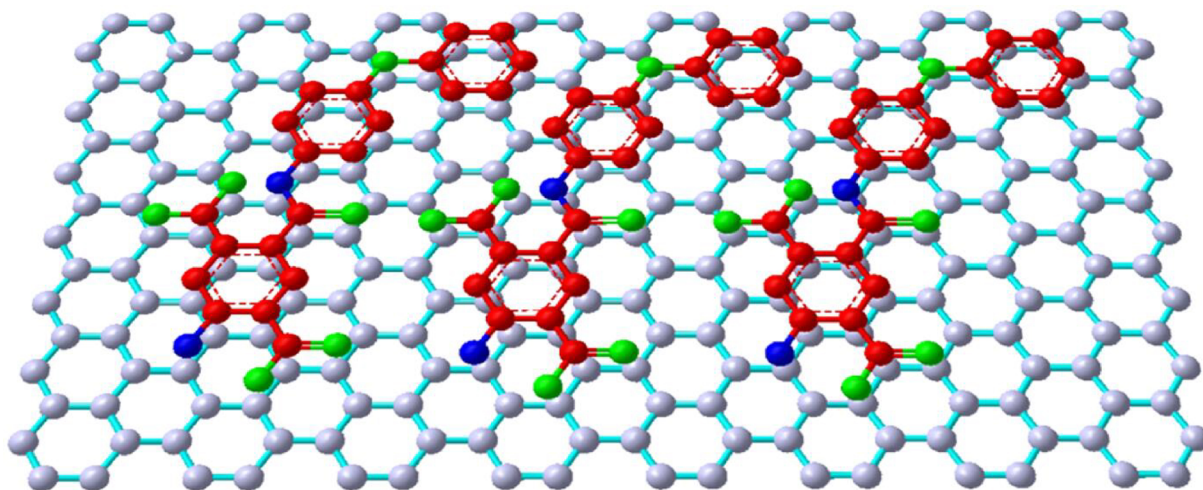


Figure 1. Illustration of the adsorption of hydrolyzed PI molecules onto graphene sheet.

Open Access

This article is licensed under a [Creative Commons Attribution 4.0 International License](https://creativecommons.org/licenses/by/4.0/).

© The Author(s) 2017

Recent research in the continuous terahertz wave on nondestructive detection of carbon fibre composite

Tielin Lu,¹ Chunxi Wang,¹ Lu Ding,¹ Xiaojing Liu,¹ Jingshui Zhang,² Lingqin Kong²

¹Instrumentation Technology and Economy Institute (Institution) 397A Guanganmenwai St., Beijing, China

²Beijing Institute of Technology (Institution) No.5 Zhongguancun South St., Beijing, China

Corresponding Author. Email: lutielin@126.com

Received: 23 May 2017, Accepted: 16 June 2017, Published Online: 30 November 2017

Citation Information: Tielin Lu, Chunxi Wang, Lu Ding, Xiaojing Liu, Jingshui Zhang, Lingqin Kong, Nano-Micro Conference, 2017, 1, 01076 doi: 10.11605/cp.nmc2017.01076

Abstract

Terahertz nondestructive detection system is to test the image of the carbon fibre composite material. We use the continuous back wave oscillator (BWO) to pump the terahertz radiation, which the frequency is range from 210-250 GHz. By the reflection type detection system, the terahertz probe focus moves from the surface of the concealed carbon fibre composite material. In order to get real-time scanning the material image, the material is located by the 2D translation machine, which is connected to the computer. The data is collected by the phase-locked amplifier and calculated by the Matlab using the least square method (LSM). The interior structure, such as cracks, inclusions, empty and bubbles, can be detected by the images nearly 1mm resolution, which is a more convenient and simple method of nondestructive detection of the carbon fiber composite material.

Introduction

The composite material is made from different materials, which is produced by physical or chemical mechanism in the macroscopic. It is largely depended on the performance of various materials, which can make it better than the original composition. For this reason, it has played an important role in many fields, such as aerospace, automobile, shipbuilding, construction and other products. As the biggest aircraft, the carbon fibre composite is used to cut down the weight of 50% less than before. So it has been in a new fashion to lightweight, energy saving, safety development and green manufacturing on changing the traditional materials. But the carbon fibre composite material is difficult to the cutting processing, the blade wear in the interaction process of fiber is still very serious. In addition, cause it has very different material properties, low bond strength between the layers, such as fiber pull out, torn between the layers, voids and the other serious problems influence the quality of the product. So how to detect the quality and nondestructive have been the key to restrict its further application.

Continuous terahertz wave have found the unique capacity to penetrate composite material and identify defects such as cracks, inclusions, voids and other [1-7]. Many years, there have been much research work done on the terahertz detecting cause of its importance character as high transmittance, safety for human beings and for other organisms. The ability of imaging the defects in aerospace composite materials, acquired during operation, by THz time-domain spectrometer (TDS) was researched in [1]. As the TDS system always needs a stable and complex optical roots, our work shows the ability of non-destructive detection in composite materials, reinforced by carbon fiber, by using continuous terahertz wave imaging system. The experimental is easy to build up and results show that the resolution is better than 1mm, and the information to collect the image of the measured sample can be obtained by two-dimensional (2D) scanning system.

Principle of the methods

With the complex structure of fibre carbon composite materials, there is a bunch of characteristic parameters that have to be focused on: fibre volume content, porosity, inclusions, voids, regions of insufficient resin infiltration and others. Continuous terahertz wave imaging system is a non-destructive and contactless inspection technique that is based on the propagation and reflection of optical waves. All the imaging system is based on source, our work is used the continuous back wave oscillator (BWO) as the source of terahertz radiation. It can easily operate the frequency and range from 160 to 2100 GHz. The output power has the relationship with the frequency, which is given by:

The U_x is the voltage diffusion in the BWO instruction and the frequency is the f . As the continuous terahertz wave incidents to the surface of the composite material, it will be directly reflected by two roots, one of the terahertz wave reflected

$$U(f) = (U_0 + U_1 f + U_2 f^2 + U_3 f^3)^2 \quad (1)$$

from the front surface of the material and the other one reflected from the material attached to the high reflective surface. From the difference for the reflective of the thickness and the surface of the sample, the intensity of the continuous terahertz wave is not the same. For the BWO is a continuous terahertz source of fixed frequency output, obtained the intensity by the detector, we use point to point scanning imaging method to record the intensity and put the relevant information into computer, which can image the composition of the sample, such as the shape and the size.

Experimental setup

Figure 1 presented the reflected imaging system from the sample of the composite material. The BWO with an output power in 0.4mW is build up as the terahertz wave source. We choose the output frequency is from 206.2 to 260 GHz,

which is extremely coherent, polarized, and monochromatic ($\Delta v/v \approx 10^{-5}$). The continuous terahertz wave generated by the BWO is modulated by a chopper. The wave exiting from BWO is divided into two parts by a high-resistivity ($R \geq 10000\Omega$) silicon wafer, with 0.5mm thick, acting as a wave splitter. One of the split beams directly incidents into the focusing lens with collecting the wave light focusing onto the sample of composite material. The focusing lens always consist with two lens, which are collimator lens. With the attenuated reflection, the polyethylene lens can get the wave focus well to the sample. The length of optical root should be short and high transmittance. In this lens group, we choose the polyethylene lens, which are well performance in terahertz wave focusing. The other split beam incidents into the detector, which converts the intensity of the terahertz into voltage signal as the input signal for the lock-in amplifier, and reference frequency for the lock-in amplifier is the same as the chopper. By this way the noise of the signal is filtered, we can obtained the intensity of the surface of the sample. After, with the acquisition unit, the data is transferred into the computer. Finally we can calculate each point by matlab and imaging the sample.

As depicted in Figure 2 is the imaging system we set up in the lab. We put one piece of paper before the sample in order to achieve the non-destructive of the material. Due to the simple system, it can easy to connect all the instrument without the external interference.

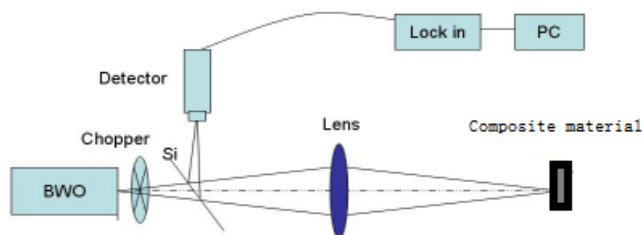


Figure 1 Schematic of the terahertz reflected imaging system.

Compared with the traditional transmission optical non-destructive system, the terahertz reflection non-destructive imaging system is a little different to set up, firstly, the terahertz is invisible, and the reflected direction is always changed, so the collection is easy to be affected by the surface of the composite material orientation, component space distribution and other

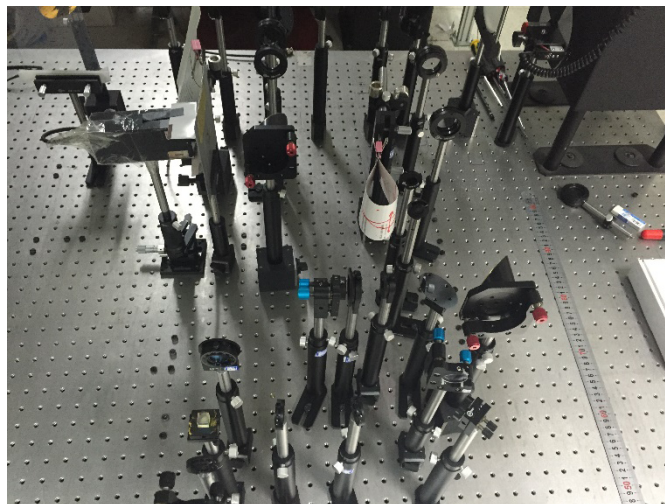


Figure 2 Schematic view of the experimental non-destructive system.

er factors. Secondly, the reflected wave consists of lens reflect wave diffuse wave and scattered wave. And the roughness, the size of the focusing and the signal to noise ratio of the sample can also influence the composition of the reflected wave and the data processing method.

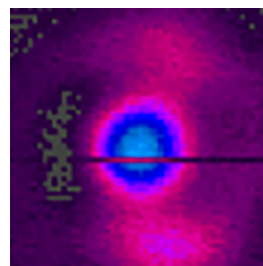


Figure 3 2D energy spot of the continuous terahertz wave.

Experimental results

For the continuous terahertz wave generated from the BWO, the optical focusing should adjust to the plate of the sample, which is highest energy point of the sample. We use the point-to-point scanning system to detect the sample, so the wave spot from the polyethylene lens is changed by the focal. The Figure 3 is the measured result of energy density distribution in the plane view, which is the sample position located, acquired by using a 2D terahertz camera. The terahertz camera is Ophir-Spiricon, made from America. In this case, the optical roots can be ready to detect the sample of the composite material.



Figure 4 The sample of fibre cabin composite material.

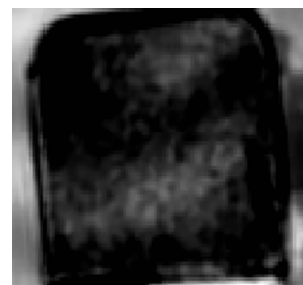


Figure 5 The image result of scanning the sample.

In order to verify the experimentally non-destructive system of modeling, Before the sample of carbon fibre composite material (as shown in Figure 4), we put a piece of paper to set up the detection system. The sample is like square with $5 \times 4 \times 0.5$ cm of the LWH size. With place the sample at the focal point of the focusing lens, the reflect wave can reach into the detector. After the data processing in the computer, the detection image of the sample is obtained with the resolution within 1 mm. The resolution depends on the output of the BWO frequency and the distance of the X-Y plane. But if the resolution

is higher, the time of the scanning image would be longer. And the theoretical focal spot diameter at 206.2GHz is 0.93 mm by the relationship of NA. Figure 5 has shown the image result of the composite material with the Matlab. It can easily present the profiles of the sample's surface with non-destructive the material. Therefore, the system can be used as a non-contact scanning image system for detecting various composite materials.

Conclusion

In this paper, the method of a reflection terahertz wave non-destructive system is demonstrated to image the carbon fibre composite material. By the pyroelectric detector to get the signal to phase-lock amplifier, it converts the optical intensity to electric signal, which we can test the sample. Compared with other image systems, the reflection terahertz imaging system has more practical application value than the transmission imaging system. It can apply on nondestructive, non-contact and extraction of material surface profile. The resolution of the measurement is higher than 1mm. But in some practical situations, the target object needs higher resolution with fast way, such as 3D imaging, recognition and tracking. In these cases, the detection imaging system will be replaced as a new detector, but the means of reflection detection would never be replaced. Meanwhile, the terahertz wave can be a powerful and easy way for imaging and detecting the composite materials.

Acknowledgment

This work was supported by a grant from Ministry of Science and Technology (No.2016YFF0202702). Thanks to Prof. Yuejin Zhao, Dr. Hui Yuan and Dr. Xiaohu Guo, giving the advice of the detection system.

References

- [1] C. D. Stoik; M. J. Bohn; J. L. Blackshire, Nondestructive evaluation of aircraft composites using transmissive terahertz time domain spectroscopy. *Optics Express* 16 (23), 17039 (2008). doi:[10.1364/OE.16.017039](https://doi.org/10.1364/OE.16.017039)
- [2] S. Wietzke; C. Jördens; N. Krumbholz; B. Baudrit; M. Bastian; M. Koch, Terahertz imaging: a new non-destructive technique for the quality control of plastic weld joints. *Journal of the European Optical Society Rapid Publications* 2, (2007). doi:[10.2971/jeos.2007.07013](https://doi.org/10.2971/jeos.2007.07013)
- [3] E. V. Yakovlev; K. I. Zaytsev; I. N. Fokina; V. E. Karasik; S. O. Yurchenko, Nondestructive testing of polymer composite materials using THz radiation. 486, 012008 (2014). doi:[10.1088/1742-6596/486/1/012008](https://doi.org/10.1088/1742-6596/486/1/012008)
- [4] T. L. Lu; H. Yuan; L. Q. Kong; Y. J. Zhao; L. L. Zhang; C. L. Zhang, Experimental research on spectrum and imaging of continuous-wave terahertz radiation based on interferometry. *Chinese Physics B*. 25 (8), 80702 (2016). doi:[10.1088/1674-1056/25/8/080702](https://doi.org/10.1088/1674-1056/25/8/080702)
- [5] C. Zhang; Y. Zhang; Q. L. Zhou, *Terahertz Sensing and Imaging*. Beijing: National defense industry press, 90 (2008).
- [6] X. H. Ge; M. Lv; H. Zhong; C. L. Zhang, Terahertz wave reflection imaging system based on backward wave oscillator and its application. *Journal of Infrared & Millimeter Waves*. 29(1), 15 (2010).
- [7] M. T. Reiten; L. Hess; R. A. Cheville, Nondestructive evaluation of ceramic materials using terahertz impulse ranging. *Nondestructive Evaluation for Health Monitoring and Diagnostics International Society for Optics and Photonics*, 6179, 617905 (2006). doi:[10.1117/12.657734](https://doi.org/10.1117/12.657734)

Open Access

This article is licensed under a [Creative Commons Attribution 4.0 International License](https://creativecommons.org/licenses/by/4.0/).

© The Author(s) 2017